# The Glass to Metal Interface during Container Forming Processes.

A thesis presented

by

*Lisa Hollands*

for the Degree of
Doctor of Philosophy
at the
University of Sheffield

Centre for Glass Research
Department of Engineering Materials
The University of Sheffield                    March 1998

# ACKNOWLEDGEMENTS

# The Glass-to Metal Interface during Container Forming Processes.

## Lisa Hollands

### *Summary*

It is known that a newly formed glass container will only possess a very small fraction of its theoretical strength. This suggests that damage occurs on the surface of the glass melt during the forming process due to glass to mould contact and hot glass handling. It might be expected that any damage inflicted on the surface of a glass article during manufacture would heal at the elevated manufacturing temperatures used, however this does not appear to be true. Therefore, the actual mechanism by which glass strength is reduced during forming needs to be fully understood and the work presented in this thesis addresses this problem.

Experiments, therefore, have been carried out here which simulate the formation of glass articles using an experimental pressing rig by systematically altering processing parameters such as the mould material, surface finish of the mould, pressing temperature and atmosphere. Processing parameters that are used industrially for the formation of glass containers were generally reproduced wherever possible in order to investigate the glass-to-mould interaction.

The interaction of both a cast iron mould material and carbon-carbon composite materials with a soda-lime-silica glass were examined using the techniques of scanning electron microscopy, x-ray photoelectron spectroscopy and atomic force microscopy in order to determine the type and extent of surface damage formed.

The surfaces of the pressed glass samples made were found to contain defects of embedded particles and indented dimples. The embedded particles found were usually due to bulk material transfer from the plunger material used. The texture found on the surface of the pressed glass samples was found to be directly affected by the surface finish of the plunger. Pressing glass samples using a cast iron plunger at an initial plunger temperature below 450°C resulted in a randomly rippled 'chilled' surface. As the initial temperature of the plunger was increased, the surface texture of the pressed glass became a closer replica of the plunger surface. The use of vacuum assistance to form the glass samples also resulted in the surface of the pressed glass becoming a closer replica of the original plunger surface, even at lower pressing temperatures.

The surfaces of the cast iron and carbon-carbon composite plungers appeared to have been affected by the initial plunger temperatures used. As the initial pressing temperature was increased, the amount of oxidation for both material types increased. In the case of the carbon-carbon composite materials investigated, both the matrix and fibres were found to have broken down at the pressing temperatures used.

X-ray photoelectron spectroscopy, of the pressed glass surfaces and the plunger materials indicated that sodium ions had migrated from the glass melt to the plunger surface during forming.

# TABLE OF CONTENTS

# TABLE OF FIGURES

# TABLE OF TABLES

# 1. INTRODUCTION

The following chapter attempts to introduce the relevant theory and literature that is pertinent in the investigation of glass-to-metal interaction during forming processes. The final sections in this chapter explain the aim of the investigation and outline the contents of the thesis.

## 1.1 Principles of Glass Forming

The forming of molten glass into its desired final shape involves the action of a number of simultaneous processes, which in turn describe the workability of the glass. Heat must be withdrawn from the viscous glass being shaped at such a rate that the object retains its desired shape throughout the process of formation. The workability of the glass is an important influence during container manufacture on factors such as glass distribution, crack formation and mechanical strength [Williams_1989]. The most important properties involved in glass forming are therefore those of viscosity and heat transfer.

### 1.1.1 Viscosity

Throughout the process of formation, the way in which the viscosity of the melt changes with temperature is of primary importance. The viscosity of the glass melt is affected by both temperature and its composition. As a glass melt is cooled, it transforms from a liquid mass to a stiff solid at the glass transformation temperature ($T_g$). The viscosity-temperature relationship of a glass therefore

determines the temperature range in which the melt can be worked before setting

(i.e. becoming too viscous for any further shaping).

The viscosity of many of the common glass forming operations in container

manufacture need to fall within specific viscosity ranges. Typical viscosity values

for glass melting and forming operations can be found in Table 1.

| Process | Log (Viscosity/dPas) |
|---|---|
| melting | 1.5 - 2.5 |
| formation of gobs for containers | 3.6 - 4.2 |
| pressing | 4.0 - 6.3 |
| surface of the parison during forming | 4.0 - 8.0 |
| surface of the bottle during blowing | 5.7 - 10.0 |

**Table 1: Typical viscosities used in glass melting and forming operations [ed. Zarzycki_1991].**

The viscosity-temperature relationship of a glass therefore needs to be determined

to ascertain its workability. Viscosity measurements at high temperatures (i.e. low

viscosity) may be carried out using techniques such as the rotating cylinder

method [Dietzel & Brückner_1955]. At low temperatures, however, where the

viscosity is too high to allow the rotation of such a cylinder, an alternative method

needs to be used (e.g. measuring the extension of a loaded uniformly heated fibre

[Boow and Turner_1942]). Additionally, the relationship between temperature and

viscosity can be determined using the Vogel-Fulcher-Tamman equation (Equation 1) [Rawson_1980]:

$$\log \eta = A + \frac{B}{T - T_0}$$

**Equation 1**

where $A$, $B$ and $T_0$ are constants for each particular glass. These constants can be obtained by measuring the viscosity of the glass melt at three different temperatures, in order to solve for the three unknown constants.

Work carried out by Lakatos et al. [1972] involved measurement of the viscosity - temperature relationships between $10^2$ and $10^{13}$ dPas of 25 different glasses in the system $SiO_2$-$Al_2O_3$-$Na_2O$-$K_2O$-$CaO$-$MgO$ typical of container glasses. The glass compositions were expressed as molar contents in relation to one mole of $SiO_2$. Statistical analysis of the results permitted the production of three equations which allowed the calculation of the constants in the Vogel - Fulcher - Tamman equation. The three equations found for calculating the constants for a glass of known composition are:

$$B = -6039.7Na_2O - 1439.6K_2O - 3919.3CaO + 6285.3MgO + 2253.4Al_2O_3 + 5736.4$$

**Equation 2**

$$A = -1.4788Na_2O + 0.8350K_2O + 1.6030CaO + 5.4936MgO - 1.5183Al_2O_3 + 1.4550$$

**Equation 3**

$$T_0 = -25.07Na_2O - 321.0K_2O + 544.3CaO - 384.0MgO + 294.4Al_2O_3 + 198.1$$

**Equation 4**

The viscosity - temperature relationship for glasses containing these components could therefore be determined by interpolation without the need for carrying out

any further experiments. This then allows the temperature range to be calculated at which each process shown in Table 1 would need to be carried out.

On formation of an article, the temperature at the surface of the glass is lower than that of the interior due to the temperature gradients produced between the glass and the relatively cool mould. The surface of the article therefore gains a very viscous surface layer with a relatively fluid interior; the solid layer enables the article to keep its shape during the formation process.

## 1.1.2 Heat Transfer

As previously mentioned, one of the most important aspects of container manufacture is the heat transfer between the glass and the mould. Heat transfer is the limiting factor in commercial production speeds as the amount of heat being transferred from the glass to the mould determines how long the glass needs to spend at each stage during production.

High heat transfer coefficients are thought to indicate good thermal contact at the glass-to-mould interface indicating that perfect contact between the glass and the mould would assist in the most rapid heat transfer and therefore increase potential production speeds. Perfect contact, however, would imply that the glass would need to adhere to the mould. Such intimate contact would be excellent for heat transfer, but would prevent the removal of the article from the mould or increase the possibility of damage to the glass surface. It has been shown that once the sticking temperature of the glass-to-mould system is exceeded, an increase in the

heat transfer at the glass-to-mould interface occurs [Fellows et al., B.T.N. 222_1976].

On contact of the glass melt with the mould, the melt contracts as it cools, whilst the mould expands as it is heated which both aid the prevention of sticking. It has been reported that the thermal contact at the glass melt-to-mould interface reduces as the melt cools due to the differences in expansion between the glass and mould [Fellows & Shaw_1978]. Theoretical investigations of how heat transfers between the glass and mould during container production have shown there to be more than one mechanism in operation. The heat transfer was determined by examining the glass-to-mould separation distance during forming and the dwell time [McGraw_1973]. It was found that as the time of glass to metal contact increased, the gap formed at the glass-to-mould interface also increased. At long dwell times, heat transfer was thought to occur across this gap due to the bulk conduction of the air in the gap. At short dwell times, however, the distance between the mould wall and the glass melt was short, meaning that gas molecule to molecule collisions were infrequent therefore indicating that heat transfer could not occur due to bulk conduction in the air.

Many parameters have been found to affect the heat transfer characteristics between the glass and mould during manufacture. When the glass is brought into contact with the mould, the initial rise in temperature has been reported to be very rapid, at several hundreds of degrees per second, and is dependent upon the initial mould temperature [Howse et al._1971]. On analysing the heat transfer at the

interface, the heat transfer coefficient (i.e. the heat flux per degree of temperature difference between the two surfaces) is found to be time dependent. The rise in mould temperature at the contact surface has also been found to depend on parameters such as the melt temperature, time of pressing and duration between pressing cycles [Michchenko_1977]. The initial temperature of the mould has been shown to affect the surface temperature of the parison formed [Foster et al., B.T.N. 276_1980] with the total heat removed decreasing with increasing mould temperature [McMinn et al., B.T.N. 236_1977]. A contradictory piece of work, however, has shown that the temperature of the parison is independent of the initial mould temperature [Clark-Monks_1974]. Reasons for this discrepancy may be due to other differences in the processing parameters used as the former work was carried out in a laboratory, whilst the latter work was carried out on an industrial scale with additional parameters involved such as the use of mould lubricants etc.. It has been shown that decreasing the initial glass temperature also decreases the amount of heat extracted from the glass [Coney et al., B.T.N. 176_1973]. The heat transfer coefficient during experimental pressing has been found to decrease with time, with the decrease being more marked the lower the applied pressure [Rawson & Wosinski_1968, Kent & Rawson_1971]. Increasing the pressing force has been shown to increase the amount of heat transfer from the glass [Coney & Kent, B.T.N. 151_1971].

Other processing variables which have been found to affect the heat transfer characteristics involve changing the mould surface. Thick oxide layers produced on the mould surface during use reduce the amount of heat transfer on contact

[McMinn et al., B.T.N. 237_1978, B.T.N. 262_1979]. The type of mould material used was found to have a different effect depending upon whether it was susceptible to the formation of oxides. The use of mould lubricants during forming acts as an insulator between the glass melt and the mould reducing the amount of heat extraction by the mould [Fellows et al., B.T.N. 215_1976, Coney et al. B.T.N. 156_1972].

## 1.2   Container Production

In the glass industry, the word container is taken to mean glass packaging including bottles and jars through to customised glass packaging such as that used for the perfume industry.

Containers are basically formed by blowing molten glass into a series of two different split moulds using either compressed air or mechanical pressing for shaping. This two step process uses two different moulds:

1.  the blank mould, where pressing or blowing may be employed for shaping and

2.  the final blow mould.

The majority of containers are manufactured using an automatic process via an I. S. Machine (see section 1.2.1). The whole process of container making can be simplified into the following main steps:

Initially, a gob of glass is made by forming a portion of the glass melt from the furnace through an orifice ring where it is sheared to form a 'gather', or gob, of

glass which is subsequently manipulated to form the article. The gob is fed into a blank mould where the neck and preformed body of the container is formed. Ideally, the gob is supplied in an isothermal state with its viscosity high enough to prevent too rapid flow under gravity. The final container is then made using stage two of the process known as either 'blow and blow' (see section 1.2.2) or 'press and blow' (see section 1.2.3).

## 1.2.1 I. S. Machines

The automatic production of glass containers is carried out almost exclusively by the use of I. S. machines. It is not certain as to whether I. S. denotes its inventors, Ingle and Smith, or its main characteristic of having 'individual sections'. The machine consists of a number of independent forming sections and can operate either on a 'blow and blow' or 'press and blow' principle and is therefore very flexible. Each forming section contains a blank mould side and final blow mould side which are coupled together. Each section works independently of each other which means that if there is a problem with one of the sections, only that section needs to be taken out of use. The I. S. machine can be made up of as many as 12 sections. The production rates for bottle making machines depends on whether the operation uses single, double, triple or quadruple gob. Production speeds are also different for different size ware, i.e. smaller ware can be produced faster than larger ware. A typical speed of production of 1-pint milk bottles for a six section double gob I. S. machine is 110 pieces per minute [Glass Manufacture[1]_module 19], (however current production speeds have now been increased).

---

1 "Glass Manufacture" is an open learning course which leads to a City and Guilds qualification in Glass Manufacture
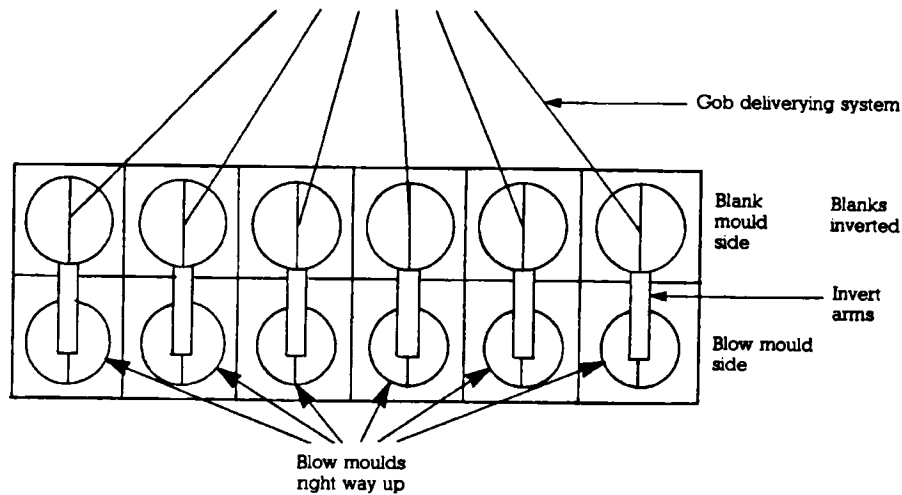
Figure 1: Schematic of the sections and moulds on a six-section I. S. machine [Glass Manufacture- module 19].

Gobs of glass of predetermined shape and weight are formed and conveyed to each blank mould in turn by an independent delivery system. The feeding of the gobs to each section in turn must be co-ordinated to ensure that there is no possibility of collision. The gob is fed to the inverted blank mould via a funnel which sits on top of the mould for a short time before being removed for the next stage of formation. The parison is then formed by either a blow and blow or press and blow process. After the parison is formed, the blank mould opens and it is held upright by its neck,but upside down, in the neck ring mould. The parison is rotated 180° so that it is now the right way up (i.e. with the rim at the top) and transferred to the final blow mould using the neck ring where it is blown into its final shape via a blow head. During the transfer of the parison from the blank mould to the blow mould, the outer surface of the glass reheats due to radiation

from the bulk of the parison which reduces the temperature gradients in the glass. The neck ring is then returned to the blank mould side of the machine to allow final blowing and the formation of the next parison to take place simultaneously. Both the blank and blow mould need to be cooled so that when they open and the container is released, the article will be rigid enough to hold its shape. After the container has been removed from the blow mould with take out tongs, it is transported to the lehr via a conveyor belt where it is annealed to remove any residual stresses before use.

## 1.2.2 Blow and Blow Process

A schematic of the blow and blow process can be found in Figure 2. If the container is made by the blow and blow process, the gob is loaded into the blank mould via a funnel and fills the ring mould where the mouth and neck (typically circular) of the container is formed. This is assisted by blowing compressed air through a baffle head placed on top of the funnel (settle blow). The head and funnel are then removed and the head is replaced directly onto the blank mould to produce a seal. The preformed body of the container is then formed by 'counter blowing' from the base of the blank mould to form the 'parison'. Heat is removed from the glass surface as it touches the relatively cool blank mould. The parison then is transferred to the final blow mould as described previously.
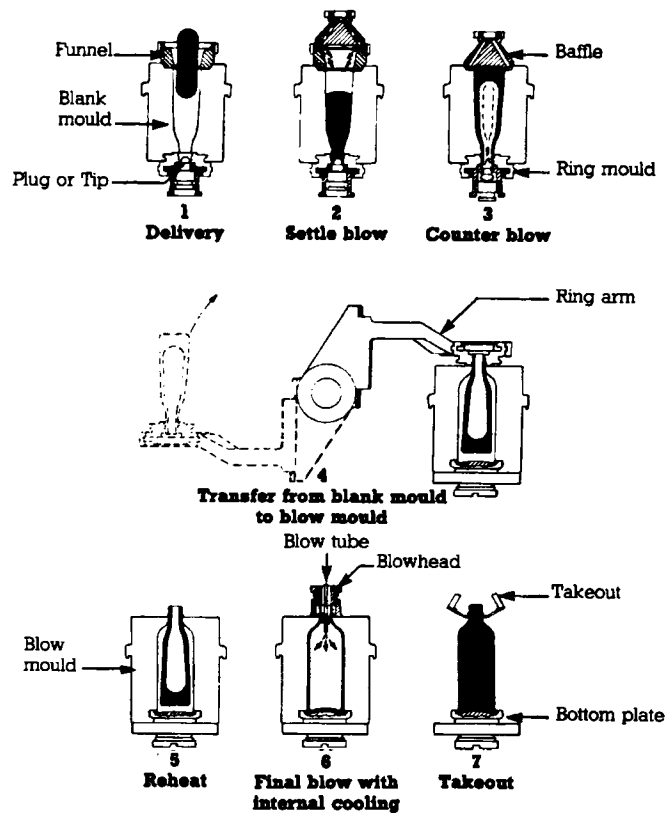
Figure 2: The I. S. Blow and Blow Process [Glass Manufacture- module 19].

During parison forming, only the outer surface is in contact with a foreign material (i.e. the blank mould and any mould lubricant which may have been used). Therefore it is only the outside of the container which can be damaged by contact with a metal surface. In theory, the inner surface should be 'pristine' as it has had no material contact. In practice, however, the blowing air is not pure, being contaminated with dust from the atmosphere even though it has been filtered. Containers made by the blow and blow process are therefore 2 - 3 times stronger on the inner surface than that of the outer surface [Evans & Davidge_1971], reaching strengths greater than 1GPa [Rawson_1988]. However, with the production of thinner walled containers, the effect of damage to the inner surface

of the container has been found to affect the general strength of containers with fracture often originating from damage to the inside surface.

The glass distribution of containers made by the blow and blow process can be uneven. The distribution of glass in the wall has been found to be affected by factors such as the gob temperature, blank mould temperatures, machine timings etc. [Foster_1984]. The variability in wall thickness is caused by temperature differences in the blank mould during forming with the area where the gob first hits the mould being the hottest. Hotter parts of the parison will be less viscous and will stretch more on the final blow than cooler parts during the final blow causing differences in the thickness of the container wall. As the wall thickness distribution using this process is difficult to control, containers formed need to be made with relatively thick walls to ensure that the thinnest part of the bottle meets the customer's specifications.

## 1.2.3 Press and Blow Process

When first developed, the press and blow process was limited to the manufacture of wide mouth containers, such as jars, but with modern techniques, such as narrow neck press and blow (NNPB), it can now be successfully used to make items such as bottles. A schematic diagram showing the press and blow process can be found in Figure 3.

In the press and blow process, a central metal plunger is used to form the central cavity in the parison and ensure the neck ring is properly filled and formed. The

gob enters the blank mould as before with the plunger in the load position via a funnel. The funnel then moves away and is replaced by a baffle. The plunger then rises and presses the glass into the shape of the blank mould to form the central cavity. The plunger is then fully retracted and the baffle is removed. The blow mould is then opened and the parison is transferred to the final blow mould.
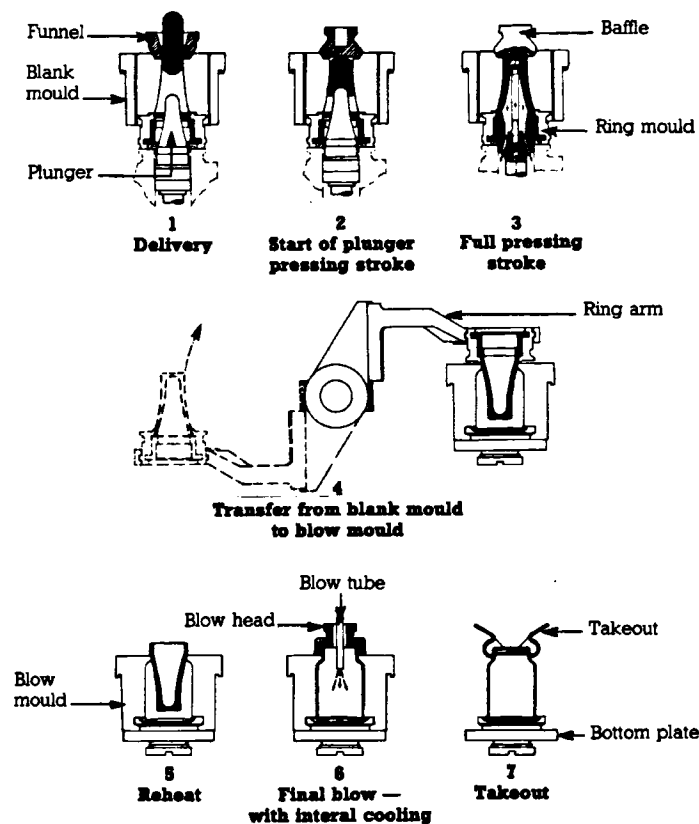


**Figure 3: The I. S. Press and Blow Process [Glass Manufacture_module 19].**

Parisons made by this process have the possibility of contamination on both surfaces due to material contact and, on the outer surface only, by mould lubricant pick up. Impurities on the plunger surface could give rise to defects on the inner surface of the mould.

The press and blow process has a number of advantages including enabling the central cavity of the parison to be made to an exact shape. This type of manufacturing process can therefore be used to produce containers with thinner walls (enabling lightweighting) as the control of the wall thickness in the parison is much improved [Edgington_1986]. The variations in gob temperature, blank mould temperature etc. do not affect the glass distribution in the parison in the press and blow process (which is true of the blow and blow process); glass distribution is controlled by the diameters of the plunger and blank mould, which are constant throughout the process. Assuming the customer requires a bottle of minimum wall thickness 0.8mm, a bottle made by the blow and blow process should have a wall thickness of 2mm whereas one made by the NNPB process should have a wall thickness of 1.33mm [Griffel_1987].

## 1.2.4 Mould Lubricants and Surface Treatments

Mould dopes, or lubricants, are universally employed throughout the glass container industry to lubricate the flow of glass in the mould and help prevent sticking. In many forming processes, the lubricant is applied manually to the mould surface using a cotton 'swab' on a metal handle. This process is potentially hazardous and therefore essential work is being carried out to eliminate that the use of manual mould lubrication. A major project has just been completed at British Glass Technology involving many of the major container manufacturers and support industries on the "The Elimination of Manual Lubrication of Forming Moulds" [1994-1997].

The majority of mould lubricants used consist of graphite with minor additions, such as sulphur, in a mineral oil or grease carrier. Any product which contains a sulphur product however has been reported to attack the mould surface which, over time can produce surface defects on the glass [Edgington 1995]. Water borne lubricants have been recently introduced in the glass container manufacture with varying amounts of success due to the rapid evaporation of water during use; rapid evaporation of the water in water borne mould lubricants has been found to result in blocked tubing in some automatic spraying processes although the results are generally good when applied manually.

An investigation has been carried out to ascertain the effect of sulphur containing hydrocarbon lubricants on the mould surface to determine whether surface corrosion was promoted or retarded. It has been shown that a flaky layer of between 1 - 10$\mu$m thick was formed on the mould surface after use which did not appear to enhance any corrosion [Golden_1983]. Graphite based mould lubricants are thought to work due to conversion of the carbon into $CO$ and $CO_2$ at normal forming temperatures which prevents sticking of glass to the mould during use [Meichel_1990].

There has been an increasing trend towards the use of some form of permanent coating on the working surface of mouldware, such as nickel or chromium. This has been found to increase the service life of moulds by up to 10 - 12 times [Orlov_1977].

Mould precoats have been shown to aid the production of containers. These precoats are applied to the working surface of the mould prior to use and have been found to reduce the amount of manual swabbing needed.

## 1.3    Moulds and Handling Equipment

Several review articles on mould materials and glass handling equipment exist in the literature [Ensor_1970, 1978, 1990] which give detailed reasons for the use of certain materials at a particular time. These reviews identify a number of properties needed for a good mould material. The preferred material properties are as follows:

- good machinability;

- high thermal conductivity;

- low thermal expansion;

- resistance to cracking at the glass contact surface;

- resistance to scaling and oxide formation;

- resistance to wear, abrasion and attack from glass volatiles;

- ability to produce a good surface finish;

- small grains with a uniform metal structure and graphite distribution;

- resistance to thermal cycling and the ability to hold its shape and not warp at the temperatures required by the process and

- low cost.


Although it does not totally satisfy all the requirements, both blank moulds and blow moulds are most commonly manufactured from an easily machinable, ferritic

grey cast iron. Other materials used include alloyed cast iron, high alloyed steels, chromium, nickel, copper and aluminium alloys and carbon.

The working surface of a cast iron mould changes substantially during the manufacture of glassware. After time, the mould gains a thick oxide layer, the morphology of which has been found, in the past, to be revealed on the resulting glass surface [Giegerich_1953, Merchant_1963]. The glass, however, did not appear to touch the complete mould surface, but only partially enter depressions of a sufficient size. This indicates that the surface finish of the mould could have a direct effect on the surface finish of the glass article made. It has also been shown that the oxide layer produced on the mould surface during use reduces the heat transfer from the hot glass to the mould [Coney et al., B.T.N. 179_1973]. The mould surface has been found to become increasingly rough with use. It has been suggested that the reason for this is due to rapid oxidation of the graphite flakes at the working surface which are destroyed during use [Kolotilkin & Volchok_1983]. Another possible theory for the increased roughness of the mould which has been postulated is that grain boundary attack or erosion in use causes 'plucking' of metal particles from the mould surface [Moder & Wasylyk_1985]. It is therefore essential that the working surface of the mould is kept in good repair and needs to be inspected and repaired regularly.

Cleaning of the moulds is carried out regularly using a shot peening technique to remove the thick lubricant layer which accumulates over a long production run. Defects are universally repaired using a nickel welding technique.

Nickel and chromium based alloys are known to be good at releasing from glass in container manufacturing processes, but are expensive. Plungers often get very hot during a typical forming cycle and therefore should be made from a material that will withstand the increased temperature without the glass sticking to the material. Plungers for use in the press and blow process are therefore commonly made from mild steel with a nickel - chromium based coating applied to the working surface.

It has been found that the harder the handling materials used with newly formed glassware, the greater the strength loss in the final container. It is thought that this is mainly due to abrasion with the harder the material giving the greater strength loss [Budd & Vickers 1990].

## 1.3.1 Mould Manufacture

The following sections introduce the manufacturing processes (including methods used for mould cooling) for the major types of mould equipment used in the glass industry for the manufacture of hollow-ware.

### *1.3.1.1 Cast Iron Moulds*

Although it does not satisfy all the requirements for the ideal mould material (see the list of requirements in section 1.3), the majority of mouldware is made from grey cast iron because of its ease of machining and low relative cost. Cast iron mould equipment is usually made using a foundry-based sand casting technique and then machined to the correct size, shape and tolerance.

Cast iron is melted using the raw ingredients of:

- pig iron;

- iron of known specification and

- glass house waste (i.e. old glassmaking moulds).

The carbon equivalent value (CEV) of the molten metal is tested, and when correct, the molten metal is poured into a ladle where the slag is skimmed off.

Green sand moulds (i.e. the sand moulds in an unfired state) are made by initially placing a wooden pattern, with the required final shape, into a steel casing block. The whole mould is made in two halves. The pattern is dusted with a release agent to stop the sand sticking to the pattern, ensuring the correct cavity shape is left after the pattern is removed. A mixture of sand, coal dust, water and clay is poured into the casing to fill it. The mould is then vibrated (rough tamping) to ensure the sand mixture fills all the gaps and is then pressed. The whole assembly is then vibrated again and the pattern is removed from the bottom. It is generally accepted that large coarse metallic grains at the working surface of the cast iron mould enables fast oxidation and degradation of the surface which is undesirable. Therefore, on manufacture, the inside face of the cast iron mould is cast against a cool blank to form a fine grained chilled structure. To form the required working surface of the final mould, a 'chill' is used which is left in the sand mould. A 'chill' is a piece of cold metal onto which the molten iron is cast; the resulting structure of a metal that has been cast against a 'chill' will be that of fine equiaxed crystals.

The two halves of the sand mould are fitted together to form the entire cavity and channels are made, by scooping out the soft sand mixture, to form the runners and risers of the casting. The runners and risers are used to enable the molten metal to reach all the areas of the cavity without the formation of bubbles. The mould cavity is then filled with the molten cast iron via an overhead ladle. After the iron has solidified, the sand mould is removed using a knock out process involving a vibrating platform over a grille. The casting and chill stay on the grille, whilst the sand goes through the holes and is transported back to the sand mill. The cast runners and risers are then removed from the casting and the remaining edges are filed smooth.

The iron which is cast directly against the chill has a martensitic structure. The final casting however requires the surface to have a fine grained ferrite and pearlite structure at the working surface of the mould. This structure is achieved by annealing at 950°C for 6 hours. The temperature is then slowly ramped down until it gets below 490°C. Below 490°C, the structure does not change any further (i.e. 490°C is the subcritical temperature) and the casting is then air cooled. The optimal structure of the iron is engineered to be approximately 5mm back from the contact surface to allow for material to be removed in machining.

The cast moulds are then roughed out to their final shape including any cooling fins. The contact edges of the mould are welded using a nickel welding technique to strengthen them. Any holes required for cooling (see section 1.3.2) or vacuum

assisted forming are then drilled into the mould. The moulds are then often finished by fine grinding and polishing of the contact surface.

### *1.3.1.2    Aluminium Bronze Moulds*

Aluminium bronzes are commonly used in areas where thermal conductivity is of primary importance such as neckrings and bottom plates. The advantage of this type of material over cast irons is that they exhibit approximately three times the thermal conductivity. The glass industry is moving towards the increased usage of these materials in other areas, but at present they cost approximately 2.5 times more than cast iron.

Aluminium bronzes are cast into a resin bonded sand mould which gives a less permeable mould than the green sand mould used for casting cast iron. Green sand moulds are used when casting iron as the combustible products in the sand mixture aid the process. When casting with aluminium bronzes, if green sand moulds were used, the final casting would be full of holes as bronzes react with the combustible gases formed. Aluminium bronzes do not need to be annealed after manufacture.

## 1.3.2 Mould Cooling Methods

During the manufacture of glass containers, the temperature of the mould increases dramatically on contact with the hot glass. The temperature of the inner wall surface in the cavity rises and falls during each production cycle. As the heat is conducted outward through the wall of the mould, there is a point where the effect of any cooling maintains a steady temperature within the body. Therefore,

after a time, the temperature within the mould reaches an equilibrium in which the temperature rises no further, but cycles slightly during production.

There are many methods employed to aid in the cooling of moulds during container production. The simplest of these involves the use of cooling fins on the outside wall (both horizontal and vertical) at which cool air is directed. Other methods used include the use of vertical mould cooling such as Vertiflow (developed by Emhart Ltd.) where holes have been drilled through the body of the mould close to the working surface (in the longitudinal direction) and cool air is passed through them.

The amount of cooling used in each production cycle is critical. If the working surface of the cavity is allowed to fall too low, it could have one of two effects. The first of these is the glass acquires a rippled wavy surface which is known as 'orange peel', i.e. a chilled surface appearance. The second is the appearance of small cracks at the glass surface. Conversely, if the temperature at the mould surface is allowed to get too high, the glass may stick to the mould.

The temperature at the plunger surface in the press and blow process, and more specifically the narrow neck press and blow processes is fundamental to its success. It has been shown that non-uniform cooling of plungers causes hot bands to be produced at the working surface [Penlington & Sarwar_1995]. Such bands have been shown to affect the hardness of the material and adhesion temperature that results in rapid uneven wear at the glass to metal contact surface [Penlington

et al._1995]. Three main types of wear mechanism have been identified in narrow neck press and blow plungers [Penlington et al._1993a]. The main form of wear has been identified as occurring on the taper. Wear at the tip has been attributed to glass adhering to the surface surrounded by areas which have been found to be richer than expected in silicon and oxygen [Penlington et al._1993b]. The appearance of silicon rich areas at the tip suggests that wetting of the surface is a chemical and not a mechanical or temperature related phenomenon. The final mechanism identified was due to the formation of an oxide surface on the inside bore of the plunger which affects its temperature characteristics and hence reduces the cooling effect of the internal plunger cooling.

## 1.3.3 Paste Moulds

Paste moulds do much less damage to the glass surface during manufacture than traditional cast iron moulds and are commonly used for making items such as tableware and lightbulbs. The use of this type of mould is restricted to the manufacture of thin walled items due to the way in which the moulds are constructed and therefore operate and to the limited amount of heat which can be removed when forming by this process. In a process that utilises paste moulds, either the glass article is rotated or the mould rotates around the article, which eliminates mould seams on the final article.

Paste moulds are made from cast iron in a similar way to a traditional container mould (see section 1.3.1.1). A relatively soft and porous carbon lining is applied to the inside surface of the mould. This is achieved by initially applying a thick

## 1.3.4 Carbon-Carbon Composites

Composite materials can be made up from particles or fibres held in a matrix, which will result in a material with tailored properties. There are many types of composite materials available which range from glass fibre reinforced polymers to particulate composites such as concrete.

Recently, carbon-carbon composite materials have been developed which use carbon fibres in a carbonaceous matrix. Even though the reinforcing fibre and the matrix are made from the same material, the properties of the composite material produced can be tailored by changing parameters such as the fibre matrix, type of reinforcing fibre, fibre volume and the matrix structure. In glass container manufacture, carbon-carbon composites have been used during hot end handling of hot glass articles, e.g. for glass contact inserts in take out tongs [Budd & Vickers_1990]. However, carbon-carbon composite materials may have a use within the glass container industry to produce self lubricating mouldware.

### *1.3.4.1    Fibre Type*

Carbon fibres can be produced by a number of different routes. The different production routes used to produce the fibres will affect such things as the thermal and mechanical properties. Two of the most common carbon fibre types are made using:

1. **polyacrylonitrile (PAN)** precursors are produced from acrylic polymers. Initially, the PAN precursor fibres are thermally stabilised and then oxidised using a combination of stretching in steam and/or air up to a temperature up to

300°C. These processes polymerise the fibre to produce long, stable, cross-linked polymeric chains which can be subsequently carbonised (and/or graphitised) in order to produce the carbon fibres. Carbonisation of the polymeric fibres is then carried out in an inert atmosphere (containing $N_2$ or Ar). Graphitisation of the carbon fibres in an inert gas up to 2800°C improves the orientation of the crystallites in the fibre direction and also the resistance to oxidation [Gerber_1994].

2. **pitch** precursors are produced from asphalt, coal tar, petroleum or PVC, which are relatively cheap raw materials. The raw materials are converted into pitch precursors by heat treatment. The precursors are then made into fibres by extrusion and spinning under tension to align the crystallites to give the fibres the desired directional properties. The pitch fibres produced are then converted to carbon, or graphite, by a carbonisation stage (at 1000-1500°C) and then graphitisation if required (at 2000-3000°C). The carbon fibres produced using this route are not as uniform or reproducible as those prepared using the PAN route and will have lower tensile strength. Carbon fibres produced using pitch precursors offer improved thermal conductivity over those produced using PAN precursors and as such may be better for use in the glass container industry.

### 1.3.4.2      Fibre Matrix

The way in which fibres are oriented and the proportion of fibres in the matrix will influence the mechanical properties of the final composite material. An increased proportion of fibres in the matrix will result in stronger final composite materials.

Oxidation of carbon-carbon composites in an oxygen containing atmosphere starts at approximately 350°C (450°C once it has been graphitised). The resistance to oxidation can be improved with the addition of a protective coating such as silicon carbide.

## 1.4 Glass to Metal Contact

Parameters such as the temperature at which adhesion between the glass melt and mould material occurs and the wetting properties of the glass melt on the mould substrate will affect the forming parameters required during the formation of glass containers.

### 1.4.1 Adhesion

Adhesion occurs between glasses and metals once a certain temperature has been exceeded. It is therefore necessary to operate container moulds below this temperature to ensure that the glass does not stick to the mould. If the sticking temperature of the tool used is exceeded, glass will adhere and, on separation, a small amount of glass may be plucked from the container surface which could produce a critical fault. If the contact temperature between the glass and metal is too low, damage could occur to the glass surface in the form of mechanical damage resulting in the weakening of the surface of the finished product, or chilling thus producing a poor surface finish [Kroptov_1975]. It is therefore better to produce bottles at temperatures closer to the sticking temperature. It has been suggested that adhesion occurs during container forming due to the chemical bonding between oxide layers of metal and non-bridging oxygens in the glass

[Pask & Fulrath_1962]. It has also been postulated that sticking occurs if the contact temperature becomes high enough to reduce the viscosity of the liquid at the contact interface and hence overcome the surface tension of the liquid. The molecules of the liquid therefore move close enough to the atoms (or ions) of the solid for Van der Waals forces to come into play [Manns et al._1995]. However, more irreversible chemical reactions may also occur with the exchange of oxygen.

Some of the most comprehensive work in this area has been carried out some years ago by Fairbanks et al. [Kapnicky et al._1949, Dowling et al._1950, Dartnall et al._1951, Fairbanks_1964]. In this case, the work has investigated the effect of different metals, surface finishes, glasses and the use of mould dopes and coatings. A series of metals was examined to investigate the effect of metal composition on the adhesion temperature. As the level of carbon in the steel was increased, the sticking temperature achieved decreased. The highest sticking temperatures were obtained for nickel, tungsten, Monel (an alloy containing nickel, copper, iron and manganese) and carbon. The effect of nickel on increasing sticking temperatures has also been reported elsewhere in the literature, although nickel coating on cast iron has been shown to decrease the sticking temperatures achieved [Oel & Gottschalk_1967]. It has been suggested that the highest sticking temperatures can be achieved for metals which are resistant to oxidation [Winther & Schaeffer_1988].

The composition of the glass has also been found to affect the sticking temperature [Smrcek_1967b], although other published work has shown this not

to be true [Abramovich & Kalashnikov_1981]. The latter work, however, only compared the effect of two different glass compositions. In common with all the work on adhesion, sticking temperatures are ill defined and each group of researchers has defined the sticking temperature differently therefore direct comparison of their work is difficult.

The use of lubricants and mould dopes on metal surfaces has been shown to increase the sticking temperatures, as would be expected [Smrcek_1967a]. It has been suggested that the viscosity of the glass at the glass-to-mould interface affects the temperature at which the glass adheres to metal with processing parameters such as the time of contact and pressure affecting the sticking temperatures achieved [Smrcek_1967c]. This would indicate that the heat transfer properties are important in avoiding sticking between glass and metal during forming.

## 1.4.2 Wetting

Wetting is essentially how a liquid spreads on a solid substrate, in this case how a glass melt spreads on metals. This property is therefore important in the manufacture of glassware and will affect, for example, the way in which a gob loads into a blank mould.

If the glass does not wet the metal at all, the glass will form droplets on the metal surface as the surface tension is minimised. If the glass, however, wets the metal substrate, it will spread out to form a thin film. A common way of describing how

a liquid will wet a solid is to examine the interfacial contact angle which decreases as the degree of wetting increases.

The wetting behaviour of glasses on metals has been associated with the stability of the metal oxide. Experimentation on the platinum group metals has shown that platinum is wetted more by glass than palladium and iridium and markedly more than rhodium [Copley et al._1975]. It was suggested that the inclination of a glass to wet a metal could be determined by the demand of the metal substrate atoms to form bonds with non-bridging oxygen atoms in the melt [Copley & Rivers_1975]. The degree of wetting has been shown to increase as temperature increases. It has been found that glass preferentially deposits at discontinuities in the metal surface such as grain boundaries and residual cracks [Copley et al._1973]. This would indicate that the melt would also preferentially attack the metal at grain boundaries.

The surrounding local atmosphere during the formation of glass containers has been shown to affect the wetting characteristics of the glass melt in addition to the oxidation state of the metal substrate. For example, it has been found that the use of an HCl atmosphere during forming affects the wetting characteristics of the glass, which in turn increases the sticking temperature [Winther & Schaeffer_1988].

## 1.5   Glass Surfaces

### 1.5.1  Strength

Mechanical damage during the manufacturing process used can affect the condition of the glass surface which has in turn been found to affect the strength of the article. It has been suggested that microcracks occur on the glass surface due to mechanical damage which accumulates through the life of the article during manufacture, handling and service [Ernsberger_1970]. Ernsberger used a lithium ion exchange process to reveal the microcracks to the naked eye. The lithium ions used in the exchange are smaller than sodium ions in the glass. On exchange, the surface of the glass is put in tension therefore extending any surface flaws to such an extent that they can be easily seen [Ernsberger_1967]. Flaws on the surface act as stress concentrators which in turn lower the strength. Etching glass surfaces in hydrofluoric acid has been shown to increase the strength [Ryabov & Fedoseyev_1968]. This strongly suggests that glass articles are covered in microcracks which are removed on etching thereby increasing the strength.

The inside of a container made using the blow and blow process should be theoretically pristine as it will have had no contact with any foreign bodies as it is blown using filtered compressed air. In reality, however, this is not the case and dust and dirt particles have been found to be introduced into the blowing air. It has been found that the strength of such a container after contact with abrasive particles both at ambient and elevated temperatures is inversely proportional to the hardness of the scratching material [Bourne et al._1984]. Therefore, the blowing

air needs to be kept as clean as possible to maximise the strength of the final article.

Even with no visible surface damage, there is still a decrease in strength from that expected from theory. This drop in strength is thought to occur due to Griffith flaws although no evidence for such flaws has been detected. It has been suggested that Griffith flaws could potentially be sodium depleted channels formed on the glass surface due to the reaction of the glass surface with water in the atmosphere [Hand & Seddon_1997]. It has been suggested that as these channels are very narrow, as they are on an atomic scale, they have therefore not been detected using conventional methods. One theory on the lowering of glass strength during forming is that the surface of the glass is modified due to the high cooling rate and temperature gradient. Following this argument, it has been suggested that the 'surface damage' is produced on glass surfaces during normal production due to the freezing in of such high temperature structure and the subsequent thermal depolymerisation under the action of rapid cooling [Sil'vestrovich et al. 1970].

A great deal of rather old work has been completed on determining factors which affect the strength of glass. Much of this work has concentrated on pulling fibres or extruding rods under different circumstances to determine the factors which affect the strength of the glass. It has been shown that the strength of fibres drawn in dirty or dusty conditions at high temperatures are considerably reduced [Holloway_1959, Proctor et al._1966]. This is thought to be due to the adhesion of

particles, such as dust, to the glass surface which produces areas of local compositional change and therefore local strength differences. A decrease in strength has also been found when the drawing load and temperature were increased [Lynch & Tooley_1957]. Fibres which have been etched to remove surface damage have been found to have increased strengths. The strength of these fibres has been found to decrease with an increase in temperature [Ritter & Cooper_1963]. It has been suggested that reasons for this could be due to devitrification or the elimination of surface water.

The effect of shear stresses at the surface during forming has been shown to affect the strength of glass rods. It has been found that glass rods which have been extruded through a stainless steel former have lower strengths to those extruded through graphite [Dengel & Roeder_1991]. Crack formation has been found to occur in glass articles at temperatures above the glass transition temperature $(T_g)$ when it is deformed at high speeds such as during pressing [Williams_1989].

How a glass article is stored after manufacture has also been found to affect the strength. If the article is stored in a humid atmosphere, the glass strength may increase [Brearley & Holloway_1963]. It is thought that this is due to the rounding off of the crack tips by water over the period of storage. However, the converse can occur if the conditions are such that further corrosion can occur.

## 1.5.2 Glass Faults

Strength reducing flaws in glass articles can originate from a number of sources throughout the life of the container. Damage can occur at every point along the journey of the container from when the shear blades cut the gob through all stages of the forming process and afterwards by contact with hot end handling equipment [Simpson_1990]. A newly formed container possesses only a minute proportion of its high theoretical strength, i.e. approximately 1% [Vickers_1988, Williams_1985]. This figure can be reduced even further by the introduction of flaws by contamination of the glass surface or abrasion whilst the glass is still at an elevated temperature.

Glass faults can occur as physical damage to the glass surface or the inclusion of foreign objects in the glass wall. Inclusions can be introduced into glass articles from two main sources. Inadequate reaction in the furnace could result in the inclusion of grains of unreacted batch known as batch stones. The glass melt could react with the furnace refractories resulting in inclusions known as refractory stones. Reaction of batch in the furnace results in the production of a substantial amount of gas. Bubbles can form near the glass surface due to the trapping of reaction gases. These are known as seeds or blisters and have been found to have twice the effect on strength compared with inhomogeneities caused by handling materials [Müller-Simon et al._1994]. Of particular importance, however, is surface damage created by contact with handling materials and other glass articles at high temperature [LaCourse_1987]. This could occur as either surface damage

such as cracking or actual reaction of the handling material with the glass resulting in potentially strength reducing embedded particles.

It has been found that many containers can fail from the inclusion of embedded materials. These materials can often be found to contain silicon and sulphur which originate from the coolants and lubricants used in manufacture [Wasylyk_1991]. One reason for this is that during use, mould lubricants can build up into thick flaky layers on the mould surface over time. Contaminating particles on the glass surface are often produced by the action of pressing pressure plus the surface thermal stresses causing spalling of the mould material. Other work has identified most embedded materials to be either carbon or iron rich which must therefore have originated from the mouldware or handling materials used [Puyane & Rawson_1979, Warren_1973]. Embedded iron particles have been found to have the largest effect on the glass strength. This may be due to differences in thermal expansion properties between the iron/iron oxide and glass. Cracking found around many of these particles was thought to occur due to differences in thermal expansion.

The temperature at which surface damage occurs during the formation of glass articles has been identified as one of the major factors involved in the strength of the glassware produced. Most damage has been found to occur at a critical temperature which is dependent on the contact material investigated [Puyane_1976]. This may be related to properties such as thermal conductivity and thermal expansion.

# 1.6 Aim of Project

## 1.6.1 Introduction

During recent years, the glass container industry has lost some of its traditional business to other materials such as plastics, metal cans and paper. Glass is still, however, a versatile, highly valued packaging material which is often the preferred material for packaging due to its transparency, non-permeability to gases, taste neutrality etc. and is the most suitable for returnable and recyclable containers. Two of the main disadvantages of glass as a packaging material, however, are its low tensile strength and high density. To be competitive in the container market, the glass industry needs to find a way of reducing the weight of each container whilst maintaining its strength.

It has been determined that damage on the glass surface is responsible for the low strengths usually achieved for newly formed containers. There is evidence that the glass undergoes surface damage during the actual forming process due to mould contact, hot glass handling etc. [Simpson_1990]. Therefore, it is important to understand how damage occurs to the glass surface during the formation of glass containers before any steps can be taken to improve the strength of the final article and hence be able to produce a lighter, thinner container.

## 1.6.2 Aims

During the formation of glass containers, there are two main problems which can arise from the contact of the glass melt with the metal forming tool:

- if the contact temperature is too high (i.e. above the "sticking" temperature), the glass melt will stick to the metal tool. On separation, threads of glass may be plucked from the surface to give a range of critical faults, including spikes and 'glass inside'. The formation of critical faults such as these will obviously result in lost production with the possibility of a product recall situation and therefore loss of reputation to the manufacturer and loss of confidence in glass as a packaging material;

- if the contact temperature is too low, the metal tool could damage the glass surface by 'chilling' and mechanical pressure. This damage will result in a weakening of the surface of the finished product and also produce a poor surface appearance.

Unfortunately, only limited amounts of work have been carried out in order to try and understand these phenomena. The main objective of this project has therefore been to try to understand how conditions at the glass-to-metal interface, under pre-sticking conditions, lead to the formation of critical faults which are not fully self healing with a view to reducing surface damage resulting during container formation. The methodology has been to simulate glass-to-metal pressing during container production by means of an experimental pressing rig. The pressed glass and metal surfaces have been investigated via a range of imaging and analytical techniques.

## 1.6.3 Thesis Outline

This thesis has been structured as follows:

Chapter 1, **Introduction**, presents a background to the field, including the basic concepts involved and introducing relevant previous work.

Chapter 2, **Experimental Procedures**, presents the way in which the experimental work has been carried out. The procedures introduced include details on how both glass and plunger samples (both cast iron and carbon-carbon composite) have been made. An introduction to the basic operation of the analytical techniques used to examine the specimens (i.e. scanning electron microscopy, x-ray photoelectron spectroscopy and atomic force microscopy) is presented including any special sample preparation techniques employed.

Chapter 3, **Results**, presents the experimental results found using scanning electron microscopy, x-ray photoelectron microscopy and atomic force microscopy for both cast iron and carbon-carbon composite plungers (and the glass samples produced). A short survey of current industrial practice used in glass container manufacture is also presented.

Chapter 4, **Discussion**, discusses the results for both cast iron and carbon-carbon composite plungers presented in Chapter 3 and attempts to relate the findings to the background ideas introduced in Chapter 1.

Chapter 5, **Conclusions and Future Work**, presents the conclusions gathered from the experimental work carried out during this project. Possible ideas for

future work to provide answers to further questions raised by the results presented here are also discussed.

.

**Figure 4: The present experimental pressing rig at British Glass Technology used to make glass samples with controlled parameters.**

**Figure 5: The press head on the experimental pressing rig at British Glass Technology just after forming a glass sample.**

Different glass container manufacturers use different production parameters (i.e. mould temperatures, production speed etc.) depending on the type of ware being made, thus it was important to cover all possible scenarios. Modifications were therefore made to the original pressing rig design to allow investigation of the effect of contact time, contact temperature, pressing force, plunger material and different atmosphere on the pressed glass and plunger contact surfaces. A schematic diagram of the experimental pressing rig can be found in Figure 6 indicating the position of the main components involved.
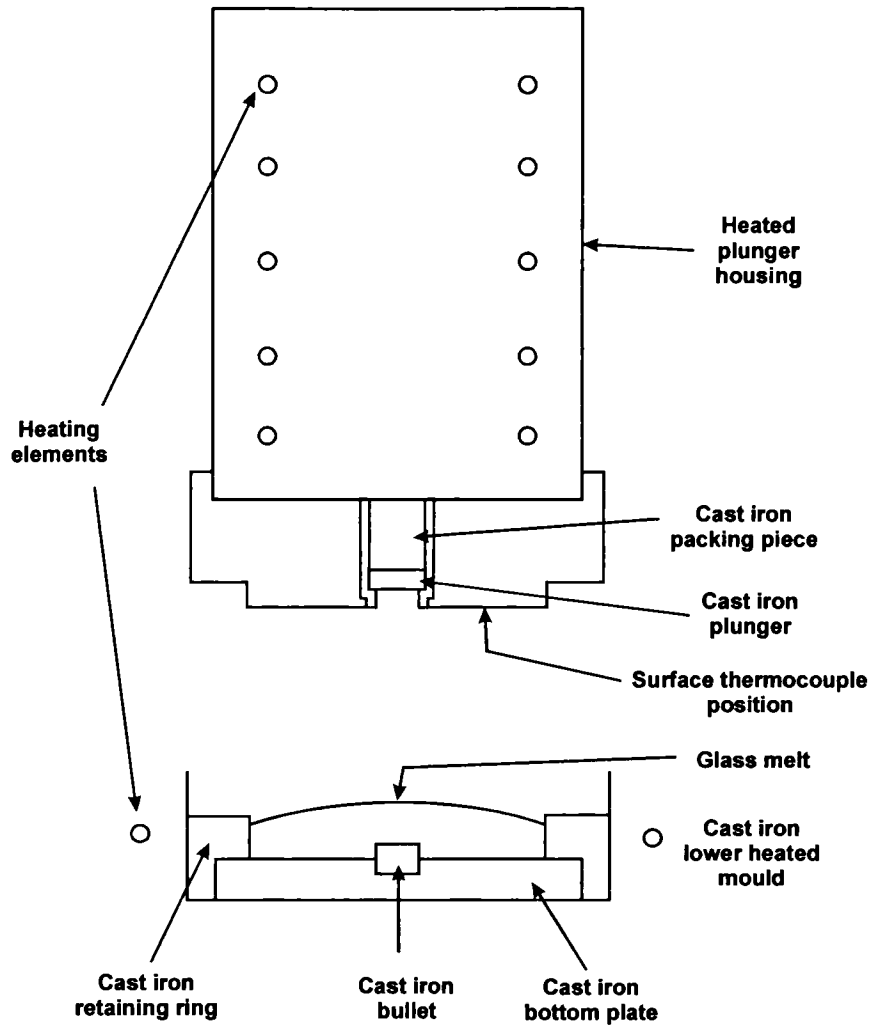
**Figure 6: Schematic of the experimental pressing rig used at British Glass Technology indicating the positions of important components.**

The experimental press consisted of a lower heated mould (made from ferritic grey cast iron similar to that used to make blank moulds) into which the glass melt was poured and a movable heated plunger mounted above it. The plunger was raised and lowered to enable the pressing of the glass samples using a pneumatic cylinder (with a pressure range 0.5 – $10\times10^5$Pa, *Norgren Martonair*) which was operated using a switch mounted on the press. The duration of the glass to metal contact during the pressing cycle was controlled using a timer. The use of the

pneumatic cylinder enabled the pressure during pressing to be easily monitored. The plunger head incorporated a removable plunger piece that enabled the effect of different plunger materials or surface finishes to be investigated.

Cullet of known composition (see Table 2), which had been obtained from a local container manufacturer (*Beatson Clark Plc., UK*), was heated in air in an electric muffle furnace situated next to the experimental pressing rig to 1450±10°C in an alumina crucible with an approximate melt capacity of 500g (99.95% alumina, *University of Sheffield*). Approximately 35–40g of the glass melt was then poured into the lower heated mould. The surface temperature of the cooling glass melt was monitored using an infra-red pyrometer (*Ircon 710S*). The pyrometer used has a filter system that was set up to enable only radiation of 5.5μm - 7.0μm to be detected. This meant that only radiation from the uppermost 0.3 ±0.05mm of the glass surface was detected. When the temperature of the glass surface fell to 950 ±10°C, the plunger was lowered by approximately 150mm and the glass melt pressed for four seconds (±0.2s). Thermocouples, mounted in the bulk mould (K type) and on the surface of the plunger housing (fast response surface thermocouple, see Figure 7), monitored how the glass melt affected the temperatures in both the centre of the lower mould (i.e. the bulk) and the glass contact surface of the plunger. Temperature data collected from the thermocouples and pyrometer, and pressing pressure data collected from the pneumatic cylinder was recorded during each pressing cycle using a digital data recorder. Once pressed, the glass sample was removed from the lower mould, by releasing the

retaining ring, and transferred to an electric muffle furnace using tongs in order to be annealed.
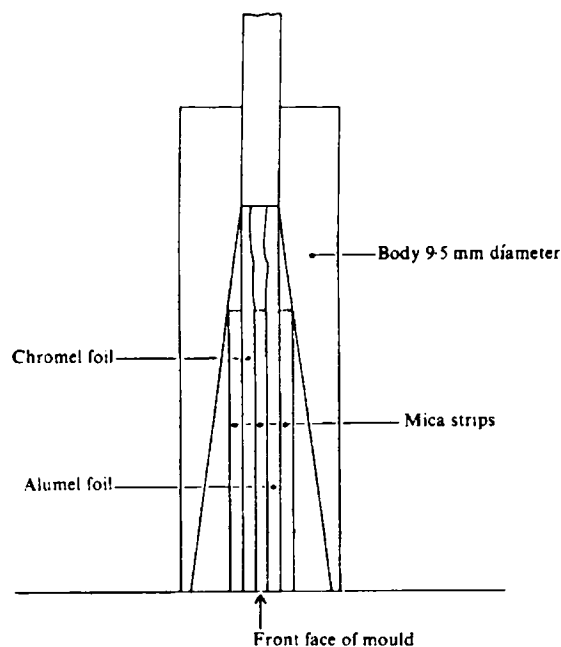


Figure 7: Sectional view of the surface thermocouple used in the experimental rig which was used to monitor the surface temperature of the plunger [Fellows & Shaw_1978].

One of the forming parameters investigated involved varying the initial temperature of the plunger prior to contact with the glass melt. Raising the temperature of the rig, however, resulted in two problems. The first of which was the need to reduce the heat losses from the plunger to ensure that the maximum possible temperature of the rig was reached. This problem was resolved by wrapping an insulating fabric (approximately 1mm thick, made from randomly oriented refractory fibres on an aluminium backing) around the plunger housing which minimised the potential heat losses to the atmosphere. Another problem

observed was that glass samples that had been pressed using initial plunger temperatures over 450°C were found to stick to the bottom plate in the lower mould (see Figure 6). This prevented easy removal of the pressed glass samples from the lower mould. The solution to this problem was found to be to use a commercially available boron nitride based paint which acted as a release agent, therefore preventing the glass from sticking (type E, *Pyrotek, UK*). The boron nitride was suspended in a water-based carrier, and after painting a thin layer onto the bottom plate, it was baked to drive off the water. The best "non-stick" results were found when the baked-on boron nitride paint was roughly polished using a cloth.

Recently, modifications have been made to the experimental pressing rig to allow for vacuum assisted forming, if required. A schematic diagram showing the principle involved in forming a vacuum between the glass melt and cast iron plunger during pressing can be found in Figure 8. These modifications did not affect the way in which the press operated when being used to press glass samples where vacuum assistance was not necessary. The way in which the vacuum assistance operates has been designed to be similar to that used universally by glass container manufactures in the formation of difficult to form parts of objects such as the shoulders of glass jars. A small hole (0.7±0.1mm in diameter) was drilled through the centre of the cast iron plunger and the cast iron packing piece (a hole of 3mm±0.2mm in diameter) which allowed air to be pulled through the system using a rotary pump. Before use, the machined plunger and packing piece were cleaned using 1,1,1 trichloroethane (Genklene, *J. Prestons Ltd., Sheffield,*

*UK*) in order to remove any debris left on the plunger from machining, then heat treated for 30 hours in static air at 470°C in order to achieve a controlled oxide layer. A low pressure of approximately 1mmHg was achieved (measured using an in line vacuum gauge) once the edge of the cavity in the plunger housing came into contact with the molten glass.
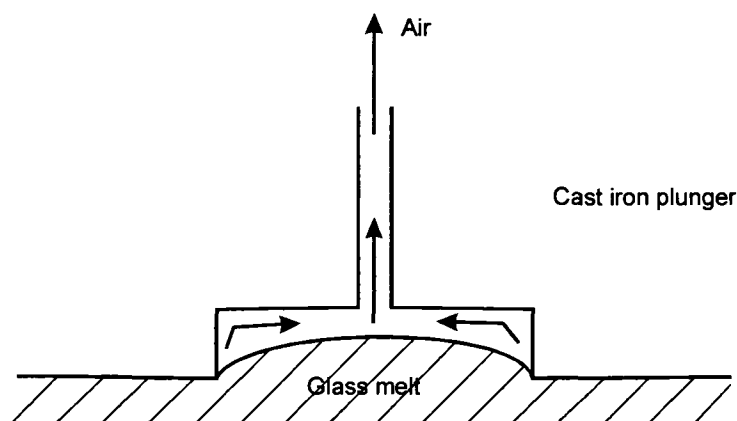


**Figure 8: Schematic diagram showing the principle involved in forming a vacuum between the glass melt and plunger during pressing.**

## 2.1.2 Glass Sample Preparation

Throughout this work the preparation and storage of glass samples has been of utmost importance; the analytical techniques utilised in this research (i.e. scanning electron microscopy (SEM), x-ray photoelectron spectroscopy (XPS) and atomic force microscopy (AFM)) have required samples to be of specific dimensions and the highest achievable level of cleanliness. It was also a requirement that glass samples should be produced so that they could be analysed without the need for additional machining which would reduce the possibility of contamination of the
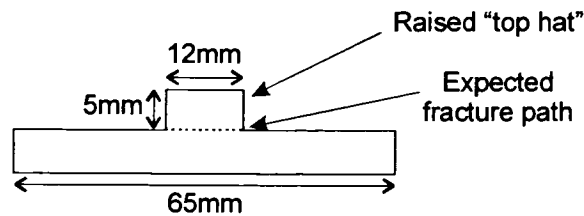
**Figure 9: Schematic diagram showing the initial shape of the pressed glass sample with a raised "top hat" with parallel sides.**

In the subsequent design, the plunger cavity was machined with a 1° taper to reduce the problem of 'keying' into the plunger cavity (see Figure 10). On pressing, the glass did not key into the plunger as before using the modified design.

It was thought that the small radius of curvature where the raised region of the glass sample met the bulk would act as a stress concentrator. This would enable the raised portion of the glass sample to be removed by knocking the point of inflexion with a sharp implement (such as the blade of a screwdriver), therefore removing the need for machining. However, it was found that the raised glass portion could not be removed without fracturing the whole sample.
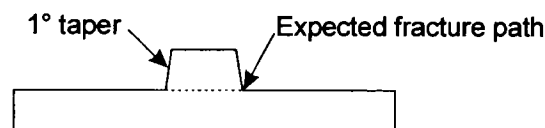


**Figure 10: Schematic diagram showing the second design shape tried for the pressed glass sample with a raised "top hat" with sides having a 1° taper.**

The eventual design utilised a cast iron bullet placed in the centre of the bottom plate in the lower mould before the glass was poured into it (see Figure 11). The "top hat" portion of the glass sample could be removed from the bulk specimen by placing the raised portion in a specially machined aluminium jig and tapping the cast iron bullet with a hammer. The raised portion of the glass sample fractured cleanly from the bulk due to the stress concentrations resulting from the corners of the bullet. The raised portion of the glass sample remained in the aluminium jig giving a sample with a flat base which could subsequently be easily mounted on the necessary stubs which were required for further sample examination.
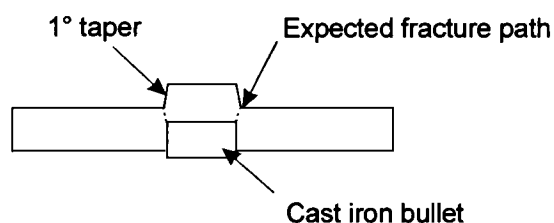


**Figure 11: Schematic diagram showing the final design shape of the pressed glass sample with a raised "top hat" with sides having a 1° taper and a cast iron bullet in the base to facilitate sample removal.**

After fracturing the glass samples from the bulk, the samples were only handled by the outer edges using metal tweezers to prevent surface contamination resulting from handling. The samples were then wrapped immediately in aluminium foil and stored in a desiccator charged with silica gel, until they were needed for examination.

## 2.1.3 Plunger Material Preparation

The level of surface contamination and size of samples of plunger material were critically important in the investigation of the interaction between the glass melt and metal plunger during forming. Naturally, the surface of the plunger material is affected by the glass melt as is the surface of the glass melt by the plunger.

Discs of each of the plunger materials investigated were machined, approximately 15mm diameter and 5mm thick. In this investigation two main types of plunger materials have been used:

1. cast iron - which is typically used in practice as a glass contact material and

2. carbon-carbon composites - which have the potential of being used as glass contact materials.

It should be noted that the carbon-carbon composites were generally easier to machine than the cast iron plungers (i.e. the cast iron used was harder than the carbon-carbon composite material).

### 2.1.3.1 Cast Iron Plunger Material

Ferritic grey cast iron is a material which is commonly used as a contact material in the glass container industry, and as such it was initially important to investigate what happens on contact with glass during normal forming practices.

As previously described in section 1.3.1.1, cast iron moulds are formed by casting against a chill to form a fine grained working surface. As the surface finish of the

mould is different from the bulk, and it was important to try and simulate the container forming process, the plunger pieces used here were made from the working surfaces of blank moulds. A number of blank moulds were therefore collected from a local glass container manufacturers (*Rockware Glass Ltd., Knottingley, UK*), which had been taken out of service due to becoming out of tolerance. Also a number of new moulds which had never come into contact with a glass melt were collected from a local cast iron mould manufacturer (*Birstall Foundry, Guildersome, Leeds, UK*) for comparison purposes.

Discs of the correct dimensions were machined from the working surface of the moulds using a lathe (*British Glass Technology*). The surface of the plunger was then finished using SiC paper by hand grinding unidirectionally using no lubricant for 1 minute for each successive finish until the surface finish which was to be investigated was achieved (i.e. 120, 600 and 1200 grit finishes). The cast iron surfaces were cleaned using 1,1,1 trichloroethane (as described in section 2.1.1) in order to degrease the surfaces and remove any contamination resulting from machining prior to heat treatment.

It was thought to be important to produce a plunger surface which would be similar to that typically found on a blank mould which had been used for a long run in practice. Therefore, before being used to press against glass, the bare, ground cast iron plungers were conditioned in a muffle furnace at 470°C for 30 hours in static air to produce a stable oxide surface similar to that found on a mould after a typical production run. The necessary heat treatment regime had

been established previously at British Glass Technology [Coney et al, B.T.N. 179_1973].

### 2.1.3.2 Carbon-Carbon Composite Plunger Material

Graphite has been reported to have high sticking temperatures with respect to glass and is used in mould lubricants due to its ability to decrease surface friction and aid loading of the gob into the blank mould. This means that it should be an excellent material for use in forming in the glass container industry. However, the mechanical properties of graphite are inadequate for this type of application as it is brittle and has a low wear resistance.

The use of a carbon based composite material (e.g. carbon-carbon composite)) has the potential, theoretically, of being an excellent glass forming material as it exhibits substantially improved mechanical properties when compared with graphite (see section 1.3.4). The properties of carbon-carbon composite materials can be varied widely by altering the fibre architecture, matrix and method of manufacture. The majority of mould lubricants contain graphite, therefore, carbon-carbon composite plunger materials may have the ability to be used as a mould material without the use of additional mould lubrication.

Three different types of carbon-carbon composite plunger materials were sourced from an American manufacturer (*HITCO Technologies Inc., USA*), having already been machined (by them) to the correct shape and dimensions (i.e. discs approximately 5mm thick with a diameter of 13mm), for evaluation for use in glass forming processes in this work and also by British Glass Technology. The

three different composite materials initially evaluated were manufactured using different production routes and therefore had different physical properties, and were as follows:

1. **NF-C T300 Laminate** - This type of material had been made by using a fabric woven from a PAN based carbon fibre in a carbonaceous matrix (see Figure 78 and Figure 79). The specimens sent were approximately ten ply thick. It was reported by the manufacturer that components which have been made using this type of construction would be among the structurally strongest forms of carbon-carbon composite.

2. **PM-C VCB-20 Chopped Squares (aeronautical brake material)** - This type of material is made of a moulding compound of fabric which has been woven from pitched based carbon fibres and subsequently chopped into 5mm squares (see Figure 86 and Figure 87). Pitch fibres offer improved thermal conductivity over PAN based fibres. This type of composite is essentially two dimensional as it is made up from layers.

3. **Carbon Felt** - This is much more of a three dimensional structure than types 1 and 2, with fibres traversing randomly in all directions. Thus there are increased amounts of voids in both the surface and bulk of the material which have been found to be between 50 to 300μm in size (see Figure 93 and Figure 94). The surface voids could therefore produce imperfections in the resulting glass surface. Carbon felt has the possibility of being the strongest (multilaterally) of these three carbon-carbon composite materials due to the three dimensional nature of the structure.

The carbon-carbon composite specimens were used in the experimental press in the as-received state, i.e. with no additional cleaning.

## 2.1.4 Forming Parameters

Forming parameters have been systematically altered to investigate the effects on the surface of the resultant pressed glass sample and plunger surface. The aim was to attempt to quantify any links between the forming parameters and the state of the surface of the samples formed and, to determine the mechanism by which any plunger-to-glass damage occurs during forming.

Most of the pressing parameters were kept constant throughout the investigation. These have included:

- container glass composition;

- plunger to glass contact time of 4 seconds and

- pressing pressure of $2\times10^5$ Pa (which is typical of that used within the glass container industry to form containers).

As mentioned above (section 2.1.3), the type of plunger material used to press the glass samples was varied as follows:

- cast iron from virgin moulds;

- cast iron sourced from used moulds which have been discarded from a container factory and

- carbon-carbon composite materials.

The majority of the investigation has, however, been carried out using cast iron plunger materials from discarded moulds.

The forming parameters which were modified during this investigation (in addition to plunger material) are:

1. cast iron plunger heat treatment;

2. cast iron plunger surface finish;

3. initial plunger temperature;

4. number of glass melt to plunger contacts and

5. vacuum assisted pressing.

The following sections introduce the forming parameters investigated. The details of the experiments carried out will be described further in Chapter 3.

### 2.1.4.1 Cast Iron Plunger Heat Treatment

In practice, after several hours of making glass containers, the cast iron mould will be coated in a thick oxide scale. It was therefore necessary to try and obtain a similar coating on the experimental plunger to simulate the type of glass-to-mould contact which would occur in practice. This was achieved by heat treating the plunger for a minimum of 30 hours at 470°C in an oven in static air (see section 2.1.3.1). In the series of pressings carried out, the majority of glass samples were made using cast iron plungers made from the working surface of discarded moulds (*Rockware Glass Ltd., Knottingley, UK*) which indeed had been heat treated prior to glass contact. In addition, however, some glass samples were also pressed using

cast iron plungers (made from the working surface of a discarded blank mould) which had had no prior heat treatment for comparison purposes.

### 2.1.4.2 Cast Iron Plunger Surface Finish

The surface finish of the cast iron plunger material was varied (for plungers sourced from the working surface of discarded blank moulds only). After machining the plungers to the correct size, the surface was finished by hand grinding using SiC paper. The finishing of the surface was carried out by hand grinding in one direction, to produce cast iron with 'equally' spaced ridges, for 1 minute for each finish. The SiC papers used have finishes of 120 grit, 600 grit and 1200 grit giving approximate resulting finishes of 200μm, 40μm and 20μm respectively. In this investigation, the majority of the pressings were carried out using cast iron plungers ground to a 120 grit finish.

### 2.1.4.3 Initial Plunger Temperature

In the glass container industry, the temperature of the blank mould depends on the type of ware being produced and the speed of manufacture. It was therefore considered important to cover all possible scenarios from cooler than is normal for the formation of containers (i.e. a typical blank mould temperature of 450°C) up to the temperature where glass-to-plunger sticking occurs. However, using the pressing rig, in its present form, it was not possible to achieve sticking temperatures due to excessive heat losses from the plunger to the surrounding atmosphere. The temperatures investigated were therefore varied between an initial pressing temperature of 300°C up to a maximum of 570°C for both cast iron

## 2.2 Analytical Techniques

Several different analytical techniques were employed in order to try to determine the effects of glass-to-metal contact during forming. The techniques used provided information on morphological and compositional changes of both the glass and plunger materials after contact.

### 2.2.1 Optical Microscopy

Optical microscopy of the glass pressed at low temperatures was carried out. It was found that it was difficult to use this technique for glass pressed at higher temperatures due to problems with the depth of focus. It has been found that when pressing glass samples pressed-in dimples were formed, and when using a higher initial plunger temperature these dimples were deeper.

#### *2.2.1.1 Optical Metallography*

Optical metallography has been used to determine the microstructure of the cast iron moulds and to ascertain how the microstructure of the cast iron changes in the mould both after use and across a section of a blank mould from the working surface through to the bulk. Optical metallography was carried out on:

1. a section which encompassed the whole thickness of the wall of the blank mould and

2. plunger specimens made from both used and new blank moulds.

The sections of cast iron blank moulds were successively ground using wet SiC papers of 120, 240, 600 and 1200 grit finish (*Buehler*) on grinding wheels. It was important that all scratches were removed before progressing to a finer grade

paper. The residual surface damage on the surface of the cast iron after grinding was removed by polishing.

Polishing of the cast iron surface was carried out using progressively finer grades of polishing cloths impregnated with progressively finer diamond pastes (6μm, 3μm and 1μm pastes, *Buehler*). The detail of the microstructure could not be seen after polishing therefore the metal surface needed to be etched.

Etching the surface of a polished metal reveals structural details such as grains, grain boundaries and phase differences. Etchants attack the metal at different rates according to such things as crystal orientation or compositional differences. The individual grains and boundaries of the cast iron were revealed by etching in a 2% Nital solution (i.e. $2cm^3$ nitric acid made up to $100cm^3$ with ethyl alcohol) for 5 seconds.

## 2.2.2 Scanning Electron Microscopy

Reflection optical microscopy requires specimens to be very flat in order be able to resolve the surface features, due to the short depth of field, and therefore imposes difficulty for focusing upon rough surfaces. Optical microscopes are also limited to magnifications of between 1 to 1,500X.

Scanning electron microscopy (SEM) is a versatile high vacuum technique which uses a beam of electrons rather than light to image surface features at magnifications of up to 10,000X with little or no sample preparation other than the application of a thin conductive coating. The electron beam interacts with the

however, can only detect elements between sodium and uranium, and hence carbon, oxygen and hydrogen are not accessible.

SEM requires the samples analysed to be clean and conductive. Therefore, the samples were cleaned by rinsing in acetone (reagent grade, *Aldrich*) and drying in air prior to examination. The plunger materials examined were all conductive (even the carbon-carbon composites) and therefore no further preparation needed to take place. The plunger materials were attached to the aluminium stubs used in the microscope using 12mm adhesive carbon discs (containing trace Si, Fe, Mg and Na, *Agar*).

The glass samples, however needed further preparation before SEM examination. The pressed glass samples were first attached to the aluminium pin-stubs using a conductive paint (silver dag, *Agar*). A conducting strip of the silver dag was then painted up the side of the sample to produce a conduction path between the top surface of the sample to be investigated and the aluminium stub beneath. A very thin layer of carbon was then evaporated, under vacuum, onto the surface of the glass samples in order to produce a conductive layer over the whole sample.

## 2.2.3 X-Ray Photoelectron Spectroscopy

X-ray photoelectron spectroscopy (XPS) is a high vacuum technique which may be used to determine the local chemistry of the top few atomic layers of the surface of a specimen. In the current work, a *VG Clam2* spectrometer (combined SIMs instrument) was used.

Photoelectrons, produced by the interaction of a beam of x-rays (in the current work produced from a MgKα source) with the surface of the sample under high vacuum, are collected and analysed to produce compositional information on the surface of the sample. In addition to providing quantitative information on the chemical composition of the surface, XPS can be used to determine the valence and co-ordination type of each of the atomic species present on the surface by examining the shift in position of the characteristic peaks produced. As the electrons produced can only escape from the very surface of the sample, information is only produced from the first few atomic layers of the specimen surface.

As the XPS technique interrogates the near surface of the sample, the cleanliness of the sample is of utmost importance. Normal handling of the sample, however careful, has the potential to contaminate the surface and therefore give erroneous results. It was therefore important to determine a rigorous sample storage and cleaning regime for both the plunger material and glass sample produced; this is described below.

### 2.2.3.1 XPS Sample Preparation Protocol

After pressing the glass samples, the plunger material was removed from the pressing rig. The plunger material was carefully handled, by its sides, using metal tweezers to prevent any contamination from handling (e.g. salts and grease from hands). The plunger sample was then wrapped individually in a piece of fresh aluminium foil to protect its surface from further contamination. Each plunger sample was then placed in a clean glass petri dish which could then be stacked in a

glass desiccator (thus enabling the plunger material and resulting glass samples to be stored together).

After removing the raised portion of the glass sample (i.e. the portion of interest) from the bulk, it was taken from the aluminium jig using metal tweezers (see section 2.1.2). Each glass sample was wrapped individually in a fresh piece of aluminium foil to prevent contamination of the surface and placed in a clean glass petri dish inside a glass desiccator charged with silica gel.

After storage in the dessicator, immediately before XPS analysis, a number of different cleaning regimes were utilised, depending on the specimen:

1.  no cleaning, i.e. 'as received';

2.  rinsing in HPLC (High Pressure Liquid Chromatography) grade hexane (*Aldrich*) to remove non-polar contaminants and HPLC grade methanol (*Aldrich*) to remove polar contaminants - glass samples;

3.  cleaning ultrasonically for 15 minutes in HPLC grade acetone (*Aldrich*) - plunger materials.

Before examination using XPS, the specimens were mounted onto aluminium pin stubs using double sided adhesive tape. Throughout each process where possible contamination might be introduced to the surface, the utmost of care and attention was exercised. Specimens were always handled using metal tweezers (to prevent contamination from handling) and stored in glass (to prevent contamination from any polymeric source).

Non-metallic samples charge up on examination. This causes the binding energy obtained to shift a few eV from their normal position. In order to compensate for this shift, the binding energy results are normalised using the position of the C 1s peak (285eV) which is present on all samples as a thin layer of carbon (usually as a hydrocarbon).

Altering the angle of the analyser to the sample surface can give depth profiling information. A greater take off angle (i.e. the angle of the emitted photons from the sample surface which are accepted by the analyser) corresponds to x-ray photons produced from deeper within the sample, however the depth is dependent on the element. Most of the XPS investigations have been carried out using take off angle of 30°. It should be noted that the angle between the analyser and the x-ray gun was fixed at 30° (i.e. altering the take off angle also altered the angle of the incoming electron beam to the sample surface).

Further information on the experimental parameters used during the XPS experiments including the quantification procedure used can be found in Appendix A.

## 2.2.4 Atomic Force Microscopy

Atomic force microscopy (AFM) is a recently developed desk-top non-vacuum technique which can be used to give high resolution three dimensional information on the surface topography of the sample. The basic principle of operation of the AFM is to scan a very sharp tip over the surface of the sample which results in an

enlarged three dimensional image of the surface (see Figure 12). In the current

work, a *Burleigh Personal* microscope was employed.
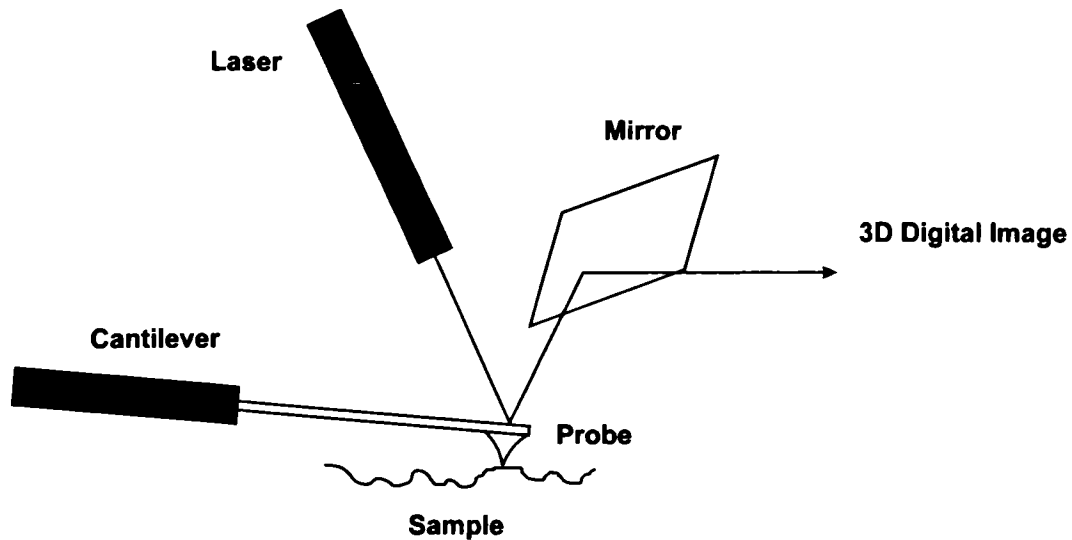


**Figure 12: Schematic diagram of an atomic force microscope.**

The surface of the sample is scanned using a cantilever with a sharp tip at its end. In the current work, 5 minute scans were carried out which gave an intermediate amount of detail. The pyramidal tip (made from silicon nitride) is placed in contact with the sample surface using a very small load (7.1nN). Any deflection of the cantilever due to surface irregularities in the sample surface in monitored by reflecting a laser beam off the cantilever and onto a photodetector. The deflection measured is proportional to the atomic forces. The signal received is then converted using a computer to give an enlarged three dimensional image of the surface of the sample. This technique can be used to give atomic resolution or low magnification surface profiles.

The surfaces of the glass specimens were examined using AFM. The specimens were prepared for examination by rinsing in acetone (reagent grade, *Aldrich*) and mounting onto an aluminium stub similar to that used in SEM.

## 2.3 Summary

This chapter has described the experimental techniques used to prepare both glass and plunger material samples and examine the resulting surfaces after controlled contact has taken place. In addition to the experimental work a short survey of local container manufacturers was carried out in order to assess the variety of mouldware used in practice. The results of this survey, together with the results from the experimental work, are described in Chapter 3.

# 3. RESULTS

The following Chapter presents the results obtained from the experimental work that was carried out to determine how glass and mould materials interact during container forming processes. The experimental procedures used to obtain these results can be found in Chapter 2. The results presented include both cast iron and carbon-carbon composite plungers which were used to press glass samples.

## 3.1  Experimental Pressings

Sections 3.1.1 and 3.1.2 present the results obtained using the analytical techniques described in Chapter 2 on cast glass (control) samples and pressed glass samples. Section 3.1.2 introduces the results from both the glass samples produced using cast iron plungers in the experimental pressing rig and the plunger material itself, whereas section 3.1.3 presents the results using carbon-carbon composite plungers. Each sub-section shows the results from each of the forming parameters that were altered during the investigation. Examples of the effect of the change of forming parameter on both the cast iron plunger material and resulting glass surfaces are presented.

To recap information previously shown in Chapter 2, all samples were pressed with a pressing pressure of $2 \times 10^5$ Pa for a duration of 4 seconds contact time. The initial temperature of the glass melt in all experiments was 950°C before any contact between the glass and plunger material took place. All glass samples were

produced in the ambient atmosphere. The glass composition used throughout the experiments, which can be found in Table 2, was kept constant.

## 3.1.1 Cast Glass

Several discs of glass were made by casting the soda-lime-silica based container glass melt into small cast iron rings (producing a cast that was approximately 15mm diameter and 5mm tall). The cast glass samples were then annealed. This was carried out in order to produce a glass surface that had not come into contact with any plunger material to form the control group of samples. The upper surface of the cast glass control samples (i.e. the surface having no contact with any plunger material) was examined using SEM together with EDS, XPS and AFM, (see sections 2.2.2, 2.2.3 and 2.2.4 respectively).

Before the control samples were examined using SEM, they were ultrasonically cleaned using reagent grade acetone to remove surface contamination. Figure 13 shows the secondary electron image obtained from the surface of a piece of a cast glass control sample. The feature in the lower right hand corner of the micrograph shown in Figure 13 is a scratch that was made using a diamond scribe to aid focusing problems.
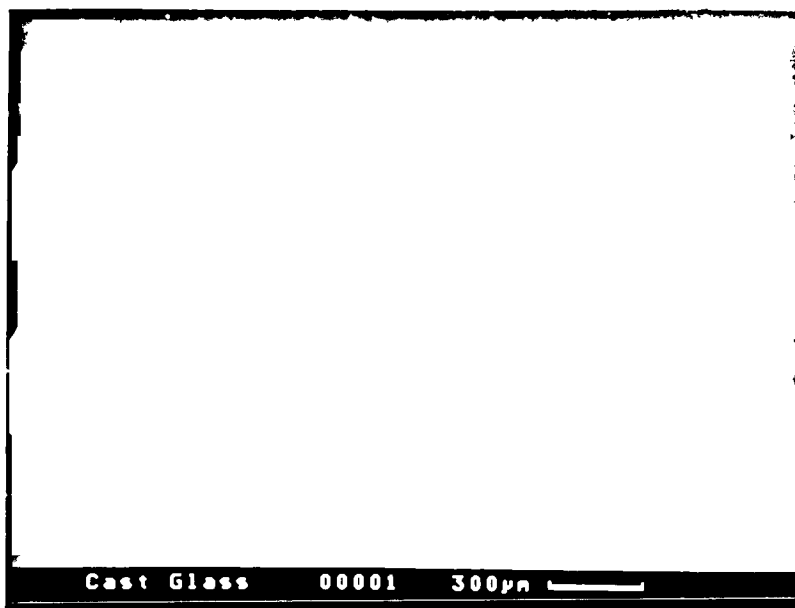
**Figure 13: Typical secondary electron image from the surface of an as-cast, control glass sample.**

It can be seen that the surface of the cast piece of glass is fairly smooth with no visible texture present. Small particles seen on the glass surface, which had not been removed by the cleaning process, were likely to be composed of glass-making batch materials (i.e. Si, Al, Ca, K containing particles were detected). These particles may have occurred inadvertently by cross contamination, as the melt was cast in a laboratory in which these types of particle are expected to be present in the atmosphere (i.e. the furnace room at British Glass).

Figure 14 shows the XPS trace obtained from the surface of a typical piece of control cast glass using x-rays from a magnesium source. The XPS data is presented as a plot of intensity (i.e. number photoelectrons emitted with a specific characteristic energy) versus electron binding energy. Please note that only the

characteristic strongest peaks of each element are labelled. Full details of all the possible peaks detected using XPS are summarised in Appendix A.
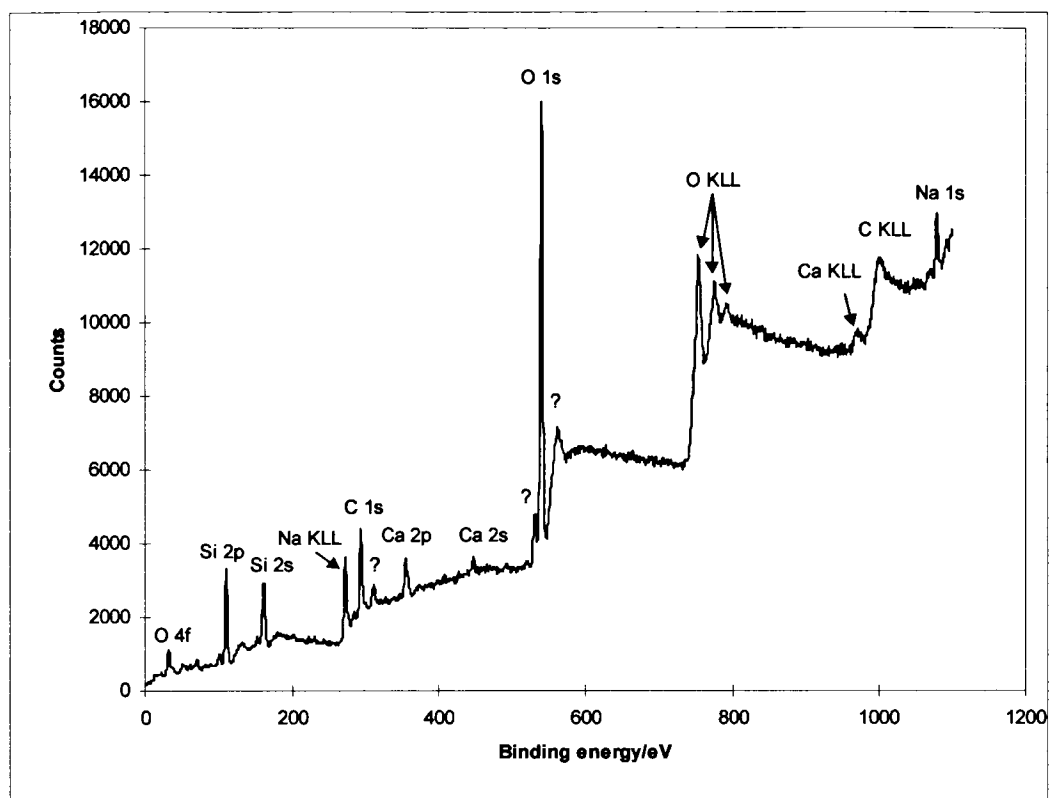


Figure 14: X-ray photoelectron spectroscopy widescan from a piece of a cast control glass sample (take off angle of 30°, using an MgKα source).

Using tabulated data [Briggs & Seah_1990], the XPS peaks were identified and the area under each of the specific characteristic peaks was used to quantify the surface. It can be seen from Figure 14 that the surface of the cast glass is made up from Si, C, Ca, O and Na. This equates to the glass surface being made up from the oxides $SiO_2$, $CaO$ and $Na_2O$. The carbon found on the surface may have occurred either due to a layer of hydrocarbon which is commonly found on most surfaces which have been exposed to the atmosphere, as an artefact of the cleaning

process used or possibly as a carbonate. Table 2 summarises the quantification results of the elemental composition of the cast control glass surface found using XPS as compared to the bulk composition using XRF.

| | Si | C | Ca | O | Na | Al | Fe | Mg | S | K |
|---|---|---|---|---|---|---|---|---|---|---|
| Concentration at the surface / atomic % | 23.2 ±2 | 29.1 ±3 | 1.8 ±0.2 | 45.4 ±5 | 0.5 ±0.05 | - | - | - | - | - |
| (atomic ratio) | (91) | - | (7) | - | (2) | - | - | - | - | - |
| Concentration of the bulk / atomic % | 25.2 | - | 4.4 | 60.6 | 8.7 | 0.7 | <0.1 | 0.1 | <0.1 | 0.3 |
| (atomic ratio) | (66) | - | (11) | - | (23) | - | - | - | - | - |

Table 2: Quantification of the elemental composition of the surface of a typical cast control glass sample using x-ray photoelectron spectroscopy compared to the bulk glass composition measured using XRF, including atomic ratios (i.e. atomic ratio of Si $=100(at\%Si)/\Sigma at\%Si,Na,Ca)$ etc.).

Quantification of the surface of the cast glass surface appears to show that it is deficient in Na, Ca and Si when compared to bulk analysis of the cullet using XRF (which had been converted from weight% of the relevant oxides to atomic %). The XRF data, however, did not include carbon. Carbon is not commonly found in bulk glass samples and as such, the XRF analytical programme used does not take it into account. Atomic ratios of Si:Ca:Na indicate that XPS shows a glass surface depleted in Na and Ca.

Atomic force microscopy of the surface of a cast glass control specimen was carried out in order to determine quantitatively the surface finish. A three

dimensional image of the cast glass surface obtained using atomic force microscopy can be found in Figure 15 with the heights represented by different colours (i.e. black is the deepest through red orange and finally yellow being the highest points).
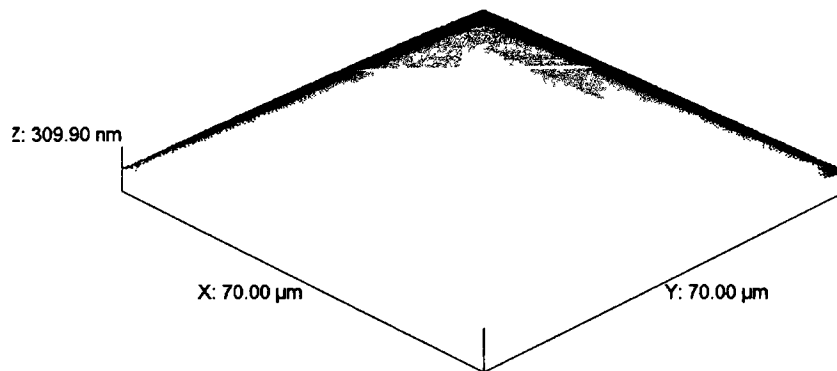


**Figure 15: A three dimensional atomic force microscopy image of a cast glass surface.**

The smooth finish imaged using AFM for the cast glass control surface (Figure 15) can be compared to an image of that of a ground glass surface (Figure 16).
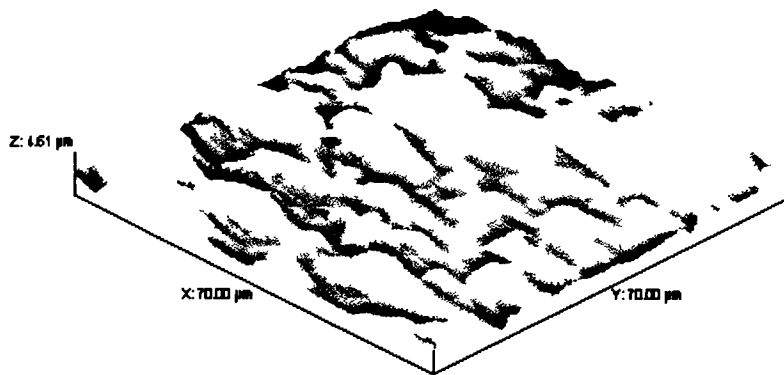
**Figure 16: A three dimensional atomic force microscopy image of a ground glass surface**

It can be seen from Figure 16 that a glass surface which had been ground using a diamond wheel with a 125-micron finish appears to be made up from random peaks (up to 4μm high) and troughs.

## 3.1.2 Cast Iron Plunger Material

The majority of the research carried out has involved investigating the material interaction of a grey cast iron plunger on a soda-lime-silica container glass during glass sample forming using the experimental pressing rig (as described in Chapter 2). The cast iron samples were made using the working surface of a cast iron blank mould in order to try to simulate a similar metal-to-glass contact to that used in practice during commercial glass container production. In particular, the same composition and microstructure of the mould material was employed as used for blank moulds at *Rockware Glass Ltd., Knottingley, UK*.

Before any controlled glass contact was carried out, the cast iron plunger materials were prepared by hand grinding in one direction using SiC paper to give a

measurable, controlled surface finish. SEM examination of the prepared cast iron plunger surfaces was carried out to examine the ground cast iron surface prior to any heat treatment. Figure 17 to Figure 19 show secondary electron images of the cast iron plunger surface with different surface finishes having had no previous heat treatment or glass contact.
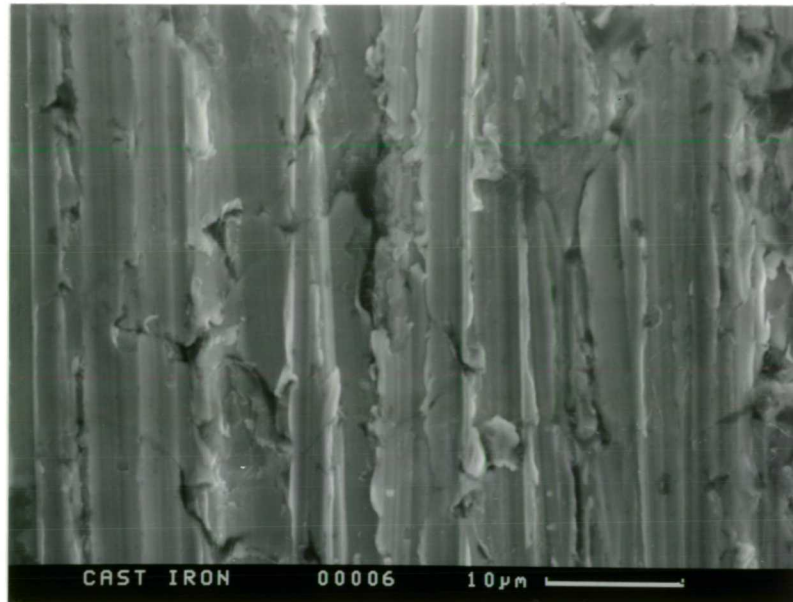


**Figure 17: Secondary electron image of a cast iron plunger surface unidirectionally ground to a 120 grit finish and having had no prior heat treatment or glass contact.**
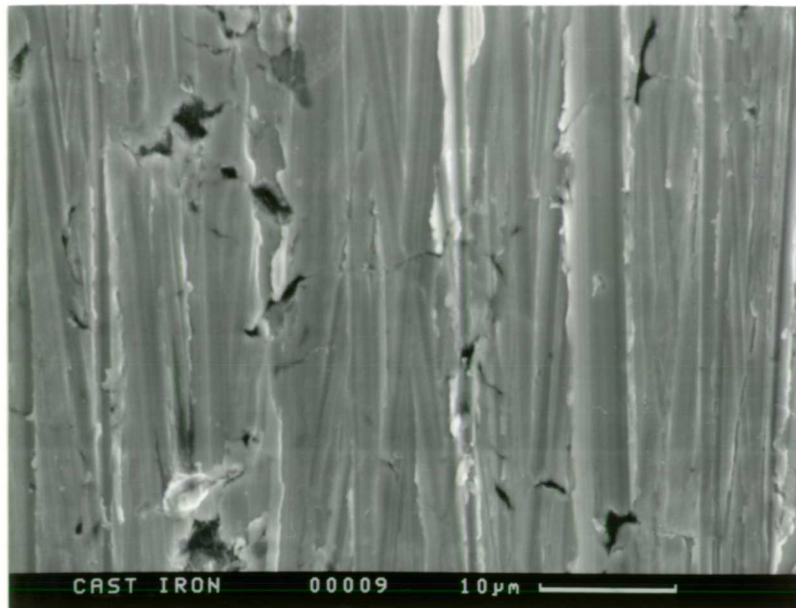
**Figure 18: Secondary electron image of a cast iron plunger surface unidirectionally ground to a 600 grit finish and having had no prior heat treatment or glass contact.**
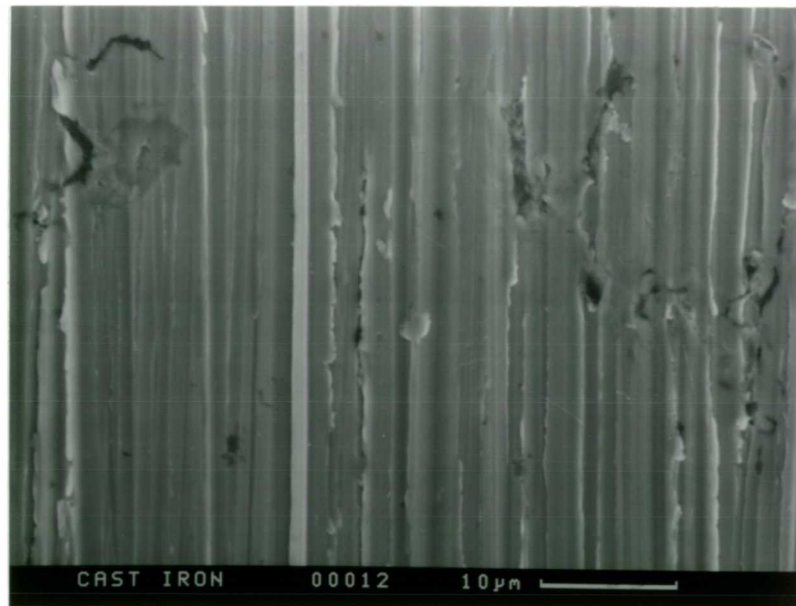


**Figure 19: Secondary electron image of a cast iron plunger surface unidirectionally ground to a 1200 grit finish and having had no prior heat treatment or glass contact.**

It can be seen from Figure 17 to Figure 19 that the prepared cast iron plunger surfaces are made up from near parallel ridges that have very little additional surface texture. The width between the ridges which stand proud appear to vary from 10μm to approximately 1μm according to Figure 17 to Figure 19.

XPS of the cast iron surface with a 120 grit finish with no previous heat treatment or glass contact was carried out to determine which species were present on the surface and in what proportions. A virgin cast iron surface (i.e. one which had been made from a brand new blank mould), which was free from significant oxide, was prepared by grinding the glass contact surface with a SiC paper in order to remove the surface oxide layers. Figure 20 shows an XPS widescan obtained from a piece of cast iron which had never come in contact with a glass melt, i.e. the sample was made from a new blank mould.
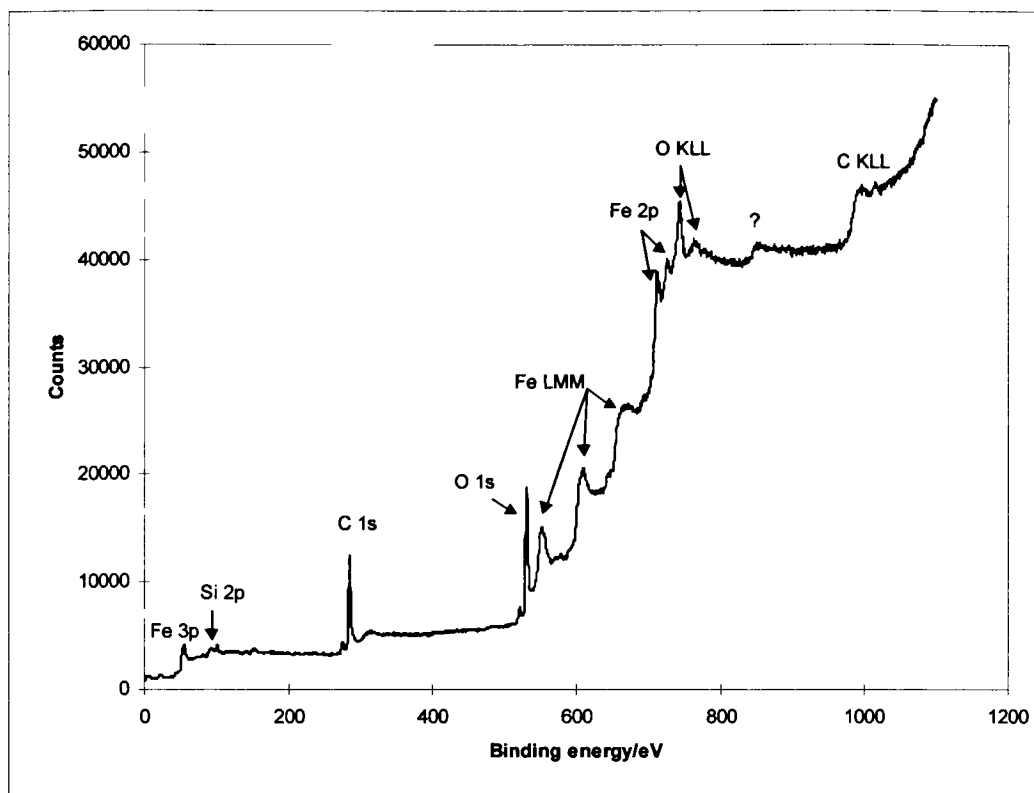
Figure 20: X-ray photoelectron spectroscopy widescan obtained from the surface of a newly ground piece of cast iron mould material with a 120 grit finish which had never had contact with glass (take off angle 30°, using a MgKα source).

It can be seen from Figure 20 that the surface of the newly ground cast iron appears to be made up of Si, C, O and Fe. It is known from the specification sheet supplied by the manufacturer of the mould (*Birstall Foundary, UK*) that the cast iron blank mould used contains other trace alloying additives that are used to alter its structural and mechanical properties. The trace alloying additives which are contained in the cast iron blank mould used include 0.4 - 0.7wt.% Mn, 0.1wt.% P, 0.1wt.% S and 0.08 - 0.12wt.% Ti. However the level of these additives is too low to be resolved on the XPS trace. The surface of the specimen needs approximately 1% of the analyte to register on the XPS trace.

Quantification using XPS (see section 2.2.3) of the surface of a piece of cast iron

that had had no previous contact with glass may be found in Table 3.

| | Si | C | Fe | O | Mn | P | S | Mo | Ti |
|---|---|---|---|---|---|---|---|---|---|
| **Concentration at the surface / atomic %** | 15.7 ±1.5 | 51.6 ±5 | 3.5± 0.4 | 29.3 ±3 | - | - | - | - | - |
| **Concentration of the bulk / atomic %** | 3.5 ±0.2 | 14.4 ±0.5 | bal | - | 0.5 ±0.2 | 0 +0.2 | 0 +0.2 | 0.3± 0.04 | 0.1± 0.04 |

Table 3: Quantification of a piece of newly ground cast iron that had had no previous contact with glass using x-ray photoelectron spectroscopy as compared to the expected composition (as supplied by the manufacturer – Birstall Foundry).

The quantification shows that, although the cast iron sample had been ground

prior to the analysis, there was still much oxide present on the surface. In addition,

the level of carbon present on the surface (51.6at.%) was higher than would be

expected from the level of carbon of the bulk (14.4at.%). This excess carbon may

indicate that there is some form of hydrocarbon contamination present on the

surface. Another explanation for the increased level of carbon on the surface may

be that there is more graphite present on the working surface of the blank mould

than is normally present in the bulk or possibly that the SiC grinding paper used

during preparation has contaminated the surface.

As described in Chapter 2, it was normal for the cast iron surface to be subjected

to heat treatment prior to glass contact. The heat treatment used involved holding

the cast-iron samples at a temperature of 470°C for a period of 30 hours in static air. This heat treatment should produce a controlled oxide layer on the cast iron surface. The heat treatment was used to produce a surface similar to one that would occur on a blank mould used in glass container manufacture after it had been in use for a production run (i.e. approximately 48 hours before cleaning and minor repairs).

An SEM examination of the cast iron plunger samples after this heat treatment was carried out in order to reveal how the surface morphology of the sample changed after the heat treatment had been applied. Figure 21 to Figure 23 show the secondary electron images of the resulting cast iron samples after heat treatment.



P120 FINISH        00003        10μm
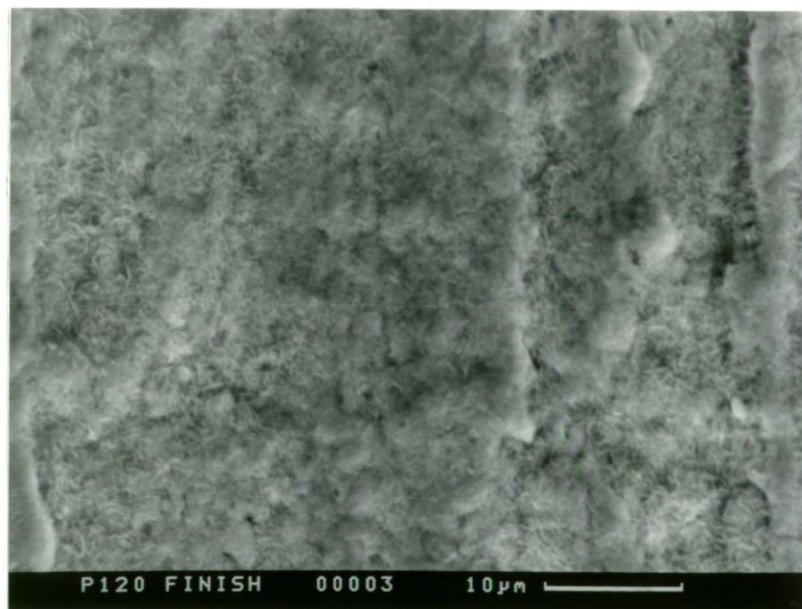
**Figure 21: Secondary electron image of a cast iron surface with a 120 grit unidirectional finish after heat treatment at 470°C held for 30 hours in air.**

It can be seen, by comparing Figure 21 to Figure 23 with Figure 17 to Figure 19, that the cast iron finish after heat treatment looks very different from a freshly ground surface. The heat treatment process appears to smooth out the ridges of the ground surface to some extent and provide each ridge with some surface texture of its own.

An XPS study of the effect of heat treatment on the chemistry of the cast iron surface was carried out. Figure 24 shows the XPS widescan obtained from the surface of a piece of cast iron after it had been subjected to the heat treatment regime and had no previous contact with glass.
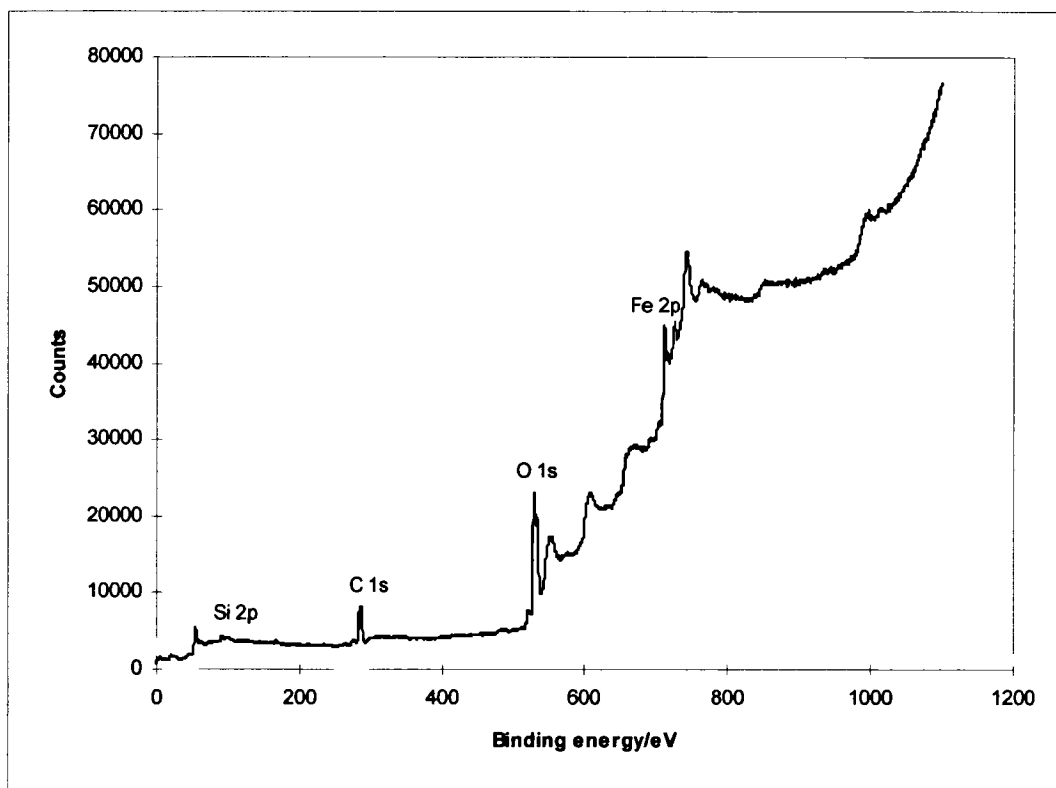


Figure 24: X-ray photoelectron spectroscopy widescan obtained from the surface of a piece of cast iron with a 120 grit unidirectional finish after heat treatment which had no prior contact with glass (take off angle 30°, using an MgKα source).

Quantification, using XPS, of the surface of the sample of cast iron with a 120 grit unidirectional finish after heat treating in air at 470°C for 30 hours, was carried out. A summary of the compositional information from the surface of the heat-treated cast iron sample using data obtained from an XPS investigation can be found in Table 4.

| Element | Concentration /Atomic % |
|---------|-------------------------|
| Si      | 13.8                    |
| C       | 36.4                    |
| Fe      | 2.9                     |
| O       | 47.0                    |

**Table 4: Quantification of the surface of a cast iron sample after heat treatment which had no previous glass contact using x-ray photoelectron spectroscopy.**

It can be seen by comparing Table 4 with Table 3 that heat treatment causes the amount of oxygen present on the cast iron surface to increase from 29.3at.% to 47.0at.%. The level of carbon, silicon and iron can be seen to decrease from 51.6at.% to 36.4at.%, 15.7at.% to 13.8at.% and 3.5at.% to 2.9at.% respectively. This decrease, however, may be an artefact of the increase in oxide produced on heat treatment that covers the underlying microstructure.

### 3.1.2.1 Cast Iron Plunger Heat Treatment

The interaction of the cast iron plunger surface with the glass melt during the formation of glass samples was carried out with the contact surface of the plunger free from significant oxide (as if the mould was new). The normal plunger materials were oxidised to produce a surface similar to that expected after a long production run (see sections 3.1.2.3 to 3.1.2.5). Pressing, using plungers free from significant surface oxide, was carried out in order to determine whether the surface of the glass sample had an increased chance of contamination from the cast iron plunger when the mould was new, compared to that if the mould had been used for a long production run.

The glass samples were pressed using cast iron plungers which had been unidirectionally finished using 120 grit SiC paper, but had been subjected to no heat treatment. Glass samples were pressed using initial cast iron plunger temperatures of 300°C and 510°C to determine whether the elevated pressing temperature had an effect on the stability of the plunger surface and the resulting glass surface. Five glass samples were pressed using cast iron plunger samples which had had no prior heat treatment at each of the initial plunger temperatures of 300°C and 510°C. The surfaces of the plunger material and the resulting glass surfaces were examined using SEM together with EDS (see section 2.2.2). The surface temperature of the plunger in contact with the glass melt in all cases, irrespective of the initial plunger temperature, has been found to rise by approximately 80°C during plunger-to-glass contact (see section 2.1.1 regarding details of the measurement techniques used).

In this investigation examining heat treatment of cast iron plungers, the initial glass melt temperature (950°C), press time (4 seconds), glass composition, atmosphere (static ambient), pressing pressure ($2 \times 10^5$ Pa ) and number of glass-to-metal contacts were held constant. Only the initial plunger temperature of the cast iron plunger, with no prior heat treatment, was varied. Between pressings, the cast iron plunger was held at the initial plunger temperature in static air for approximately 20 minutes to ensure that it was evenly heated.

Figure 25 shows the secondary electron image of the surface of a cast iron plunger sample that had had no previous heat treatment and was used to make 5 glass samples.



Figure 25: Secondary electron image of a cast iron surface with a 120 grit finish having no previous heat treatment after 5 contacts with glass using an initial plunger temperature of 300°C.

It can be seen from Figure 25 that the surface of this cast iron plunger, that had had no previous heat treatment prior to making glass samples, appears to have formed an oxide layer. The surface of this plunger (seen in Figure 25) does not have the smooth surface of a freshly ground surface (as seen in Figure 17) leading to the conclusion that an oxide layer had formed. Comparing Figure 25 with Figure 21 of a cast iron sample which had been subjected to the normal initial heat treatment regime of 470°C held in static air for 30 hours, it can be seen that the oxide layer formed only by pressing glass melts does not appear to be as substantial and fibrous (i.e. not as thick and does not appear to smooth out the ridges formed by grinding).

Figure 26 shows a secondary electron image of the surface of the 5$^{th}$ pressed glass sample made using the same cast iron plunger which had no prior heat treatment. Thus Figure 26 is the secondary electron image of the glass which was last in contact with the plunger surface shown in Figure 25.

Figure 26: Secondary electron image of the 5$^{th}$ pressed glass surface made using a cast iron plunger with a 120 grit finish having no previous heat treatment using an initial pressing temperature of 300°C.

The glass surface, shown in Figure 26, made using a cast iron plunger with no previous heat treatment at an initial plunger temperature of 300°C, appears different from that of the as-cast control glass surface (Figure 13) which was generally smooth. The surface of the pressed glass (see Figure 26) can be seen to have numerous randomly distributed dimples in the surface, which have probably been formed on contact with the plunger, and is covered in small particles. The secondary electron image of one of these particles (in Figure 26) can be seen in Figure 27.
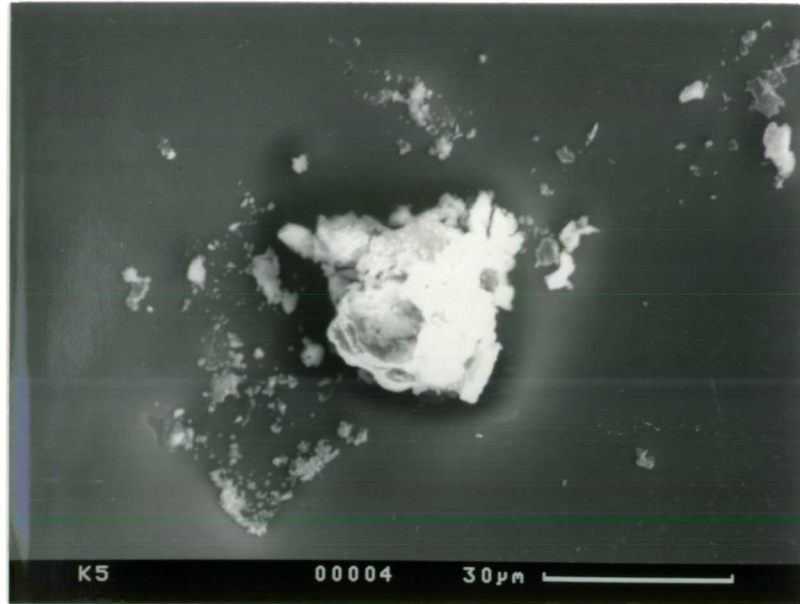
**Figure 27: High magnification secondary electron image of an embedded particle approximately 25μm in size found on the surface of the 5<sup>th</sup> glass sample, pressed using a cast iron plunger with a 120 grit finish with no previous heat treatment.**

EDS analysis of particles like that shown in Figure 27, revealed them to be iron rich. It is therefore likely that these particles seen on the pressed glass surface have originated from the oxide scale formed on the cast iron plunger surface during use. The quantity of particles found on the glass surface may indicate that the oxide scale formed on the cast iron surface only loosely adhered to the plunger surface.

As a comparison, glass samples were pressed using cast iron plungers which had had no previous heat treatment with a higher initial plunger temperature of 510°C, rather than 300°C, as above. The cast iron samples were prepared using 120 grit SiC paper to give a controlled (unidirectional) finish. Figure 28 shows a secondary electron image of the surface of a cast iron plunger sample that had had no prior

heat treatment, which had then been used to make 5 glass samples at an initial plunger temperature of 510°C. Each glass sample was pressed using an initial plunger temperature of 510°C. The cast iron plunger was held in static air for 20 minutes between contacts with the glass melt to allow the temperature of the plunger to stabilise.
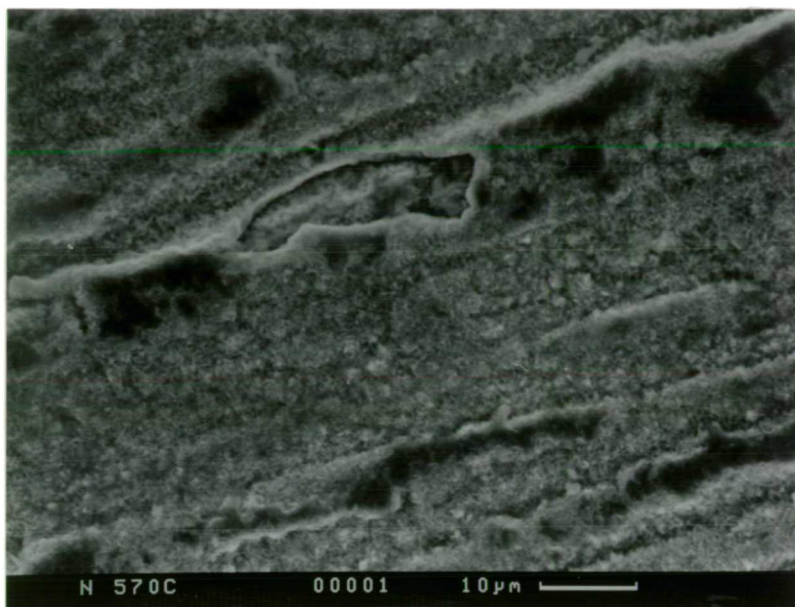


**Figure 28: Secondary electron image of a cast iron surface with a 120 grit finish with no previous heat treatment after 5 contacts with glass using an initial plunger temperature of 510°C.**

It can be seen by comparing Figure 28 and Figure 25, that increasing the pressing temperature from 300°C to 510°C also appears to increase the thickness of oxide layer formed. The surface of the cast iron plunger which had been used to make glass samples at an initial plunger temperature of 510°C appears to be more like that of the conditioned cast iron plunger surface (Figure 21) which was held at

470°C for 30 hours in static air, where the ridges have been smoothed out to some extent.

Figure 29 shows an area of the cast iron plunger surface after it had been used to make 5 glass samples using an initial plunger temperature of 510°C, with no prior heat treatment. It can be seen from Figure 29 that there is an area on the right hand side of the micrograph where the oxide scale has become detached from the cast iron plunger sample.
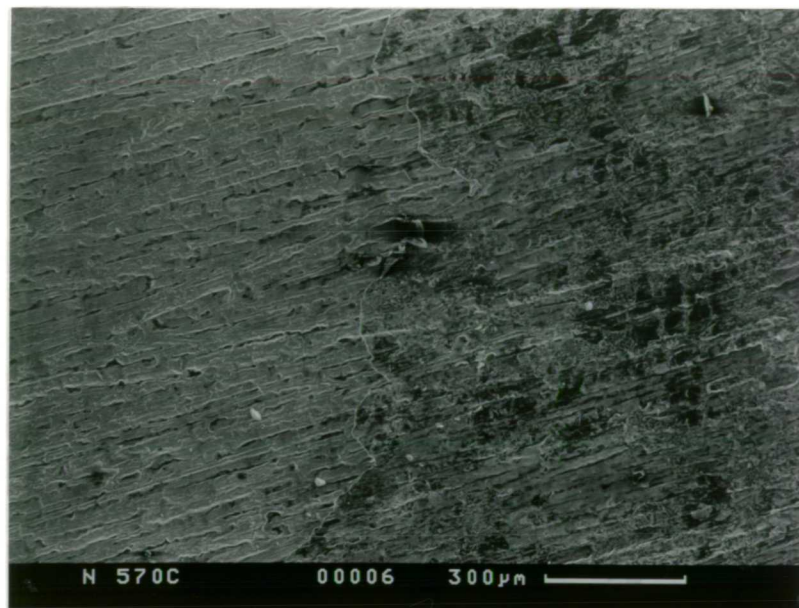


**Figure 29: Secondary electron image of a cast iron surface with a 120 grit finish with no previous heat treatment after making 5 glass samples using an initial plunger temperature of 510°C, the right hand half shows an area where the oxide has become detached.**

It can be seen that the oxide scale has come loose from an area approximately 800μm in size on the surface of the plunger. It is possible that the loosened oxide may have become embedded in the resulting pressed glass surface during pressing.

Figure 30 shows a secondary electron image of the surface of the 5th glass sample made using a cast iron sample with a 120 grit finish, that had had no prior heat treatment, using an initial plunger temperature of 510°C.
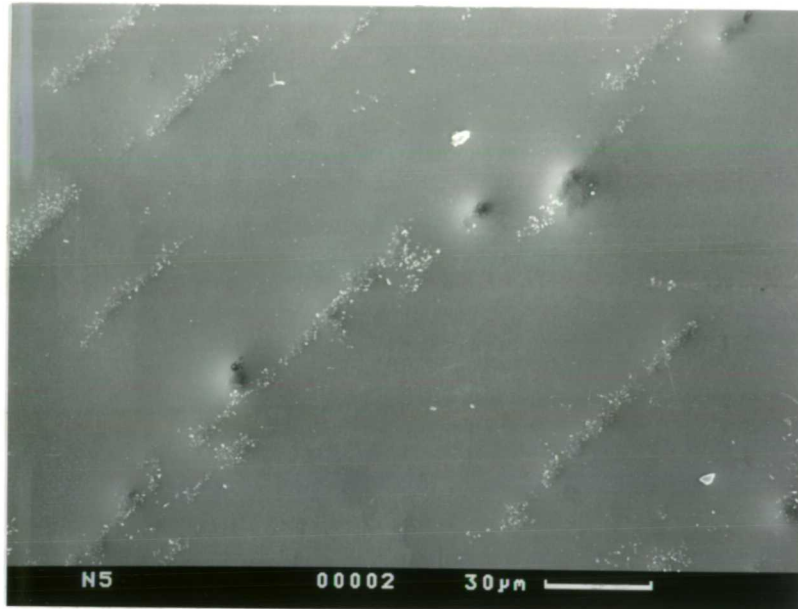


Figure 30: Secondary electron image of the 5$^{th}$ pressed glass surface made using a cast iron plunger with a 120 grit finish which had no previous heat treatment using an initial plunger temperature of 510°C.

It can be seen that the surface of the pressed glass is covered in dimples. This glass surface does not appear to be the same as one which was pressed at a lower temperature (i.e. using an initial plunger temperature of 300°C) where the dimples appeared to be randomly distributed and shallow (Figure 26). The dimples seen in the glass surface that had been pressed using an initial plunger temperature of 510°C can be seen to be in rows and appear fairly deep. This may indicate that at a

higher pressing temperature, there is increased glass flow around the defect ridges left from grinding in the plunger surface.

Another feature that may be seen in Figure 30 is the appearance of numerous sub-micron particles. Analysis of these particles using EDS has shown them to be iron rich. These particles generally appear to lie along the lines of the ridges, left over from grinding, in the surface of the cast iron plunger which would have come in contact with the glass during pressing. Figure 31 shows the evidence of glass surface damage resulting when a glass sample is made using a cast iron plunger with a 120 grit finish with no previous heat treatment at an initial plunger temperature of 510°C.
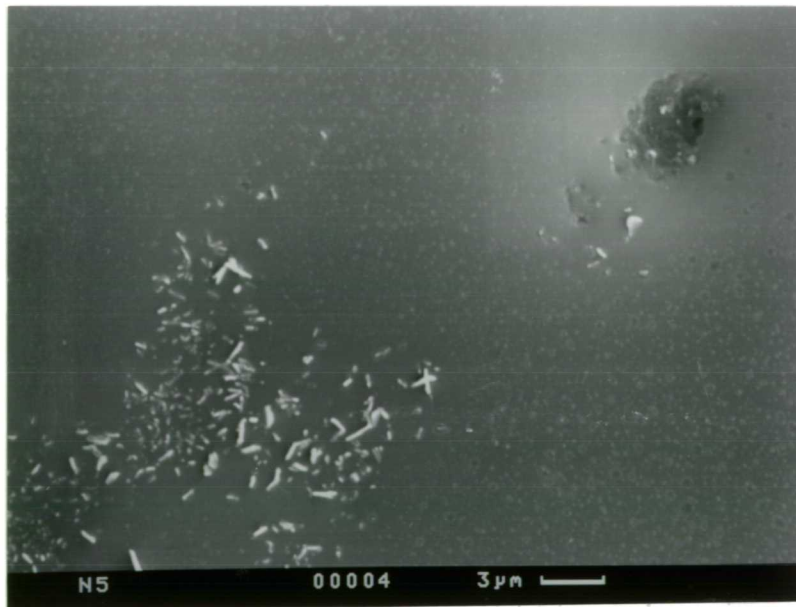


Figure 31: Secondary electron image of the surface damage on the 5th pressed glass sample made using a cast iron plunger with a 120 grit finish having no previous heat treatment with an initial plunger temperature of 510°C.

It can be seen from Figure 31 that dimples made in the pressed glass surface, when it is pressed at an initial plunger temperature of 510°C, do not appear to be smooth but have a roughened finish. This roughening may indicate that there was some form of localised sticking between the glass and plunger on contact during forming. The iron rich particles which can be seen in Figure 31 to be embedded in the pressed glass surface, are randomly oriented and sub-micron in size. They have the general appearance of the woolly oxide scale seen in Figure 28 on the plunger surface. The appearance of the particles therefore indicates that the oxide scale formed on the plunger surface (at an initial plunger temperature of 510°C) with no previous heat treatment on contact with glass is not very stable and is prone to becoming detached from the plunger.

### 3.1.2.2 Cast Iron Plunger Surface Finish

The effect of the surface finish of the plunger material on the resulting surface finish of the glass samples was investigated by carrying out a series of glass pressings using plungers with different finishes. This was carried out to determine whether the surface finish of the plunger had any effect on the surface finish of the resulting glass sample at different temperatures.

The cast iron plungers used were given controlled unidirectional surface finishes of 120 grit, 600 grit and 1200 grit. The plungers were then heat treated for 30 hours at 470°C in order to try and give a stable oxide surface as described in section 2.1.3. Glass samples were then pressed using an initial cast iron plunger temperature of 300°C with one of the three plunger grit finishes. Further glass samples were made using an initial plunger temperature of 510°C with plungers

having a 120 grit, or 1200 grit finish, as a comparison. Five glass samples were made using each plunger sample. Again, for this series of pressings the initial glass melt temperature (950°C), press time (4 seconds), glass composition, atmosphere (static ambient), number of glass-to-metal contacts and pressing pressure ($2\times10^5$ Pa) were kept constant with only the plunger surface finish being varied.

The resulting glass samples were examined using reflection optical microscopy, SEM together with EDS and atomic force microscopy. The composition of the glass surfaces were examined using XPS. The cast iron plunger surfaces were examined using SEM.

Figure 32 shows the surface of a pressed glass surface, using reflection optical microscopy, which had been made using a cast iron plunger with a 120 grit finish and an initial plunger temperature of 300°C.

225μm
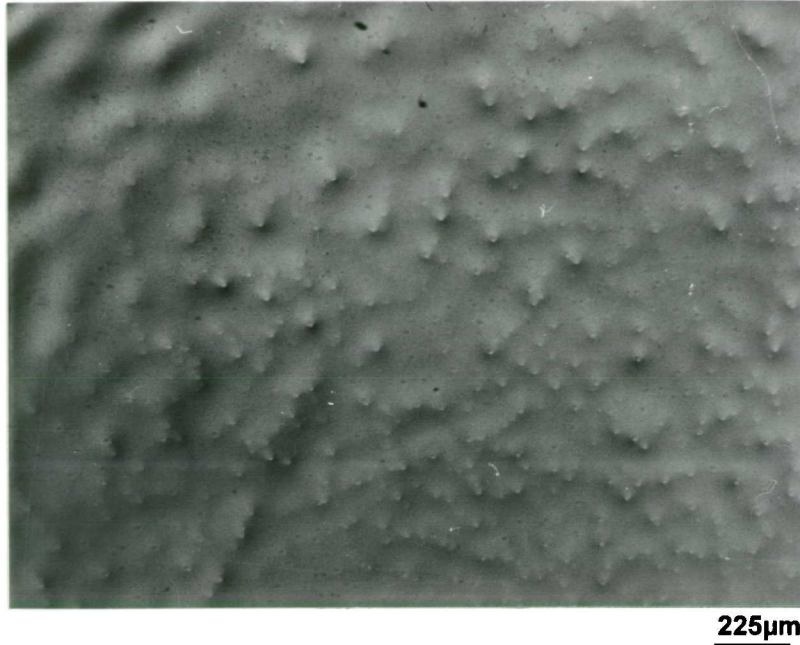
**Figure 32: Optical micrograph of a pressed glass surface made using a cast iron plunger with a 120 grit finish at an initial pressing temperature of 300°C (4$^{th}$ sample).**

It can be seen that the surface of the pressed glass is covered with randomly oriented large dimples that appear to be approximately 50μm across and are approximately 200μm apart. Closer examination of the pressed glass surface shows it to be covered in numerous particles up to 30μm in size. Figure 33 shows a secondary electron image of a typical particle which could be found on a glass surface which had been pressed using a cast iron plunger with a 120 grit finish at an initial plunger temperature of 300°C.
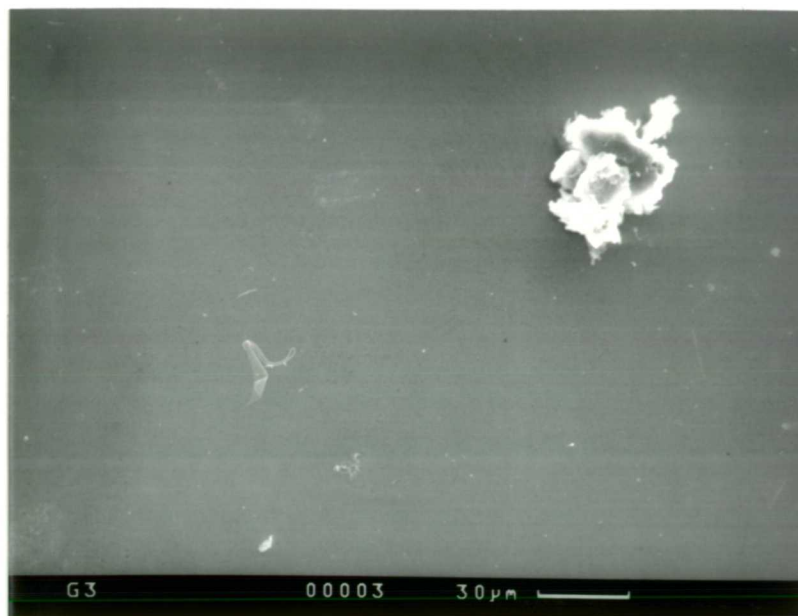
**Figure 33: Secondary electron image of a typical embedded particles found on a glass surface which had been pressed using a cast iron plunger with a 120 grit finish at an initial plunger temperature of 300°C (3$^{rd}$ sample).**

Analysis of such embedded particles using EDS/SEM have shown them either to be iron rich or to appear to be made from the glass itself, although the majority are iron rich.

XPS of the surface of the glass sample pressed using a cast iron sample with a 120 grit finish at an initial plunger temperature of 300°C was carried out to determine which species were present and in what amounts. An XPS widescan of the first glass surface produced using these parameters may be seen in Figure 34.
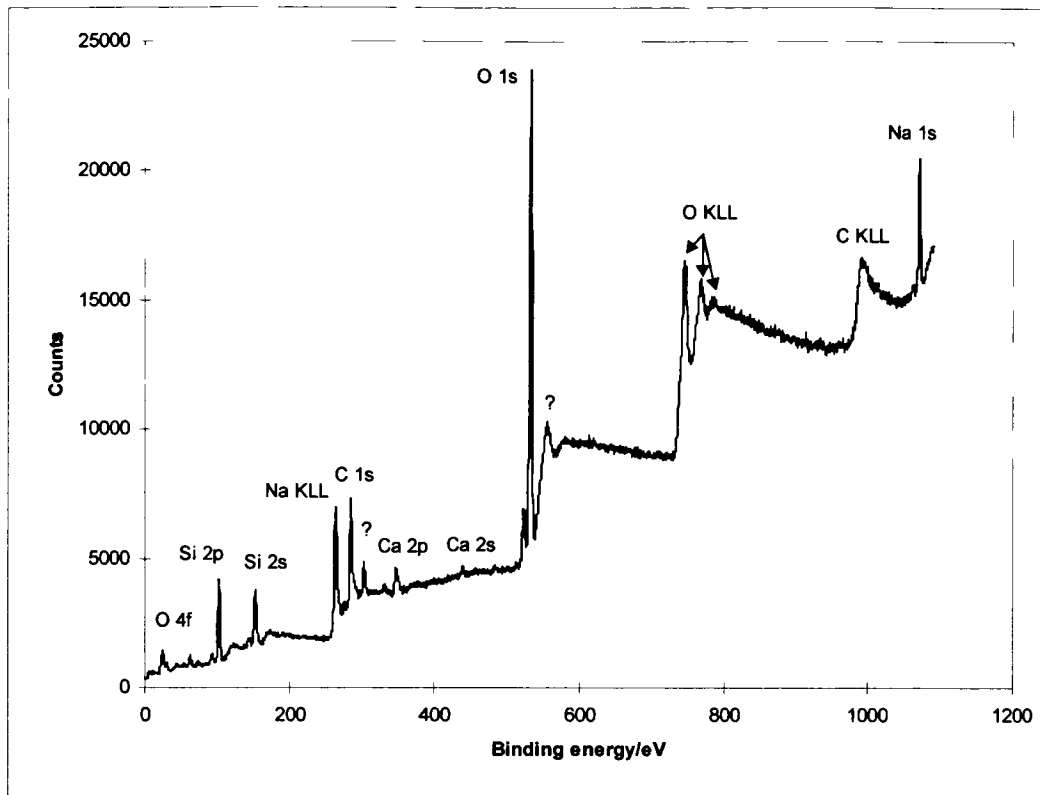
**Figure 34: X-ray photoelectron spectroscopy widescan of the first glass surface produced using a cast iron plunger with a 120 grit finish using an initial plunger temperature of 300°C (30° take off angle, using a MgKα source).**

The surface of the first glass sample pressed using a cast iron plunger with a 120 grit finish at an initial plunger temperature of 300°C can be seen from Figure 34 to be made up from Si, Ca, Na, O and C. The absence of other elements which should be present in the glass (e.g. K, Mg etc.) would indicate that there was less than 1 atomic% of these elements present on the surface. Although iron rich particles were located on the surface using SEM and EDS, no iron was found using XPS. This would therefore indicate that there was less than 1 atomic% of iron present on the surface of the pressed glass sample.
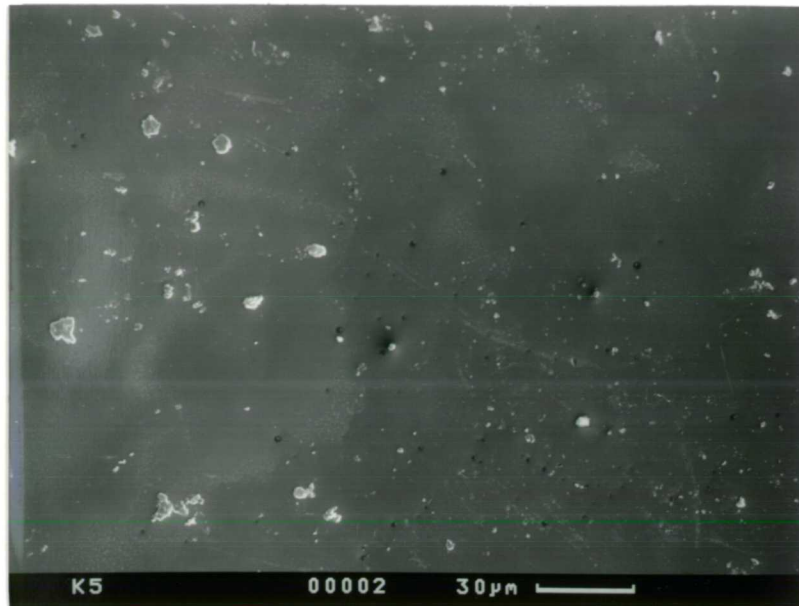
**Figure 36: Secondary electron image of a pressed glass surface made using a cast iron plunger with a 600 grit finish using an initial plunger temperature of 300°C (2$^{nd}$ sample).**

It can be seen that there appears to be rows of dimples present (approximately 300μm apart) on the glass surface which was pressed using a cast iron plunger with a 600 grit finish at an initial plunger temperature of 300°C. Between the rows of dimples, however, there appears to be a more random pattern of dimples present. It can also be seen that there are numerous particles less than 30μm in size evident on the surface. These particles have been found to be either iron rich or silicate glass.

XPS of the first pressed glass surface produced using a cast iron plunger with a 600 grit finish at an initial plunger temperature of 300°C was carried out in order to determine which species were present and in what concentrations (survey scan in Figure 37).
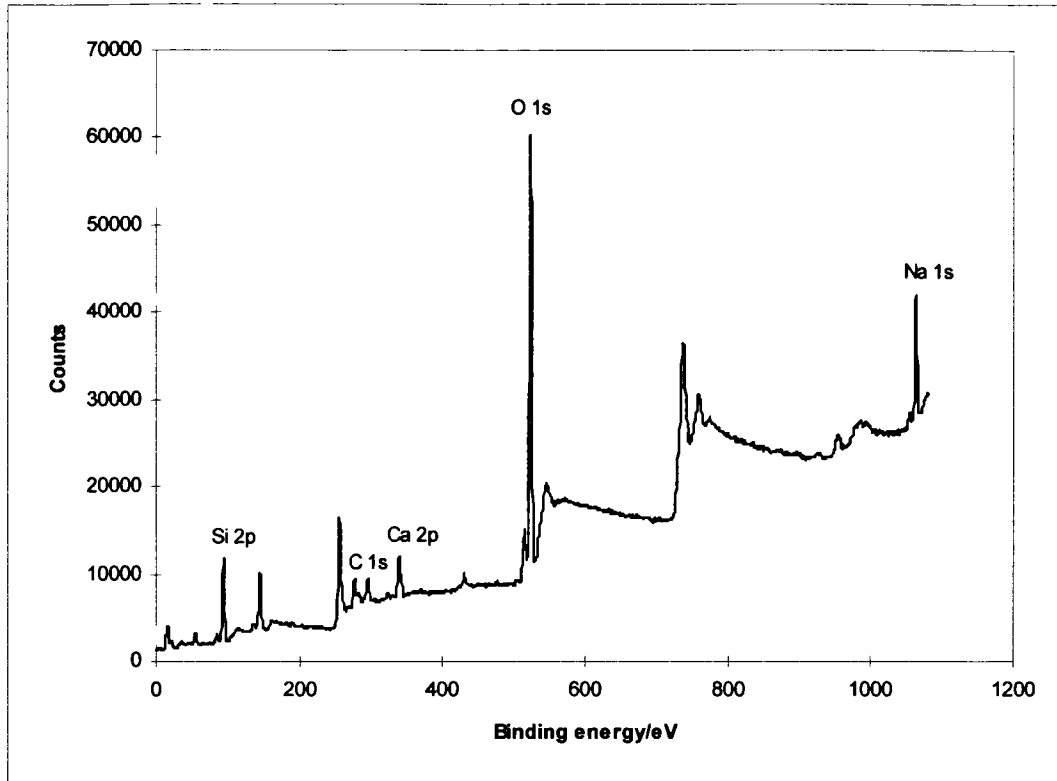
**Figure 37:** X-ray photoelectron spectroscopy widescan of the first pressed glass surface produced using a cast iron plunger with a 600 grit finish using an initial plunger temperature of 300°C (30° take off angle, using a MgKα source).

It can be seen from Figure 37 that the surface of the first glass sample which was pressed using a cast iron plunger with a 600 grit finish at an initial plunger temperature of 300°C can be seen to be made up from Si, Ca, Na, O and C. Quantification of the species detected can be found in Table 5.

| Element | Concentration /Atomic % |
|---------|-------------------------|
| Si | 27.3 |
| C | 13.0 |
| Ca | 2.5 |
| O | 55.5 |
| Na | 1.7 |

**Table 5: Quantification of the species detected on the first glass sample pressed using a cast iron plunger with a 600 grit finish at an initial plunger temperature of 300°C.**

When the data presented in Table 5 are compared against that from a cast glass surface - i.e. one having no contact with a plunger material (summarised in Table 3), it can be seen that there is some variation in the composition of the two surfaces. After contact with a cast iron plunger material (600 grit finish at an initial plunger temperature of 300°C) it can be seen that there appears to be an increase in the oxygen, calcium and sodium levels, but a decrease in the level of carbon present.

The effect of a relatively smooth (i.e. an even finer finish which is close to being polished) cast iron plunger surface on that of the resulting pressed glass surface was investigated using cast iron with a 1200 grit finish. Figure 38 shows the surface of a glass sample which had been pressed using a cast iron plunger with a 1200 grit finish at an initial plunger temperature of 300°C.

225µm

**Figure 38: Optical micrograph of a glass surface which had been pressed using a cast iron plunger with a 1200 grit finish at an initial plunger temperature of 300°C (4th sample).**

The surface of the glass sample which had been pressed using a cast iron plunger with a 1200 grit finish appears to have some randomly oriented dimples on it especially near the centre at the edge. However, the surface of the glass sample can be seen to have rings of ripples evident. This type of rippled surface is normally found in glass containers when they have been formed with too cool a mould and is often termed a chilled surface. Numerous particles less than 50µm in size can be seen on the surface. Figure 39 shows a secondary electron image of one of the embedded particles which was found on the surface of a glass sample which was pressed using a cast iron plunger with an initial plunger temperature of 300°C; these particles were typically iron or silicate glass.
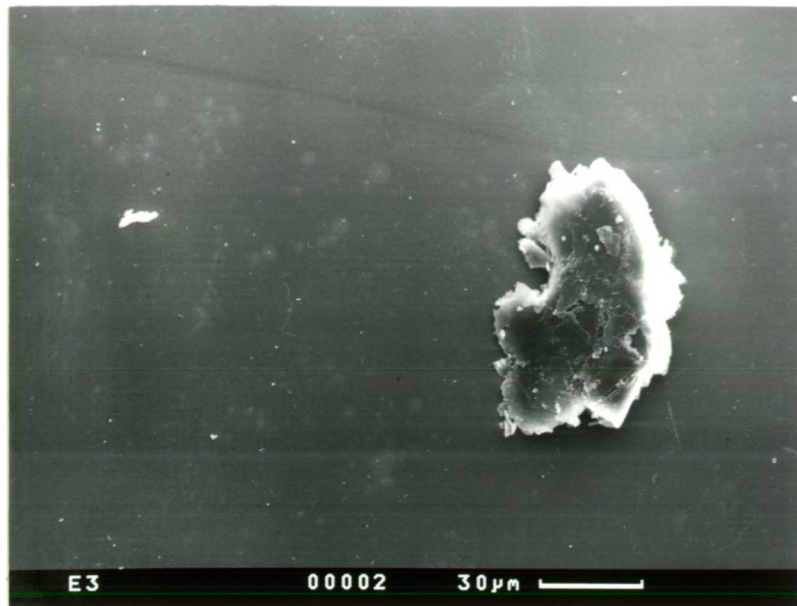
**Figure 39: Secondary electron image of an embedded particle found on the surface of a glass surface pressed using a cast iron plunger with a 1200 grit finish at an initial plunger temperature of 300°C (3$^{rd}$ sample).**

An XPS investigation was carried out on the first pressed glass sample produced using a cast iron plunger with a 1200 grit finish at an initial plunger temperature of 300°C to determine what species were present on the surface and in what quantities.
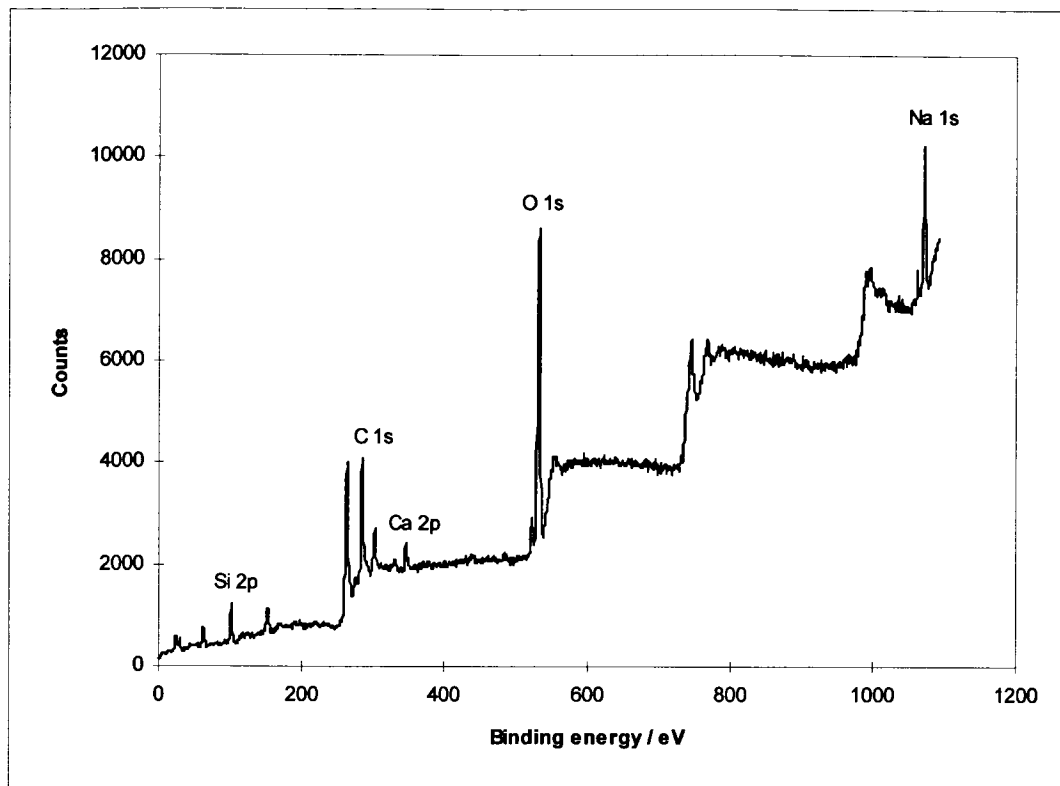
**Figure 40: X-ray photoelectron spectroscopy widescan of a pressed glass surface produced using a cast iron plunger with a 1200 grit finish at an initial plunger temperature of 300°C (30° x-ray gun to sample angle, using magnesium x-rays).**

From the XPS survey scan in Figure 40, the surface of the pressed glass surface formed using a cast iron plunger with a 1200 grit finish at an initial plunger temperature of 300°C is composed of Si, O, Na, Ca and C. The results from quantification of these detectable elements using XPS at a x-ray gun to sample angle of 30° are summarised in Table 6.

| Element | Concentration /Atomic % |
|---------|-------------------------|
| Si | 25.8 |
| C | 21.7 |
| Ca | 2.8 |
| O | 48.4 |
| Na | 1.3 |

Table 6: Quantification of the first pressed glass surface made using a cast iron plunger with a 1200 grit finish at an initial plunger temperature of 300°C using XPS.

Quantification of the pressed glass surface produced using a cast iron plunger with a 1200 grit finish at an initial plunger temperature of 300°C as summarised in Table 6 shows that the surface has a similar composition to that of a glass sample pressed using a cast iron plunger with a 600 grit finish at an initial plunger temperature of 300°C (Table 5).

Survey scans were repeated on the pressed glass surface produced using a cast iron plunger with a 1200 grit finish at an initial plunger temperature of 300°C by altering the take off angle of the x-ray gun to angles (i.e. take off angles) of 15°, 60° and 90° to give a crude form of depth profiling. The shallower the angle of the x-ray gun to the specimen gives a more surface specific result, however this is elemental specific (e.g for carbon, oxygen and silicon, a 15° take off angle would approximately equate to the top 1nm, whereas a 90° take off angle would approximately equate to 4.5nm for carbon, but deeper for sodium). Figure 41 shows a graph of how the concentration of the detected elements on the pressed

glass surface varies with increasing the penetration depth of x-rays on the sample

surface giving a crude form of depth profiling.
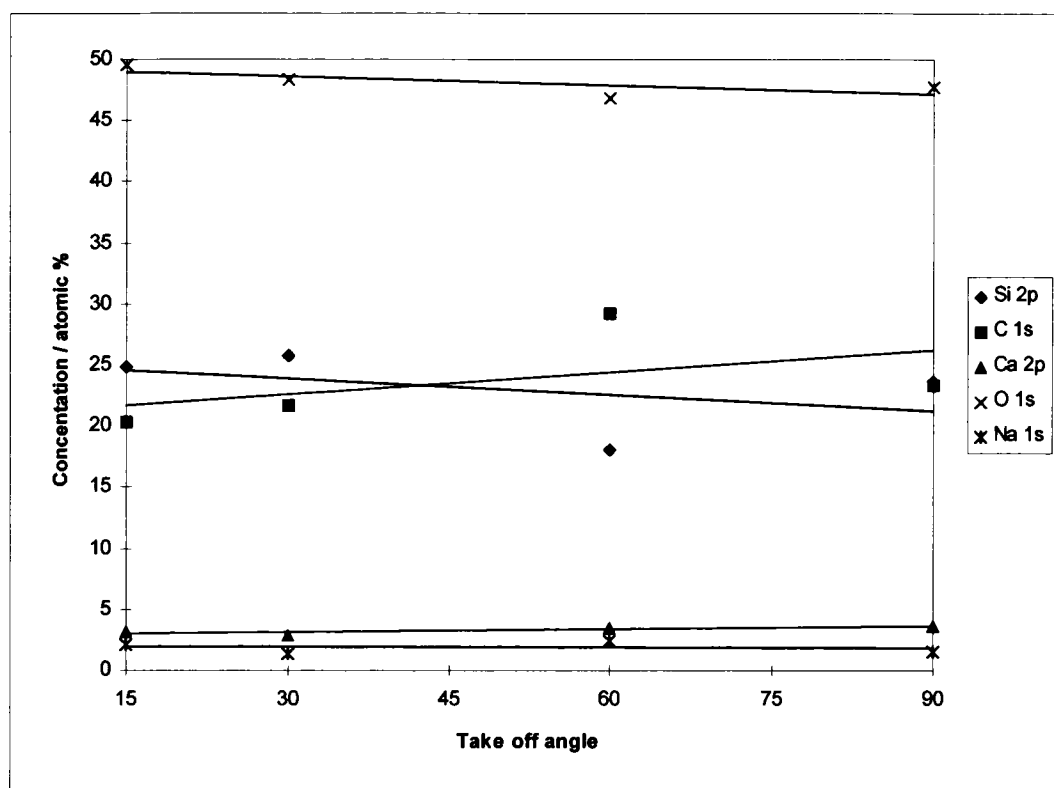


**Figure 41: Crude depth profiling, with the increasing depth indicated by an increase in take off angle, carried out using x-ray photoelectron spectroscopy on the first glass sample pressed using a cast iron plunger with a 1200 grit finish at an initial plunger temperature of 300°C (using a MgKα source).**

The crude depth profiling carried out on the pressed glass surface produced using

a cast iron plunger with a 1200 grit finish at an initial plunger temperature of

300°C suggests that the composition of the surface of the glass sample is similar

however deep the penetration. The slight gradients seen on the traces in Figure 41,

appear to indicate a decrease in the level of silicon and oxygen present deeper in

the sample whilst the sodium and calcium levels stay constant. However, the random error on the silicon trace, in particular, is quite large.

Atomic force microscopy was carried out in order to determine quantitatively the finish of the 4th pressed glass surface which had been made using a cast iron plunger with a 1200 grit unidirectional finish at an initial plunger temperature of 300°C (Figure 42)
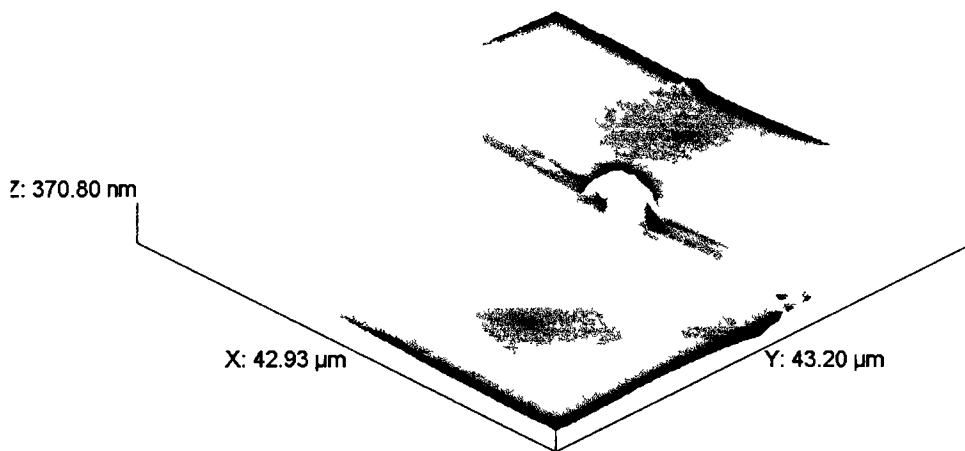


**Figure 42: Three dimensional atomic force microscopy image of the 4th pressed glass surface made using a cast iron plunger with a 1200 grit unidirectional finish at an initial plunger temperature of 300°C.**

It can be seen from Figure 42 that there are both dimples (shown in black) and embedded particles (shown as yellow) present on the surface. The dimples appear to be approximately 20µm apart from each other and are about 150-200nm deep and approximately 15µm across with fairly shallow sides.

Figure 43 shows a secondary electron image of the surface of a cast iron plunger sample that had been used to press 5 glass samples. The plunger has a 1200 grit surface finish and was used to make the glass samples using an initial plunger temperature of 300°C.
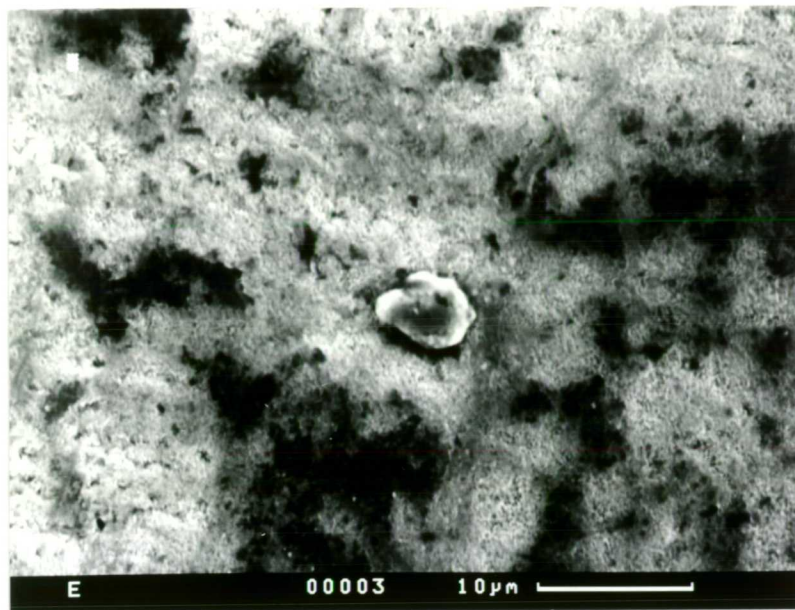


**Figure 43: Secondary electron image of a cast iron sample with a 1200 grit finish used to press 5 glass samples using an initial plunger temperature of 300°C.**

It can be seen that the surface of the cast iron plunger does not appear to have any of the original grinding lines present on the surface (*cf.* Figure 19). The surface of the cast iron plunger appears to be covered in a thick fibrous appearing oxide coating (*cf.* Figure 17 showing a newly ground cast iron surface). The particle seen in the centre of the micrograph shown in Figure 43 analysed as that of the glass pressed.

As a comparison to the glass samples which were pressed using an initial plunger temperature of 300°C, glass samples were also pressed using cast iron plungers (which had been initially heat treated in air for 30 hours at 470°C) with an initial plunger temperature of 510°C. This was carried out for plungers with both 120 grit and 1200 grit finishes.

Figure 44 shows a secondary electron image of the surface of a glass sample which had been pressed using a cast iron plunger with a 120 grit finish using an initial plunger temperature of 510°C.



**Figure 44: Secondary electron image of a glass surface which has been pressed using a cast iron plunger with a 120 grit finish at an initial plunger temperature of 510°C (1ˢᵗ sample).**

It can be seen from Figure 44 that the pressed glass surface appears to have rows of dimples that seem to have particles in them. EDS analysis has shown that these particles are iron rich. This would indicate that there has been intimate contact at

certain points between the plunger and glass during pressing which has caused a certain amount of the oxide scale from the plunger surface to become attached to the glass.

A three dimensional image using atomic force microscopy of the 4th glass surface pressed using a cast iron plunger with a 120 grit finish at an initial plunger temperature of 510°C can be found in Figure 45.
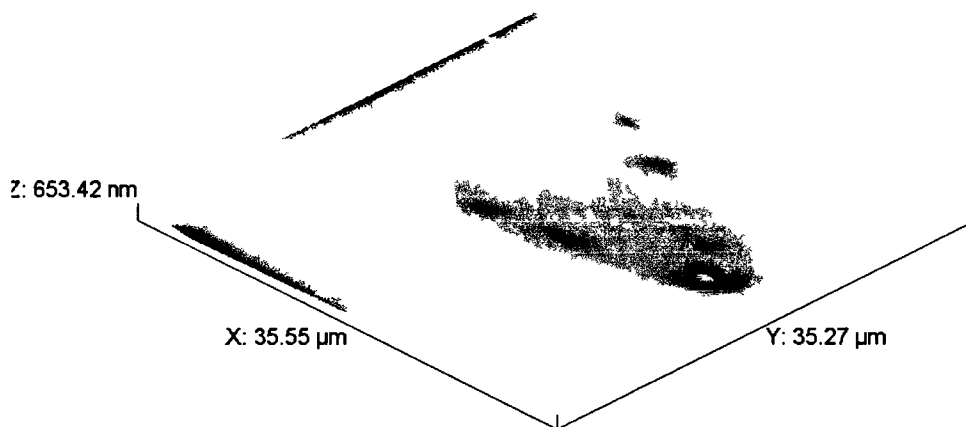


**Figure 45: Three dimensional atomic force microscopy image of the 4th glass surface which had been pressed using a heat treated cast iron plunger with a 120 grit unidirectional finish using an initial plunger temperature of 510°C.**

It can be seen from Figure 45 that there are both dimples and pressed-in particles present. However, the image seen shows a cluster of small sub-pits inside a large dimple. These sub pits are approximately 300-350nm deep and 2μm across inside a dimple which is about 30μm across. The evidence of the smaller sub-pits inside

the larger dimple would suggest that the glass melt has flowed to fill imperfections in the grooves of the 120 grit cast iron plunger during pressing.

Figure 46 shows a secondary electron image of the surface of a cast iron plunger that had been used to press 5 glass samples using an initial plunger temperature of 510°C.
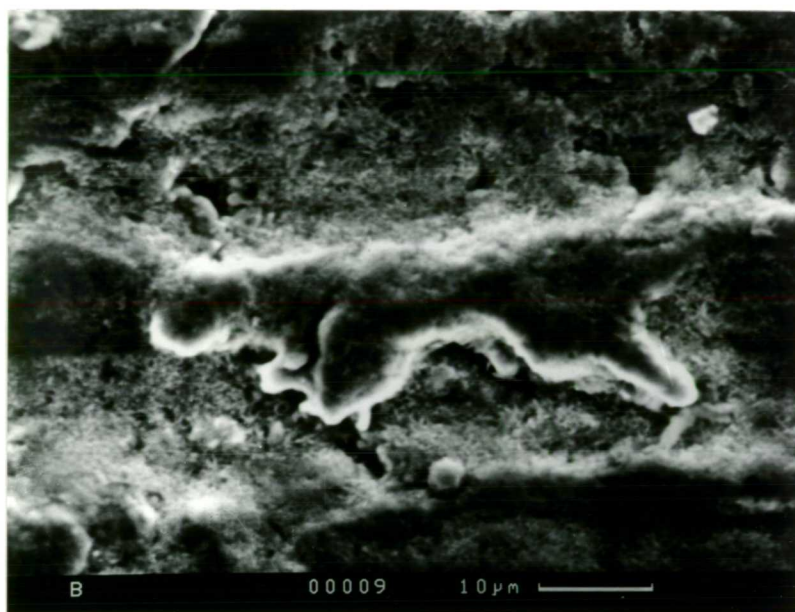


Figure 46: Secondary electron image of a cast iron plunger surface, which had been heat treated for 30 hours in air at 470°C, that has a 120 grit finish and has made 5 pressed glass samples using an initial plunger temperature of 510°C.

The morphology from the surface of the cast iron plunger with a unidirectional 120 grit finish which had been used to press 5 glass samples using an initial plunger temperature of 510°C (Figure 46) appears to be covered in a thick coating of oxide.

As a comparison, glass samples were pressed using a cast iron plunger with a finer 1200 grit finish using the same initial plunger temperature of 510°C. Figure 47 shows a secondary electron image of a glass surface which had been pressed using a cast iron surface with a 1200 grit finish using an initial plunger temperature of 510°C.



**Figure 47: Secondary electron image of a glass surface pressed using a cast iron plunger with a 1200 grit finish using an initial plunger temperature of 510°C (2$^{nd}$ sample). The length of the bar is 10 microns.**

Compared to the glass surface which had been pressed using a cast iron plunger with a 1200 grit finish using an initial plunger temperature of 300°C (Figure 39), it can be seen that increasing the plunger temperature to 510°C increases the amount of ripple present on the glass surface. The dimples seen are closer together than those found on a glass sample which had been pressed using a cast iron plunger with a coarser 120 grit finish using the same initial plunger temperature of 510°C

(Figure 44). The embedded particles seen in Figure 47 have been found to be iron rich using EDS.

A high magnification three dimensional image of the 4$^{th}$ glass surface pressed using a cast iron plunger with a unidirectional 1200 grit finish at an initial plunger temperature of 510°C can be found in Figure 48.
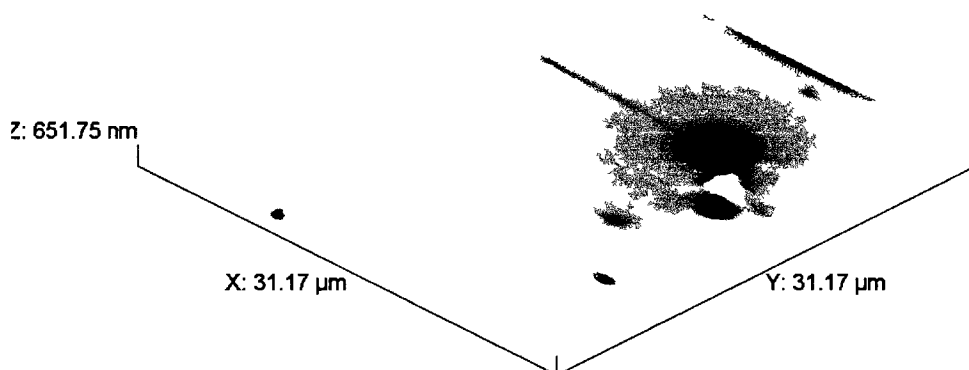


**Figure 48: Three dimensional atomic force microscopy image of the 4$^{th}$ glass surface pressed using a cast iron plunger with a 1200 grit surface finish at an initial plunger temperature of 510°C.**

It can be seen from Figure 48 that there are both dimples and pressed-in particles evident on the surface of the glass sample which had been pressed using a cast iron plunger with a 1200 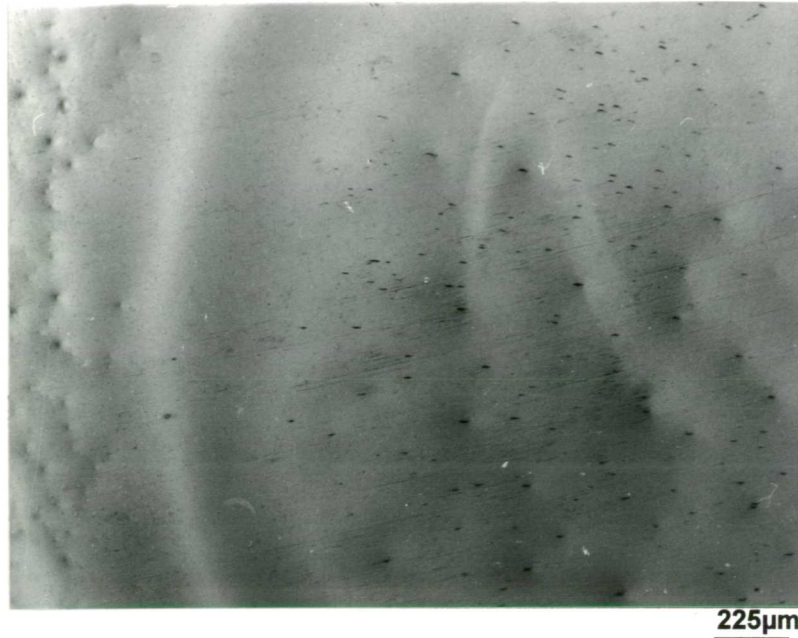grit surface finish at an initial plunger temperature of 510°C. The large dimple seen on the right hand of Figure 48 has been found to be approximately 8μm across and is 400nm deep. These dimples are narrower and deeper that those found on glass which had been pressed at an initial plunger temperature of 300°C using a cast iron plunger with a 1200 grit finish (i.e. dimples

which were 15μm across and 150-200nm deep seen in Figure 42). The depth of the dimple seen in Figure 48 is similar to that of the glass surface which had been pressed using a cast iron plunger with a 120 grit finish at an initial plunger temperature of 510°C, but is narrower.

Figure 49 shows a secondary electron image of the surface of a cast iron plunger (prepared to 1200 grit finish) sample used to press 5 glass samples using an initial plunger temperature of 510°C.
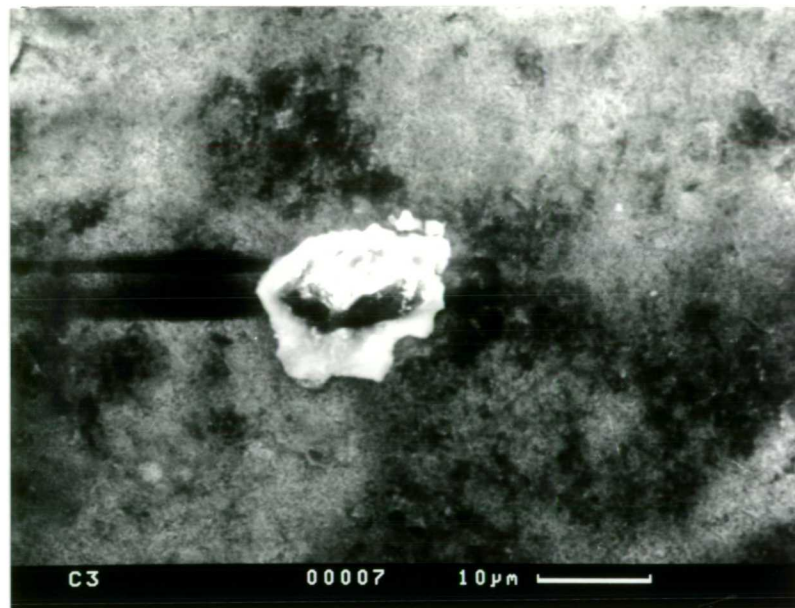


**Figure 49: Secondary electron image of a cast iron plunger surface with a 1200 grit finish used to make 5 glass samples with an initial plunger temperature of 510°C.**

It can be seen from Figure 49 that the ridges on the surface of the cast iron plunger with a 1200 grit finish after pressing 5 glass samples using an initial plunger temperature of 510°C appear to have been smoothed out. The oxide coating on the

plunger surface appears to have become thick enough to even out the ridges. The particle seen on the surface analysed as being iron rich using EDS.

### 3.1.2.3 Initial Plunger Temperature

The initial temperature of the plunger has been varied from lower than would be used in practice to form containers (i.e. 300°C) to that which is close to that expected for the glass to adhere to the plunger (i.e. 570°C). The temperature range investigated was chosen to cover all possible scenarios which might be encountered during glass container manufacture as different temperatures are used in blank moulds depending upon parameters such as production speeds and the size of ware being produced. It is also possible that different areas of the blank mould will have different temperatures due to differential cooling and the area where the gob hits the mould will have a higher temperature.

Glass samples were all pressed using cast iron plungers made from the working surface of discarded moulds (*Rockware Glass Ltd., Knottingley, UK*) with a 120 grit finish at a range of temperatures (300°C to 510°C in 30°C intervals and 510°C to 570°C in 20°C intervals). In this series of pressings the initial glass temperature (950°C), press time (4 seconds), glass composition, mould composition, atmosphere (ambient) and pressing pressure ($2 \times 10^5$ Pa) have all been kept constant with only the initial plunger temperature being varied. The maximum initial plunger temperature investigated (i.e. 570°C) did not appear to cause any large scale sticking of the glass to the plunger during contact. Unfortunately, the temperature of the plunger could not be raised to any higher temperature than

570°C due to thermal losses of the plunger to the atmosphere when the heating element was run at its maximum setting.

Results from the pressing of glass samples using a heat treated cast iron plunger with a 120 grit finish at an initial plunger temperature of 300°C have been presented in section 3.1.2.2 (i.e. Figure 32 to Figure 35 show results form both the pressed glass sample and cast iron plunger sample).

Glass surfaces pressed using an initial plunger temperature below 450°C were found to have a large randomly rippled texture (e.g. as seen in Figure 32 to Figure 38). This would have occurred as the surface of the glass melt would have set (i.e. become too viscous for flow to occur) before being pressed into the grooves in the cast iron plunger surface. There appears to be a gradual change in the appearance of the dimpled surfaces of the pressed glass samples between the initial plunger temperatures of 300°C and 510°C from randomly oriented large shallow pits at the lower temperatures to aligned deeper pits at the higher temperatures. In all cases, iron rich particles have been found on the glass surface.

Results from the pressing of glass samples using a heat treated cast iron plunger with a 120 grit finish at an initial plunger temperature of 510°C have been presented in section 3.1.2.2 (i.e. Figure 44 to Figure 46 show results from both the pressed glass sample and cast iron plunger sample).

The maximum initial plunger temperature reached using the pressing rig was 570°C due to problems with heat losses to the ambient atmosphere. Even at this elevated temperature, there did not appear to be any large scale glass-to-plunger sticking evident. Figure 50 and Figure 51 show secondary electron images of the 5th glass surface pressed using a heat treated cast iron plunger with a 120 grit finish using an initial plunger temperature of 570°C.
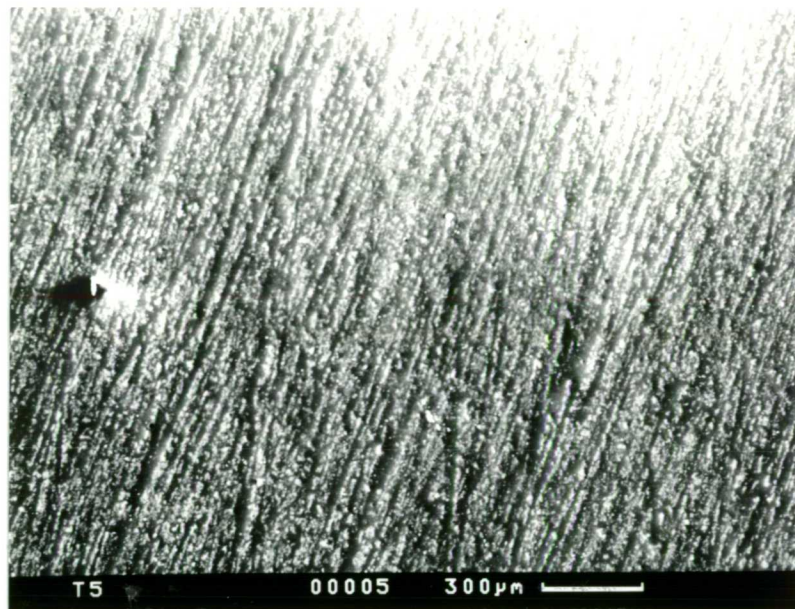


**Figure 50: Secondary electron image of the 5th glass surface pressed using a cast iron plunger with a 120 grit finish at an initial plunger temperature of 570°C.**

It can be seen from Figure 50 that the glass surface which had been pressed using a cast iron plunger with a 120 grit finish at an initial plunger temperature of 570°C appears to have deep grooves present which are less than 100μm apart.
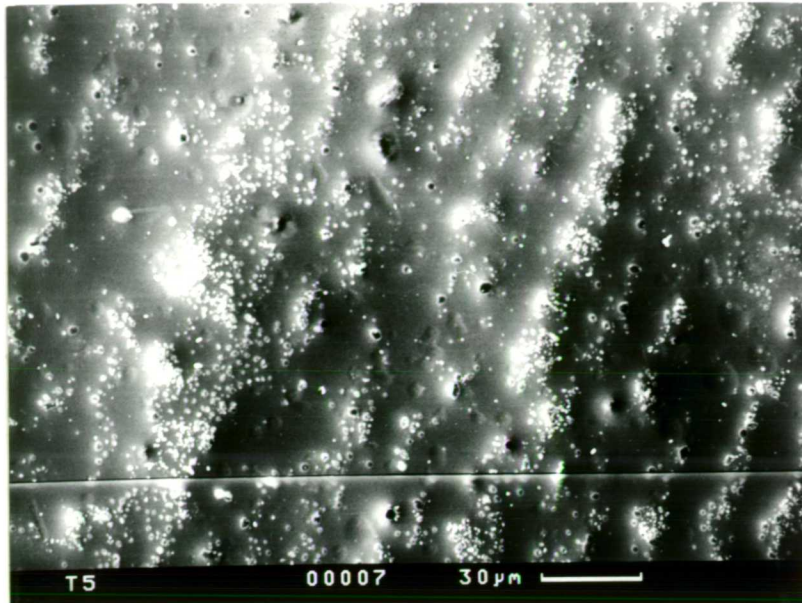
**Figure 51: High magnification secondary electron image of the 5th glass surface pressed using a cast iron plunger with a 120 grit finish at an initial plunger temperature of 570°C.**

Figure 51 shows that at higher magnifications, there appears to be numerous shallower dimples between the deeper grooves seen on Figure 50. This may indicate that using a cast iron plunger with an initial plunger temperature of 570°C enables easier flow of the glass melt into imperfections on the plunger surface. Although there appeared to be a roughened surface seen at the base of the dimples, it did not appear to be any more advanced that the surface of the glass samples pressed at lower plunger temperatures.

Figure 52 and Figure 53 show secondary electron images of the surface of the heat treated cast iron plunger with a 120 grit finish which was used to press 5 glass samples using an initial plunger temperature of 570°C.

It can be seen from Figure 52 and Figure 53 that the surface of the heat treated cast iron plunger with a 120 grit surface finish which had been used to press 5 glass samples at an initial plunger temperature of 570°C does not appear to be covered in the same sort of fine fibrous oxide seen previously for plungers used at lower temperatures, but it appears more blocky and substantial.

### 3.1.2.4 Number of Glass-to-Metal Contacts

Increasing the number of glass to metal contacts (i.e. the number of pressed glass samples made) has been investigated using plungers made from both a virgin cast iron blank mould (*Birstall Foundry, UK*) and a discarded, used cast iron blank mould (*Rockware Glass Ltd., Knottingley, UK*) for clarification. In the majority of the glass pressing experiments, only 5 glass samples were made. In this investigation, however, as many glass samples were made using one plunger sample as was possible in one week as a comparison; this turned out to be 30 pressings. The initial pressing temperature used was 510°C in both experiments as it was decided that this was a typical blank mould temperature used in container manufacture and any material transfer which may occur between the glass and plunger on contact (and *vice versa*) would be accelerated. In this series of pressings the initial glass temperature (950°C), press time (4 seconds), glass composition, atmosphere (ambient) and pressing pressure ($2 \times 10^5$ Pa) have all been kept constant with only the number of glass-to-metal being varied.

A virgin cast iron plunger was prepared by machining a disc 13mm in diameter by 5mm high (at *British Glass Technology*) from the working surface of a newly formed blank mould which had had no prior contact with a glass melt. These discs

were given a 120 grit finish using SiC paper and then heat treated by holding at 470°C in static air for 30 hours to form a stable oxide surface. The virgin cast iron plunger was used to press 30 glass samples in total. An SEM examination was carried out on 3 glass samples (i.e. the first, the middle sample (15th) and the last glass sample (30th) made) and the cast iron surface after it had pressed 30 glass samples.

Figure 54 shows a secondary electron image of the first glass sample made using the heat treated virgin cast iron plunger with a 120 grit finish at an initial plunger temperature of 510°C.
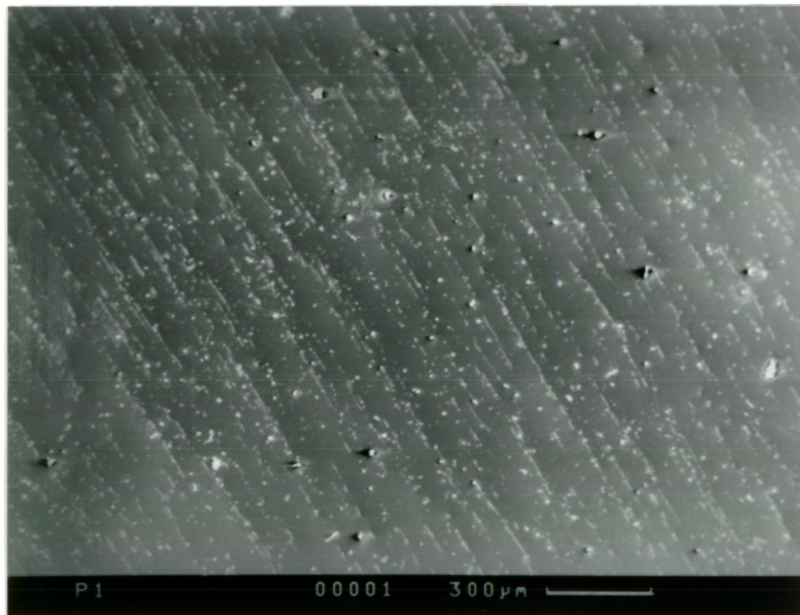


**Figure 54: Secondary electron image showing the first glass surface pressed using the heat treated virgin cast iron plunger with a 120 grit finish at an initial plunger temperature of 510°C.**

It can be seen from Figure 54 that the pressed surface of the first glass sample is made up from parallel rows of dimples. The glass surface is also covered in particles. Figure 55 shows a back-scattered electron image of the pressed glass surface at the same magnification to show areas with differing composition.
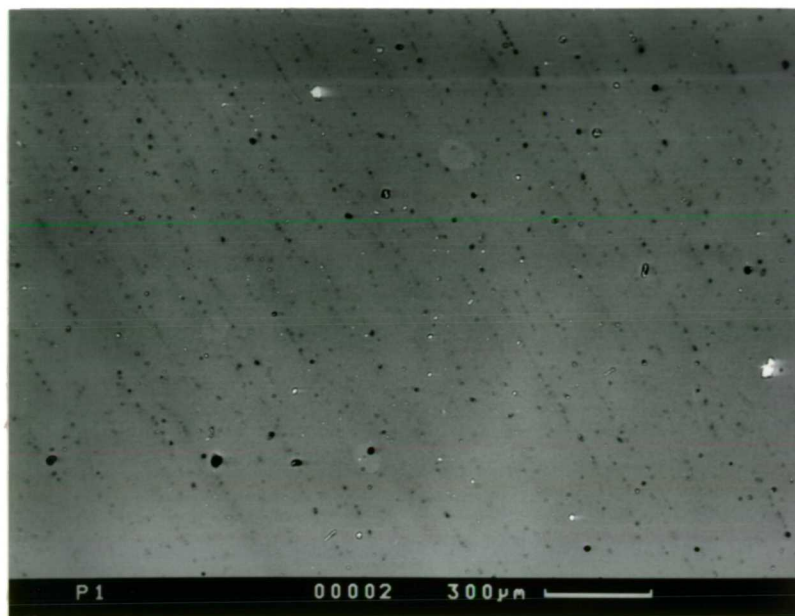


**Figure 55: Back-scattered electron image of the first glass surface pressed using the heat treated virgin cast iron plunger with a 120 grit finish at an initial plunger temperature of 510°C.**

The bright particles seen on the surface of the first pressed glass sample have analysed as being iron rich and are therefore most likely to have originated from the cast iron plunger. The dark areas seen on Figure 55 have been found to be that of glass or are deep dimples.

At a higher magnification, it can be seen that the bright particles on the surface of the pressed glass sample are made up of different sizes. Figure 56 and Figure 57

respectively show the secondary electron and back-scattered electron images of the first glass sample pressed using the heat treated virgin cast iron plunger with a 120 grit finish at an initial plunger temperature of 510°C.
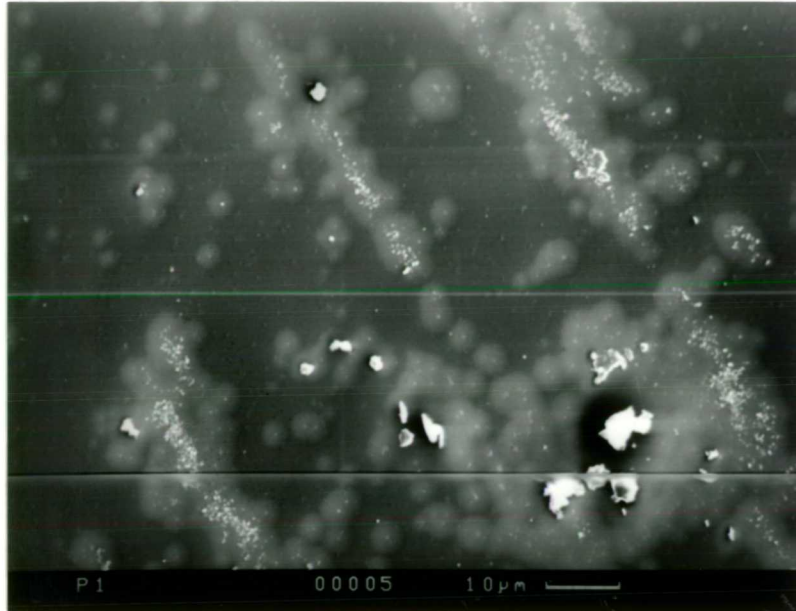


Figure 56: Secondary electron image of the surface of the first pressed glass sample produced using the heat treated cast iron plunger with a 120 grit finish at an initial plunger temperature of 510°C (please note: the parallel lines seen on the micrograph are not real features, but occurred during the electron scan possibly due to vibration).

**Figure 57: Back-scattered electron image of the surface of the first glass surface produced using the heat treated virgin cast iron plunger with a 120 grit finish at an initial plunger temperature of 510°C.**

It can be seen from Figure 56 and Figure 57 that at higher magnifications, the surface of the first glass sample pressed using the heat treated virgin cast iron plunger with a 120 grit finish at an initial plunger temperature of 510°C that sub-micron particles appear to be clustered around the pressed-in grooves. In addition, larger particles can be seen which appear to be sited in a more random fashion. EDS analysis has revealed that both types of particles are iron rich.

A high magnification three dimensional image of the 2<sup>nd</sup> glass surface which had been pressed using a cast iron plunger with a 120 grit finish at an initial plunger temperature of 510°C can be found in Figure 58.

Figure 58: Three dimensional atomic force microscopy image of the 2$^{nd}$ glass surface which had been pressed using a cast iron plunger with a 120 grit unidirectional finish at an initial plunger temperature of 510°C.

It can be seen in Figure 58 that there are a group of dimples present on the glass surface together with evidence of pressed-in particles. The dimples are between 9 and 17μm across and 350-500nm deep. The base of the large dimple seen in the centre of Figure 58 can be seen to have small protrusions attached to it. This corresponds with the iron rich particles seen previously in Figure 56.

Figure 59 and Figure 60 respectively show low magnification secondary electron and back-scattered electron images of the fifteenth (middle) glass sample pressed using a heat-treated virgin cast iron plunger with a 120 grit finish at an initial plunger temperature of 510°C.
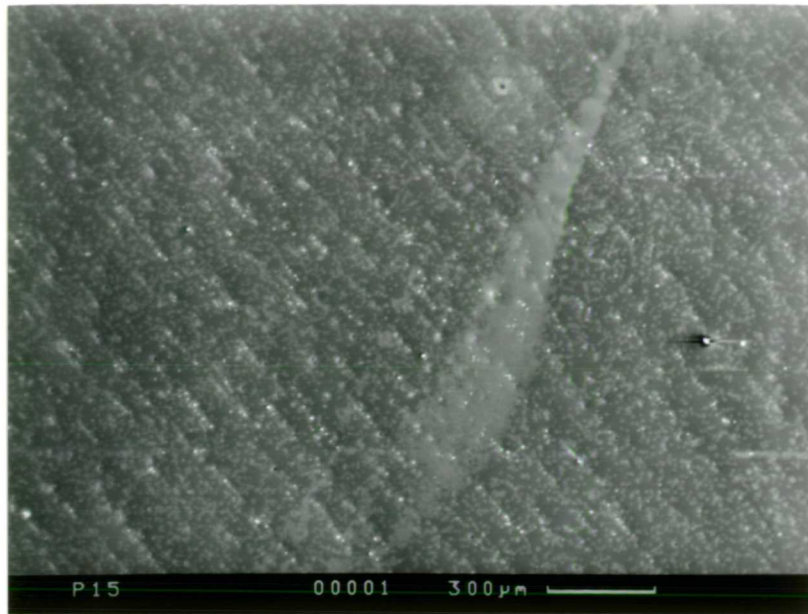
Figure 59: Secondary electron image of the fifteenth (middle) glass sample made using the heat treated virgin cast iron plunger with a 120 grit finish at an initial plunger temperature of 510°C.
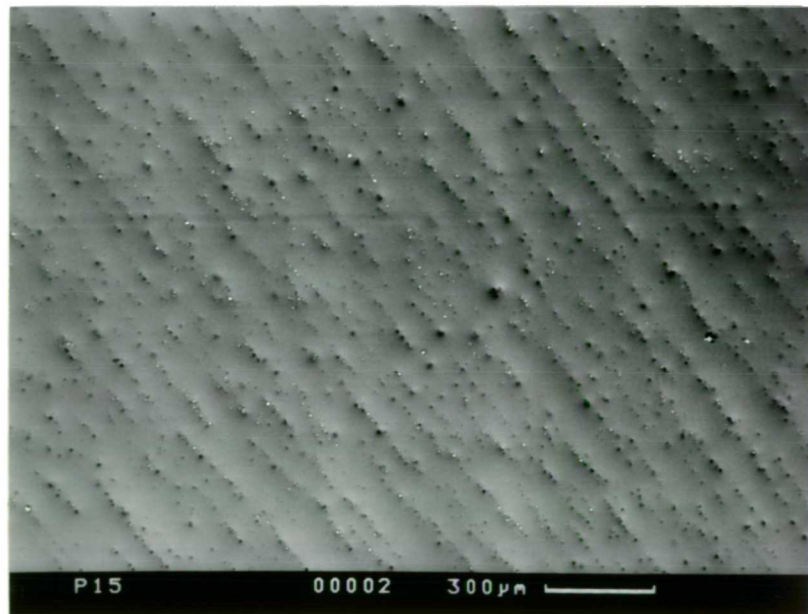


Figure 60: Back-scattered electron image of the fifteenth (middle) glass sample made using the heat treated virgin cast iron plunger with a 120 grit finish at an initial plunger temperature of 510°C.
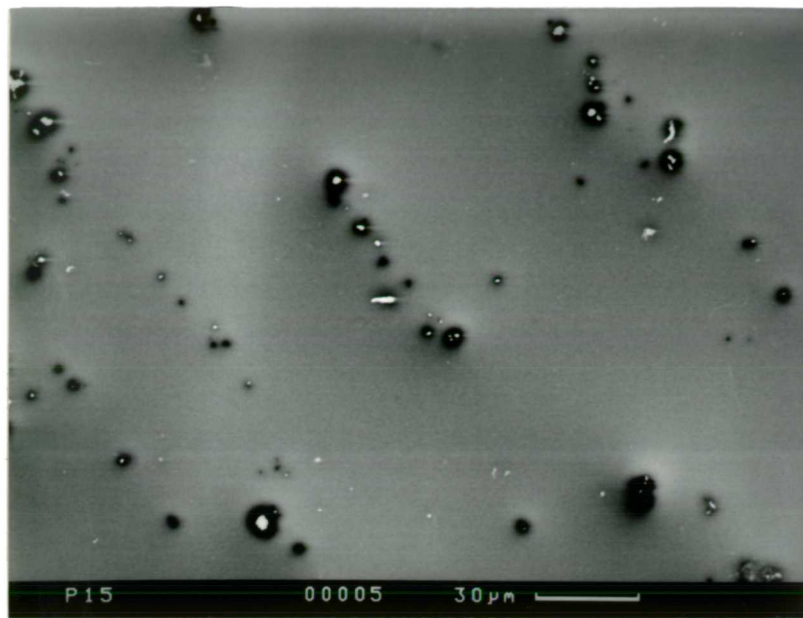
**Figure 62: Back-scattered electron image of the fifteenth (middle) glass sample made using the heat treated virgin cast iron plunger with a 120 grit surface finish at an initial plunger temperature of 510°C.**

It can be seen from Figure 61 and Figure 62 that the sub-micron iron rich particles seen in Figure 56 and Figure 57 are not present on the fifteenth pressed glass surface. However, the larger particles are still evident but these now appear to correspond to being sited in the base of dimples.

Figure 63 and Figure 64 respectively show low magnification secondary electron and back-scattered electron images of the thirtieth (i.e. last) glass sample pressed using the heat-treated virgin cast iron plunger with a 120 grit finish at an initial plunger temperature of 510°C.
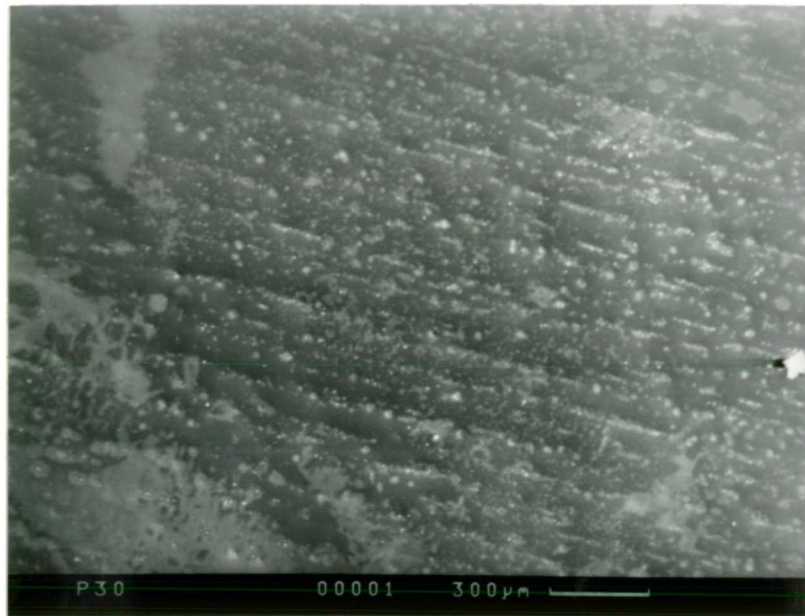
Figure 63: Secondary electron image of the thirtieth (last) glass sample made using the heat treated virgin cast iron plunger with a 120 grit surface finish at an initial plunger temperature of 510°C.
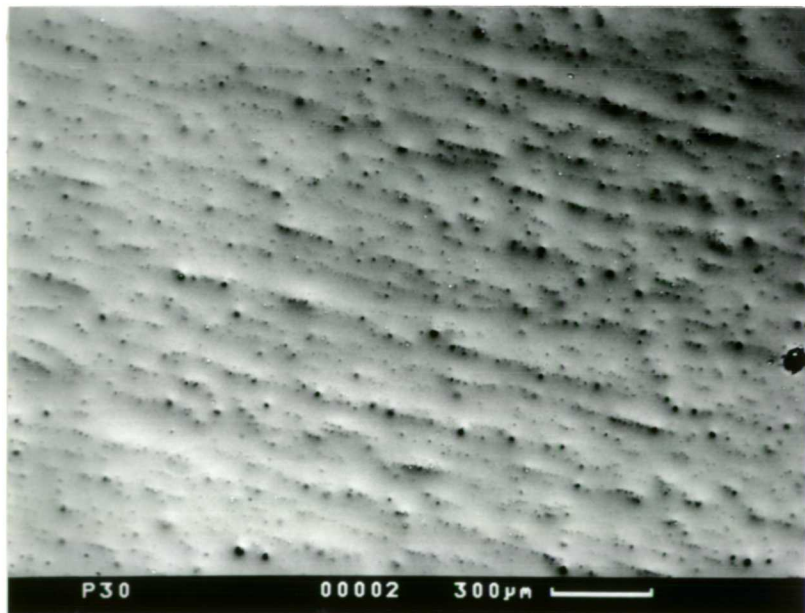


Figure 64: Back-scattered electron image of the thirtieth (last) glass sample made using the heat treated virgin cast iron plunger with a 120 grit finish at an initial plunger temperature of 510°C.

It can be seen from Figure 63 and Figure 64 that the thirtieth glass sample made still appears to have the rows of dimples present as seen in the glass samples which had been pressed earlier (i.e. the first (Figure 54 and Figure 57) and fifteenth (Figure 59 and Figure 62) pressed glass samples). The iron rich particles seen on previous samples, however, do not appear to be present on the thirtieth pressed glass sample in the same quantities, with very few being seen.

A high magnification three dimensional atomic force microscopy image of the $29^{th}$ glass surface which had been pressed using a cast iron plunger with a 120 grit finish at an initial plunger temperature of 510°C can be seen in Figure 65.
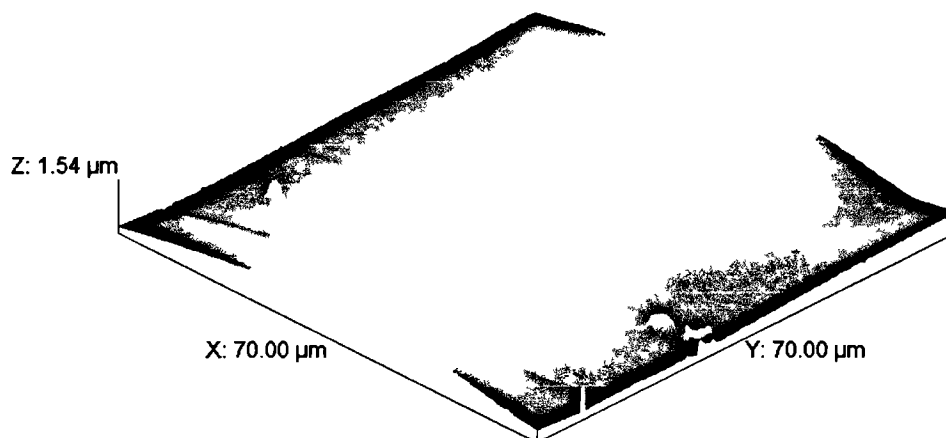


Figure 65: Three dimensional atomic force microscopy image of the $29^{th}$ glass surface which had been pressed using a cast iron plunger with a 120 grit unidirectional finish at an initial plunger temperature of 510°C.

The pressed glass surface seen in Figure 65 can be seen to consist of rows of dimples which are approximately 60μm apart. These dimples have been found to

be approximately 300nm deep and 15μm across. This indicates that the dimples formed by pressing using a cast iron plunger with a 120 grit finish at an initial plunger temperature of 510°C become shallower after time (i.e. the dimples formed in the 2nd pressed sample were 350-500nm deep as seen in Figure 58). This may indicate that the difference in height between the ridges and troughs of the cast iron used to press reduces after each contact producing shallower pressed-in dimples in the pressed glass sample.

Figure 66 shows the secondary electron image of the heat treated virgin cast iron plunger with a 120 grit finish which had been used to produce thirty pressed glass samples at an initial plunger temperature of 510°C.
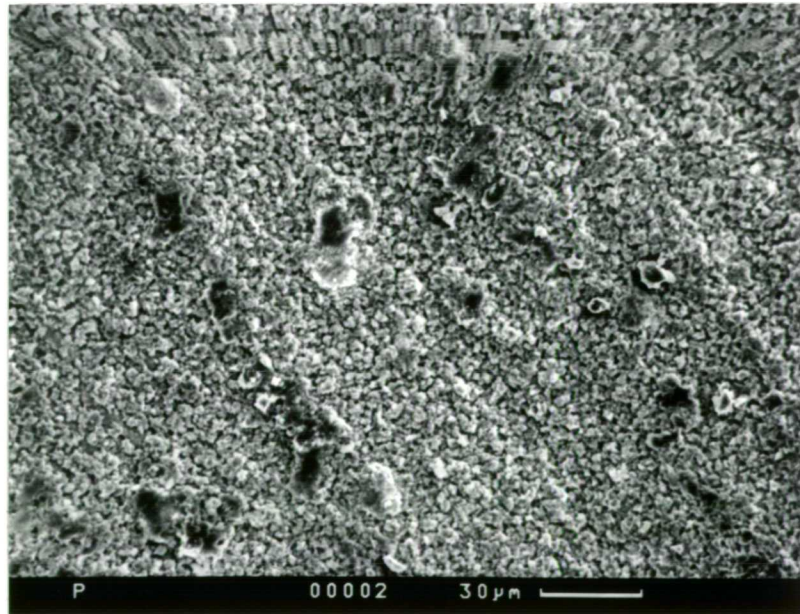


**Figure 66: Secondary electron image of the heat treated virgin cast iron plunger with a 120 grit finish which had been used to press thirty glass samples at an initial plunger temperature of 510°C.**

It can be seen from Figure 66 that the surface of the heat treated virgin cast iron plunger with a 120 grit finish which had been used to press thirty glass samples at an initial plunger temperature of 510°C appears very different from a similar plunger which had pressed 5 glass samples (Figure 28). The finer fibrous appearing particles, which have been seen previously, have disappeared. It is likely that these fine particles were loosely adhering and have been transferred to the surface of the pressed glass samples during contact. In addition, the heat-treated virgin cast iron plunger surface also appeared to have a few particles adhered to it. Figure 67 shows a back-scattered electron image of one of the particles, approximately 40μm in size, found adhered to the surface of the heat treated virgin cast iron plunger with a 120 grit finish used to press 30 glass samples at an initial plunger temperature of 510°C. It should be noted that the finer bright particles seen in Figure 67 were found to be iron rich and were likely to be iron oxide.
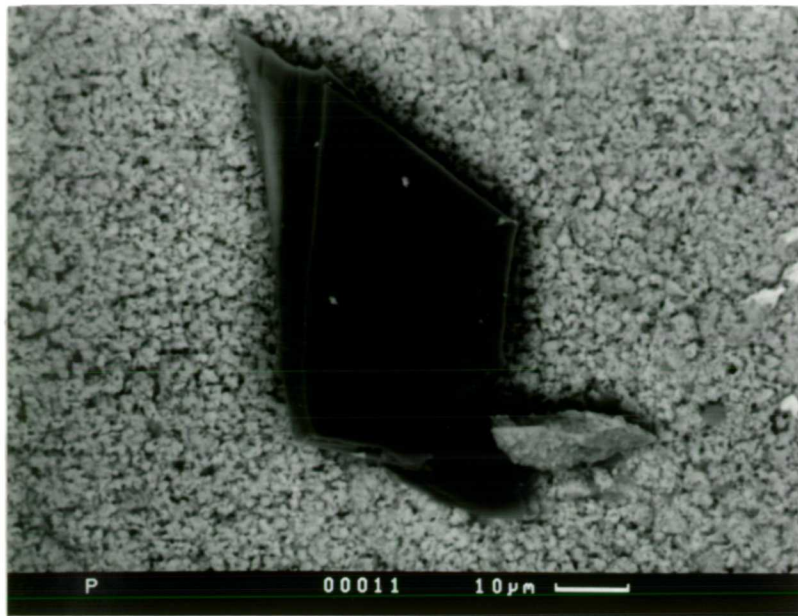
**Figure 67: Back-scattered electron image of the heat treated virgin cast iron plunger with a 120 grit finish which had been used to press thirty glass samples at an initial plunger temperature of 510°C showing a particle approximately 40μm in size.**

An x-ray photoelectron spectroscopy investigation of the heat treated cast iron sample which had been used to make 30 pressed glass samples at an initial plunger temperature of 510°C was carried out to determine whether any material transfer from the glass to the plunger had occurred during contact. Figure 68 shows the XPS widescan of the heat treated virgin cast iron surface used to press 30 glass samples at an initial plunger temperature of 510°C.
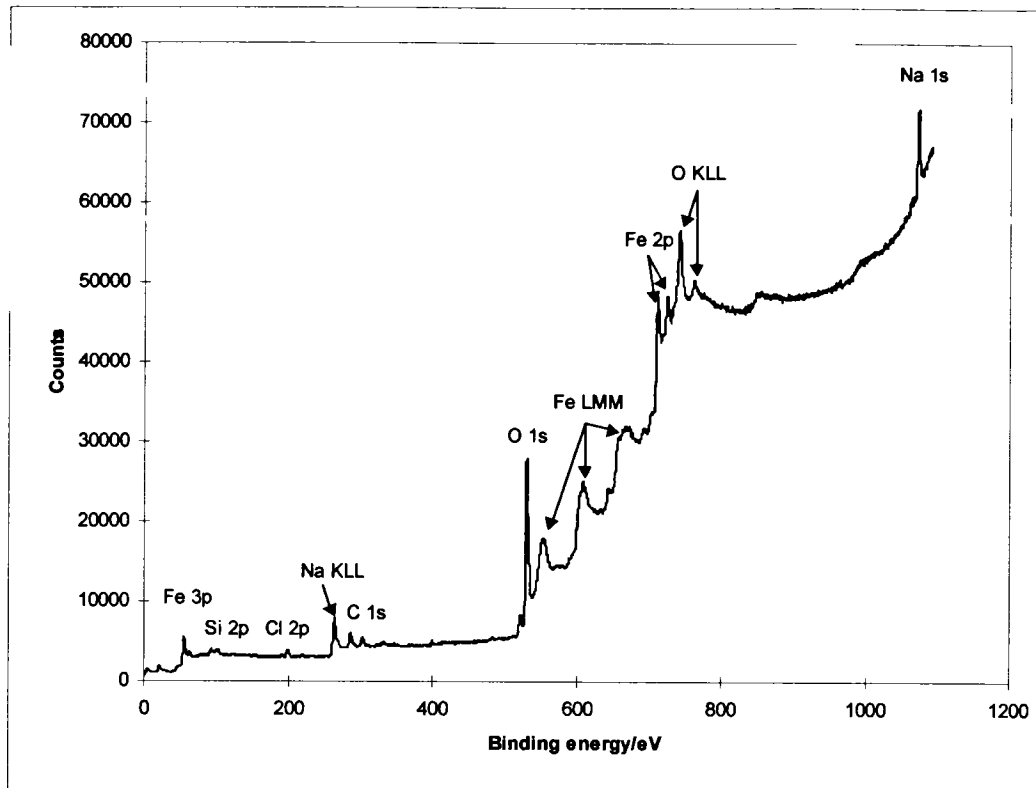
**Figure 68:** X-ray photoelectron spectroscopy widescan of a heat treated virgin cast iron plunger which had been used to make 30 pressed glass samples at an initial plunger temperature of 510°C (30° take off angle using a MgKα source).

It can be seen from Figure 68 that the surface of the heat treated virgin cast iron plunger with a 120 grit finish which had been used to make 30 glass samples at an initial plunger temperature of 510°C is made up from Si, C, O and Fe but also appears to contain Cl and Na.

Quantification of the results obtained from the widescan seen in Figure 68 can be found in Table 7.

| Element | Concentration /Atomic % |
|---------|------------------------|
| Si | 31.8±3 |
| C | 13.3±1.5 |
| Fe | 4.1±0.4 |
| O | 46.5±5 |
| Na | 2.1±0.2 |
| Cl | 2.1±0.2 |

**Table 7: Quantification of the heat treated cast iron plunger with a 120 grit finish used to make 30 pressed glass samples at an initial plunger temperature of 510°C.**

From Table 7 it can be seen that after glass contact, the iron and silicon levels in the surface of the cast iron plunger increase whilst the carbon level decreases when compared to a cast iron surface with heat treatment, but no glass contact (Table 4). The increase in silicon levels may indicate the presence of glass on the surface of the cast iron plunger after contact. The decrease in the carbon level after glass contact probably indicates that the soft graphite in the plunger surface has been removed during pressing.

As it was possible that the Na and Cl could be present on the plunger surface as contamination from handling, an XPS widescan was repeated after the plunger had been ultrasonically cleaned in HPLC grade acetone for 15 minutes to remove any surface contamination. Figure 69 shows the survey scan obtained from the heat treated virgin cast iron plunger with a 120 grit finish after making 30 pressed

glass samples at an initial plunger temperature of 510°C after being ultrasonically

cleaned in HPLC grade acetone for 15 minutes.
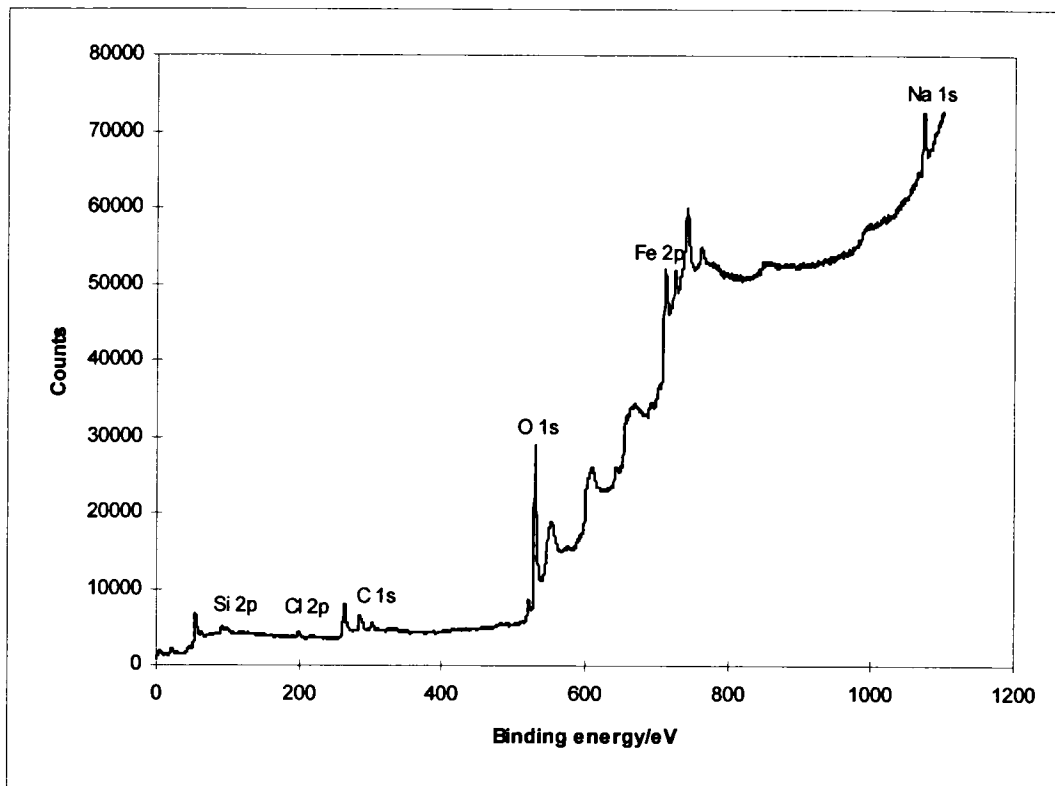


**Figure 69:** X-ray photoelectron spectroscopy widescan of a heat treated virgin cast iron plunger with a 120 grit finish which had been used to make 30 pressed glass samples at an initial plunger temperature of 510°C after being ultrasonically cleaned in HPLC grade acetone (30° take off angle using a MgKα source).

It can be seen from Figure 69 that the surface of the heat treated virgin cast iron

plunger used to make 30 pressed glass samples still appears to contain sodium and

chlorine. Therefore narrow scans (i.e. scans in finer detail) were carried out over

the binding energies where sodium and chlorine lay (see Figure 70 and Figure 71

respectively). This was done to try and determine in which chemical state (i.e.

what the sodium and chlorine were most likely to be bonded to) the two possible

contaminants were to decide whether they were due to contamination from handling or due to material transfer which occurred during pressing.
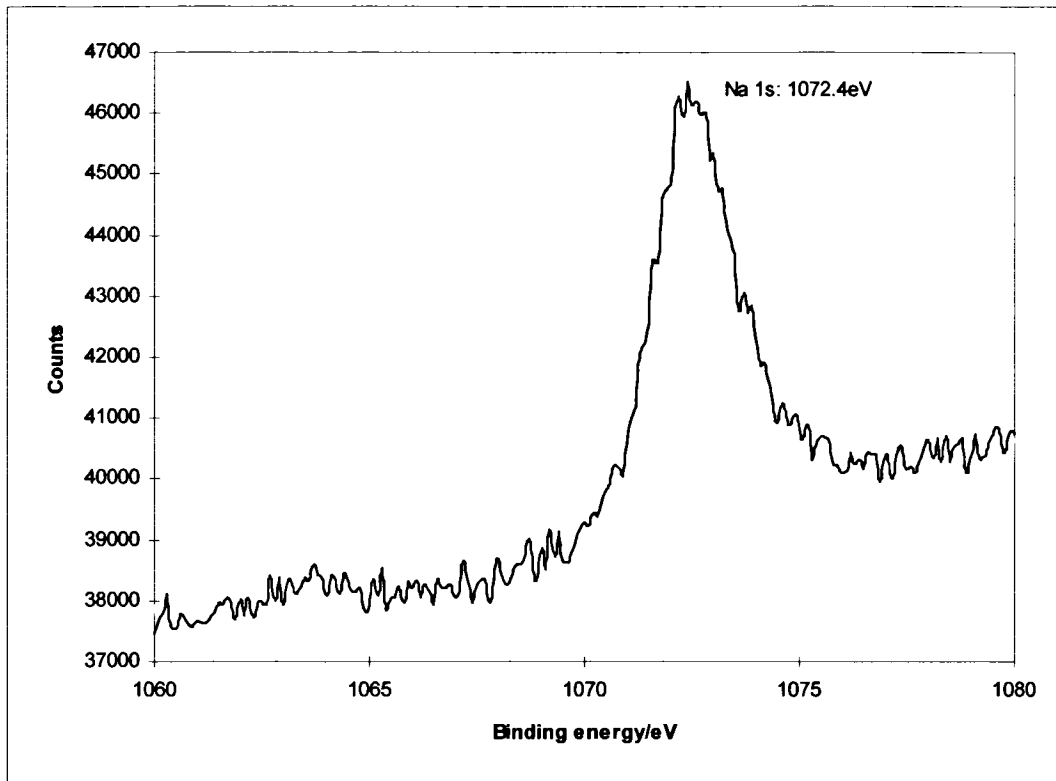


**Figure 70:** X-ray photoelectron spectroscopy narrow scan of the sodium peak from the heat treated virgin cast iron plunger with a 120 grit finish after making 30 pressed glass samples at an initial plunger temperature of 510°C (30° take off angle using a MgKα source).
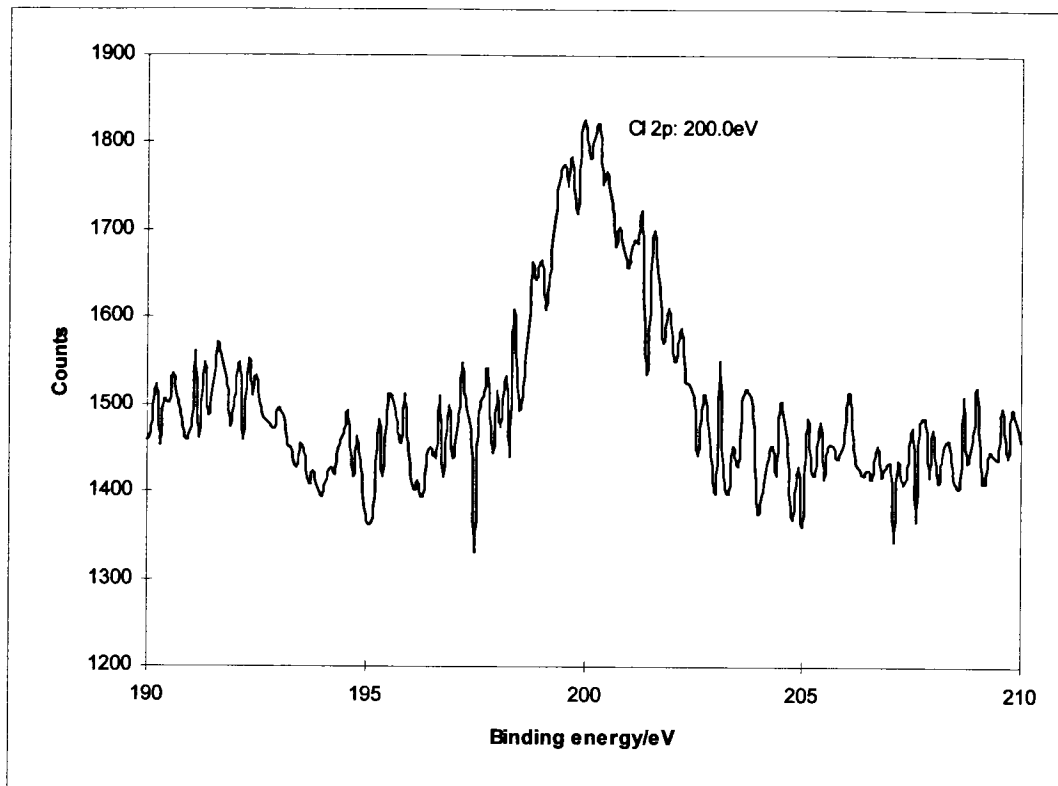
**Figure 71: X-ray photoelectron spectroscopy narrow scan of the chlorine peak from the heat treated virgin cast iron plunger with a 120 grit finish after making 30 pressed glass samples at an initial plunger temperature of 510°C (30° take off angle using a MgKα source).**

The positions of the sodium and chlorine peaks achieved discount the possibility that these species are present due to contamination of NaCl from handling (i.e. the expected peak position for Na would be 1071.6 eV and the expected peak position for Cl would be 198.6 eV for NaCl). The peak position obtained for sodium (i.e. 1072.4 eV) could possibly be due to $Na_2O$ (1072.5 eV). A table of the observed peak positions for Na and Cl compared with those expected for NaCl can be found in Table 8.

| | Peak position / eV | | |
|---|---|---|---|
| | **Observed** | **Expected for NaCl** | **Expected for Na₂O** |
| **Na** | 1072.4 | 1071.6 | 1072.5 |
| **Cl** | 200.0 | 198.6 | - |

**Table 8: Comparison of the observed and theoretical x-ray photoelectron spectroscopy peak positions for sodium and chlorine using magnesium x-rays [Briggs and Seah_1990]**

As the data sets available regarding XPS peak position data are limited, no conclusions could be reached regarding the position of the chlorine.

Quantification of the results obtained from the widescan seen in Figure 69 can be found in Table 9.

| **Element** | **Concentration /Atomic %** |
|---|---|
| Si | 18.0±2 |
| C | 20.5±2 |
| Fe | 4.6±0.5 |
| O | 53.5±5 |
| Na | 2.0±0.2 |
| Cl | 1.5±0.15 |

**Table 9: Quantification of the heat treated virgin cast iron plunger used to make 30 pressed glass samples at an initial plunger temperature of 510°C after ultrasonic cleaning in HPLC grade acetone.**

Table 9 shows that after cleaning the cast iron plunger, the silicon level on the surface decreases (*c.f.* Table 7). This may indicate that any glass on the surface of the plunger was loosely adhering and was therefore removed by the cleaning procedure. The sodium level present on the plunger surface after cleaning, however, appeared to stay constant indicating that there may have been some form of sodium ion transfer from the glass to the plunger on pressing.

A cast iron plunger with a unidirectional 120 grit finish which had been made from the working surface of a discarded blank mould (supplied by *Rockware Glass Ltd., Knottingley, UK*, see section 3.1.2.4) and heat treated by holding at 470°C in static air for 30 hours was used to press 23 glass surfaces using an initial plunger temperature of 510°C. Both the pressed glass samples and the cast iron plunger surface appeared very similar to those prepared using the virgin cast iron (supplied by *Birstall Foundary, UK*, see section 3.1.2.4).

### 3.1.2.5 Vacuum Assisted Pressing

Several glass containers have regions which are difficult to form without the aid of vacuum assistance. These difficult to form regions would include areas such as the shoulders of jars as these regions have a fairly sharp radius of curvature where it is difficult for the glass melt to flow to fill the mould without assistance. Vacuum assistance is therefore used to pull the glass melt into areas where it would have difficulty in flowing before becoming too viscous for further flow to take place.

It was therefore for this reason, in addition to forcing the glass and plunger to have more intimate contact during pressing without the possibility of an air cushion

being present, that glass samples were pressed using vacuum assisted pressing. The vacuum assisted pressing was achieved by drilling a hole of 0.7mm in the centre of the plunger sample through which air was pulled using a rotary pump producing a small pressure of 1mmHg to be formed when the glass melt came into contact with the plunger housing (see Figure 6). Glass samples were pressed at the two extreme initial plunger temperatures of 300°C and 510°C using plungers made from discarded cast iron blank moulds (supplied by *Rockware Glass Ltd., Knottingley, UK*) for comparison. In this series of pressings the initial glass temperature (950°C), press time (4 seconds), glass composition, number of glass-to metal contacts, atmosphere (crude vacuum) and pressing pressure ($2 \times 10^5$ Pa) have all been kept constant with only the initial plunger temperature being varied.

Figure 72 and Figure 73 show secondary electron images of the 5th glass surface that had been pressed using a cast iron plunger with a 120 grit finish at an initial plunger temperature of 300°C using vacuum assistance.
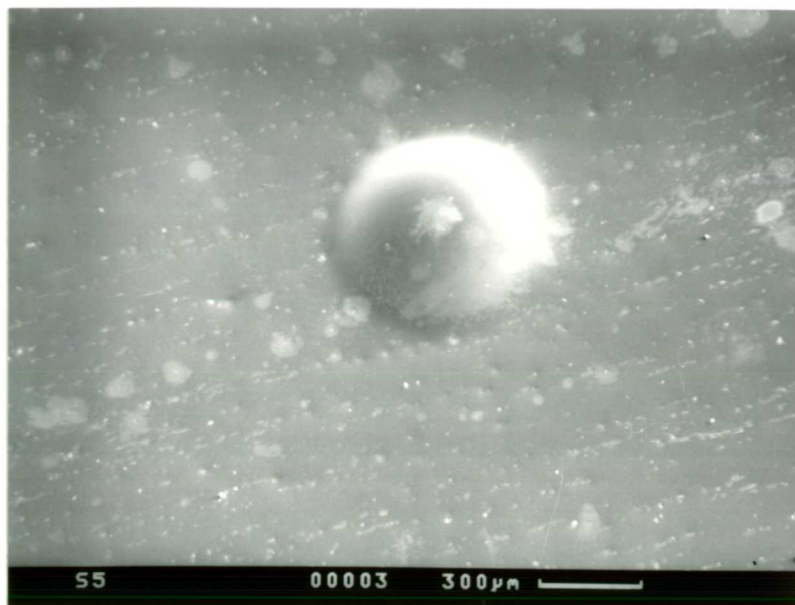
**Figure 72: Secondary electron image of the 5<sup>th</sup> glass surface pressed using a heat treated cast iron plunger with a 120 grit finish at an initial plunger temperature of 300°C using vacuum assistance showing a protruding pimple approximately 600µm in diameter.**

The protruding pimple which is approximately 600µm in diameter seen in the centre of Figure 72 has resulted due to the glass melt being pulled into the hole in the centre of the cast iron plunger by the vacuum during pressing. It can be seen that rows of pressed-in dimples are present on the pressed glass surface. The glass surface which was pressed using the same conditions (i.e.120 grit finish and initial plunger temperature of 300°C) without vacuum assistance does not have these aligned dimples present, but randomly oriented pressed-in dimples (Figure 26). This may therefore suggest that there is closer contact of the glass to the plunger when vacuum assistance is utilised. This closer contact may be due to either the extra 'pressing force' exerted due to the vacuum or that a possible air cushion has been removed which inhibited close contact previously.
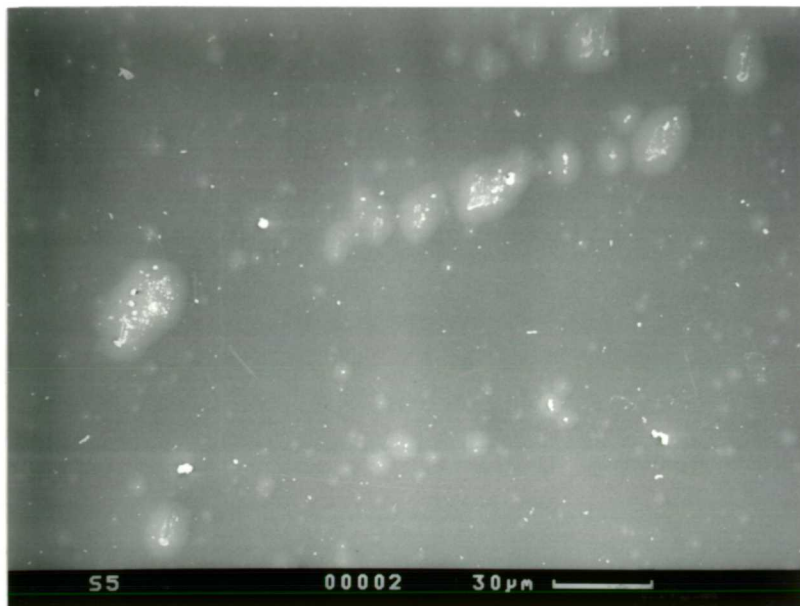
**Figure 73: High magnification secondary electron image of the 5th glass surface pressed using a heat-treated cast iron plunger with a unidirectional 120 grit finish at an initial plunger temperature of 300°C using vacuum assistance.**

Figure 73 shows that there are numerous sub-micron particles present on the glass surface pressed using a heat-treated cast iron surface with a 120 grit finish at an initial plunger temperature of 300°C. These particles appear to be concentrated on the bases of the dimples seen on the pressed glass surface. EDS analysis has revealed these particles to be iron rich. The glass surface which had been pressed using the same initial plunger temperature and plunger surface finish without vacuum assistance, did not appear to have these particles concentrated at the base of the dimples, but were more randomly oriented (see Figure 33).

Figure 74 shows a secondary electron image of a heat-treated cast iron plunger with a 120 grit finish that had been used to make 5 pressed glass samples at an initial plunger temperature of 300°C using vacuum assistance.
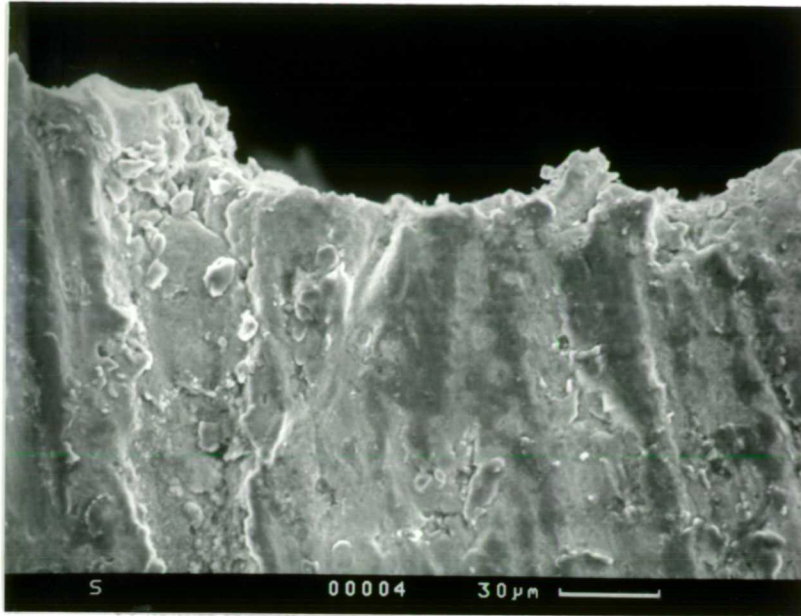
**Figure 74: Secondary electron image of a cast iron surface with a 120 grit finish which had been used to press 5 glass samples with an initial plunger temperature of 300°C using vacuum assistance (showing the central hole in the plunger that was used to pull the air through as the black area at the top).**

Figure 74 appears similar to the plunger used with the same pressing parameters without vacuum assistance (Figure 25).

Figure 75 and Figure 76 show secondary electron images of the 5th pressed glass surface made using a cast iron plunger with a 120 grit finish at an initial plunger temperature of 510°C using vacuum assistance.

Figure 75: Secondary electron image of the 5th pressed glass surface made using a cast iron plunger with a 120 grit finish at an initial plunger temperature of 510°C using vacuum assistance showing the raised pimple, with particles attached at its apex, approximately 650μm diameter in the top right hand corner resulting from the hole in the cast iron plunger used for applying the vacuum.
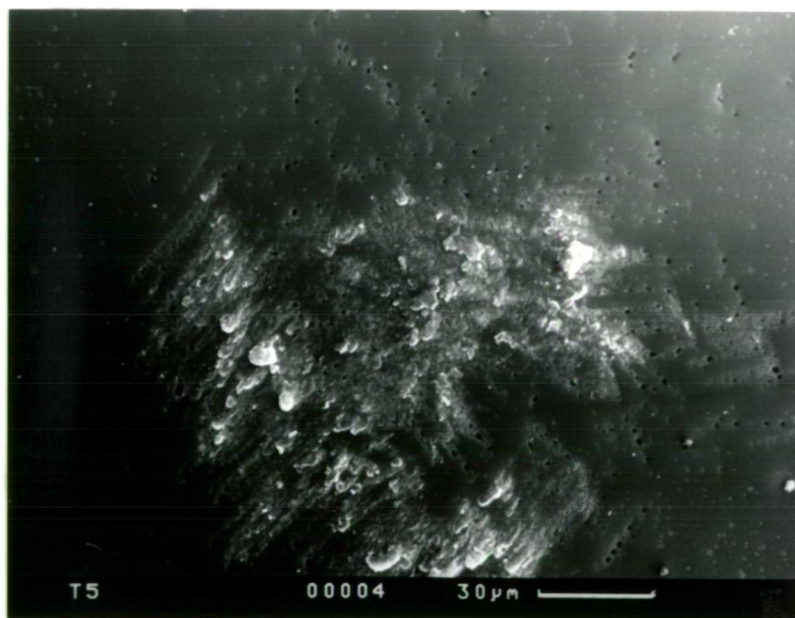


Figure 76: Secondary electron image of the central raised pimple (seen in Figure 75) formed on the 5th pressed glass surface made using a cast iron plunger with a 120 grit finish at an initial plunger temperature of 510°C using vacuum assistance.

It can be seen from Figure 75 that the surface of the 5$^{th}$ glass sample made using a heat treated cast iron plunger with a 120 grit finish at an initial plunger temperature of 510°C with vacuum assistance is made up from what appears to be parallel grooves. These grooves appear to be closer together on the glass sample prepared at an initial plunger temperature of 510°C when compared to the sample made at 300°C (Figure 72). The particles found in the centre of the raised pimple (Figure 76) on the glass sample seen in Figure 75 have been found to be iron rich using EDS. The presence of the raised pimple on the surface of the pressed glass samples is inevitable due to the design of the vacuum pressing rig.

A three dimensional atomic force microscopy image of the 4$^{th}$ glass sample pressed using a cast iron plunger with a 120 grit finish at an initial plunger temperature of 510°C using vacuum assistance can be found in Figure 77.



Z: 1.62 μm

X: 70.00 μm

Y: 70.00 μm
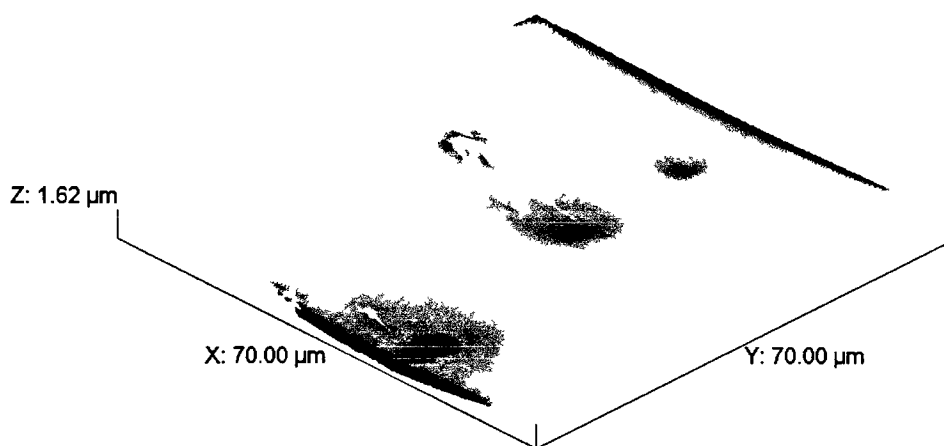
Figure 77: Three dimensional atomic force microscopy image of the 4$^{th}$ glass surface made using a cast iron plunger with a 120 grit unidirectional surface finish at an initial plunger temperature of 510°C using vacuum assistance.

Figure 77 shows that there is a row of dimples present on the pressed glass surface which are approximately 30μm apart. Also present on the surface are pressed in particles.

### 3.1.3 Carbon-Carbon Composite Plunger Material

In addition to the traditional blank mould material commonly used in glass container manufacture (i.e. grey cast iron with a fine equiaxed grained working surface), behaviour of carbon-carbon composite materials on pressing glass samples was investigated to determine whether they were suitable for this type of application. In practice, glass container manufacturers use carbon based mould dopes to aid the loading of the gob into the blank mould and to avoid sticking between the melt and the hot metal. The use of a graphite-based material might eliminate the need for manual mould doping (see Chapter 1). Unfortunately, graphite does not have good mechanical properties on its own and a mould made from this would not last the long enough for a full production run. It was postulated that the use of a graphite based composite material may therefore be a potential mould material which could be engineered to give the benefits of a graphite material with additional thermal and mechanical properties. The use of carbon-carbon composite materials as a possible hot glass contact material has therefore been examined here.

Glass samples were pressed at the two extreme initial plunger temperatures of 300°C and 510°C using plungers made from each of the carbon-carbon composite materials. NF-C T300 laminate, PM-C VCB-20 chopped squares and carbon felt plunger samples were received (from *HITCO Technologies Inc., USA*) which had

already been machined to the correct shape and size (see section 2.1.3.2). In this series of pressings the initial glass temperature (950°C), press time (4 seconds), glass composition, number of glass-to metal contacts, atmosphere and pressing pressure ($2\times10^5$ Pa) have all been kept constant with only the initial plunger temperature being varied.

### 3.1.3.1 NF-C T300 Laminate

This type of carbon-carbon composite was made up from woven carbon fibres (produced from poly-acrylo-nitrile) in a carbon matrix.

Figure 78 and Figure 79 show secondary electron images of the carbon-carbon composite laminate material prior to any glass contact.



**Figure 78: Secondary electron image of NF-C T300 laminate carbon-carbon composite material before glass contact.**
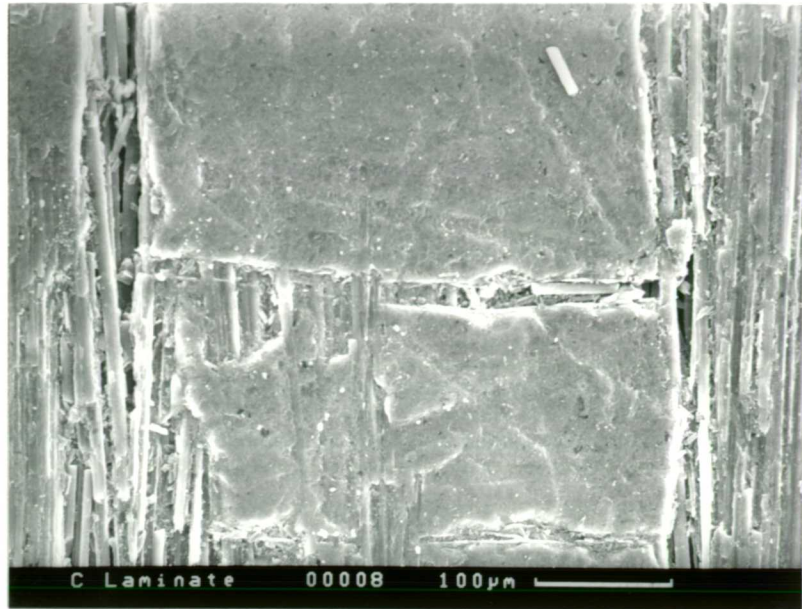
**Figure 79: High magnification secondary electron image of NF-C T300 laminate carbon-carbon composite material before glass contact.**

It can be seen from Figure 78 and Figure 79 that the carbon-carbon composite laminate material appears to be made up from parallel carbon fibres approximately 10μm in diameter. Figure 79 shows large areas where the carbon matrix has been revealed at the surface. EDS analysis revealed particles containing iron, manganese and chromium in the gaps between the fibres of the composite. The manufacturers of the composite may have introduced these particles during the machining/preparation of the plunger samples.

Figure 80 shows a secondary electron image of the fifth pressed glass surface made using a carbon-carbon composite laminate material plunger at an initial plunger temperature of 300°C.
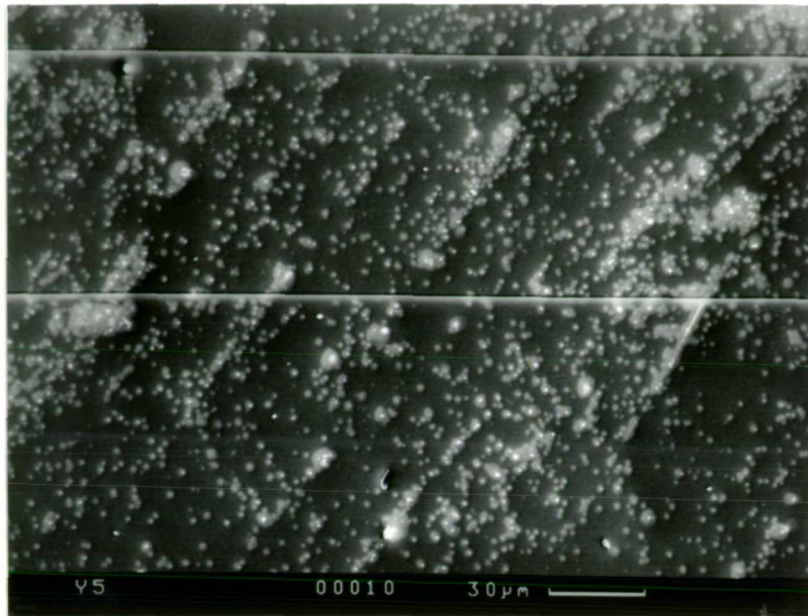
**Figure 80: Secondary electron image of the 5$^{th}$ glass surface made using the carbon-carbon composite NF-C T300 laminate material plunger at an initial plunger temperature of 300°C.**

It can be seen from Figure 80 that there appear to be grooves on the surface of the pressed glass sample. These grooves are likely to have occurred due to the glass melt flowing between the fibres in the composite. Situated in these grooves, small particles less than 5μm in size can be found. These particles were either found to contain iron, manganese and chromium or could not be analysed. As carbon can not be detected with the EDS detector used, it is likely that the latter particles were carbon from either the carbon matrix or fibres of the plunger material.

Figure 81 and Figure 82 show secondary electron images of the carbon-carbon composite laminate plunger after it had been used to make 5 pressed glass samples at an initial plunger temperature of 300°C.

It can be seen from Figure 81 that there are numerous bright particles covering the surface of the composite that had come into contact with the glass during pressing (the area without particles was contained in the retaining ring in the experimental press and had therefore not come in contact with any glass). These were found to be potassium chloride using EDS. The appearance of the laminate material after making glass samples at an initial plunger temperature of 300°C (Figure 82) is similar to the sample that had had no contact with glass (Figure 79).

Figure 83 and Figure 84 show secondary electron images of the 5th pressed glass surface made using the carbon-carbon composite laminate plunger material with an initial plunger temperature of 510°C.



**Figure 83: Secondary electron image of the 5th glass surface made using the carbon-carbon composite NF-C T300 laminate material plunger at an initial plunger temperature of 510°C.**

**Figure 84: High magnification secondary electron image of the 5ᵗʰ glass surface made using the carbon-carbon composite NF-C T300 laminate material plunger at an initial plunger temperature of 510°C.**

It can be seen from Figure 83 and Figure 84 that the glass sample made using the carbon-carbon composite NF-C T300 laminate material at an initial plunger temperature of 510°C appears to be a close replica of the composite surface. The grooves seen in the pressed glass surface would have been made due to the indentation of the fibres in the relatively fluid glass that solidified around them. The particles seen on the glass surface either contain iron, manganese or chrome which may have been introduced during machining of the plunger discs by the manufacturer, or carbon from the composite itself.

Figure 85 shows the secondary electron image of the carbon-carbon composite NF-C T300 laminate plunger material that had been used to make 5 pressed glass samples at an initial plunger temperature of 510°C.

**Figure 85: High magnification secondary electron image of carbon-carbon composite NF-C T300 laminate material plunger after making 5 pressed glass samples at an initial plunger temperature of 510°C.**

It can be seen from Figure 85 that there appears to be much less of the solid matrix present on the surface of the carbon-carbon composite laminate material after contact with hot glass at an initial plunger temperature of 510°C when compared to one with no glass contact (Figure 79). This would mean that the fibres close to the contact surface would be loose and these could therefore become detached from the bulk material and become embedded in the glass surface on contact during pressing. A small cluster of particles containing iron, chrome and manganese can be seen on the surface of the laminate plunger material in Figure 85 which may have been introduced during machining by the manufacturer.

### 3.1.3.2 PM-C VCB-20 Chopped Squares

This type of carbon-carbon composite was made up from woven carbon fibres (produced from pitch) which had been chopped into squares and held in a carbon matrix.

Figure 86 and Figure 87 show secondary electron images of the carbon-carbon composite chopped square material that had no previous contact with glass.
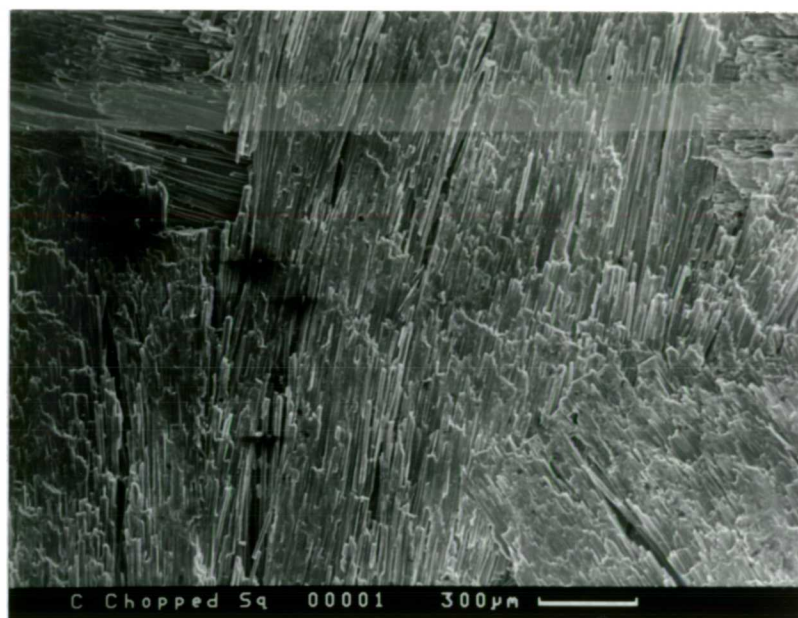


**Figure 86: Secondary electron image of carbon-carbon composite PM-C VCB-20 chopped squares material with no prior glass contact.**
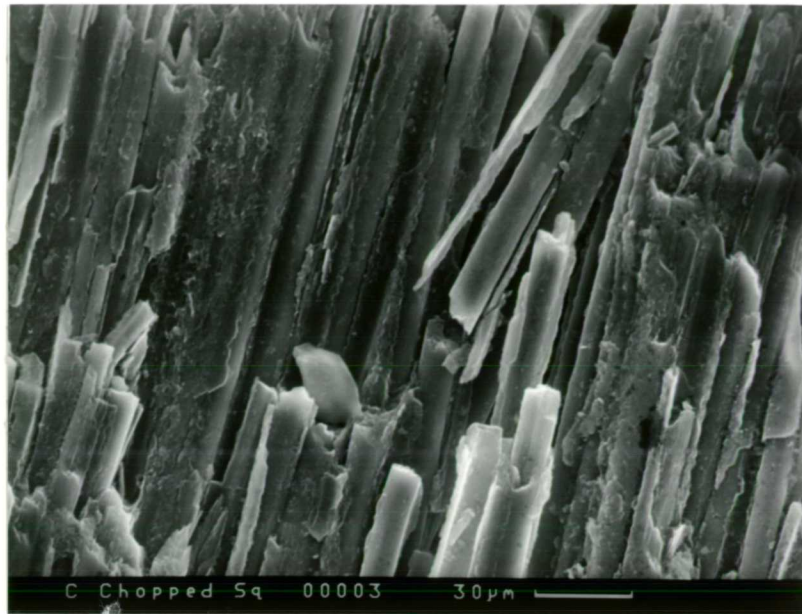
**Figure 87: High magnification secondary electron image of carbon-carbon composite PM-C VCB-20 chopped squares material with no prior glass contact.**

It can be seen in Figure 86 and Figure 87 that the carbon-carbon PM-C VCB-20 chopped squares composite material is made up from parallel carbon fibres that are approximately $10\mu m$ in diameter. EDS analysis revealed particles containing iron, manganese and chromium in the gaps between the fibres of the composite. As this type of particle appears to be present in all of the supplied carbon-carbon composite materials, as stated earlier, the manufacturers of the composite may have introduced these particles during the machining/preparation of the plunger samples.

Figure 88 shows a secondary electron image of the 5th pressed glass sample made using a carbon-carbon composite chopped squares plunger material at an initial plunger temperature of 300°C.

**Figure 88: Secondary electron image of the 5<sup>th</sup> pressed glass surface made using a carbon-carbon composite PM-C VCB-20 chopped squares plunger material at an initial plunger temperature of 300°C.**

It can be seen from Figure 88 that the surface of the pressed glass sample made using a carbon-carbon composite chopped squares plunger material at an initial plunger temperature of 300°C appears to have randomly oriented shallow grooves and dimples present. Particles seen on the pressed glass surface were either metallic or thought to be carbon.

Figure 89 shows a secondary electron image of the carbon-carbon composite chopped squares plunger material that had been used to press 5 glass samples at an initial plunger temperature of 300°C.
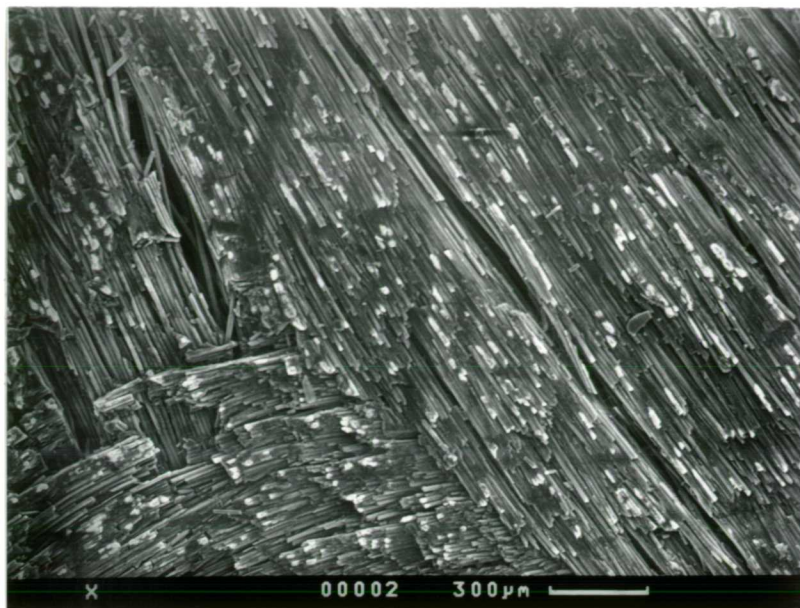
**Figure 89: Secondary electron image of the carbon-carbon composite PM-C VCB-20 chopped squares plunger material used to make 5 pressed glass samples at an initial plunger temperature of 300°C.**

It can be seen from Figure 89 that the carbon-carbon composite chopped squares plunger material which had been used to make 5 pressed glass samples at an initial plunger temperature of 300°C appears to have a small amount of debonding present (i.e. disappearance of the matrix material, causing the fibres to loosen) when compared to the same material with no glass contact (Figure 86). The bright particles seen in Figure 89 on the surface of the plunger were found to be potassium chloride (as described earlier in section 3.1.3.1).

Figure 90 and Figure 91 show secondary electron images of the 5th pressed glass surface made using the carbon-carbon composite PM-C VCB-20 chopped squares plunger material at an initial plunger temperature of 510°C.
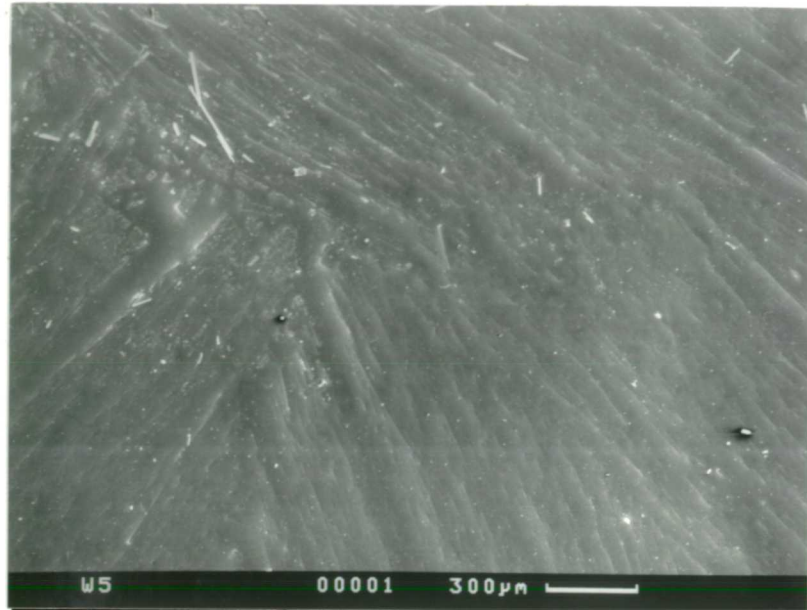
Figure 90: Secondary electron image of the 5<sup>th</sup> pressed glass surface made using the carbon-carbon composite PM-C VCB-20 chopped squares plunger material at an initial plunger temperature of 510°C.
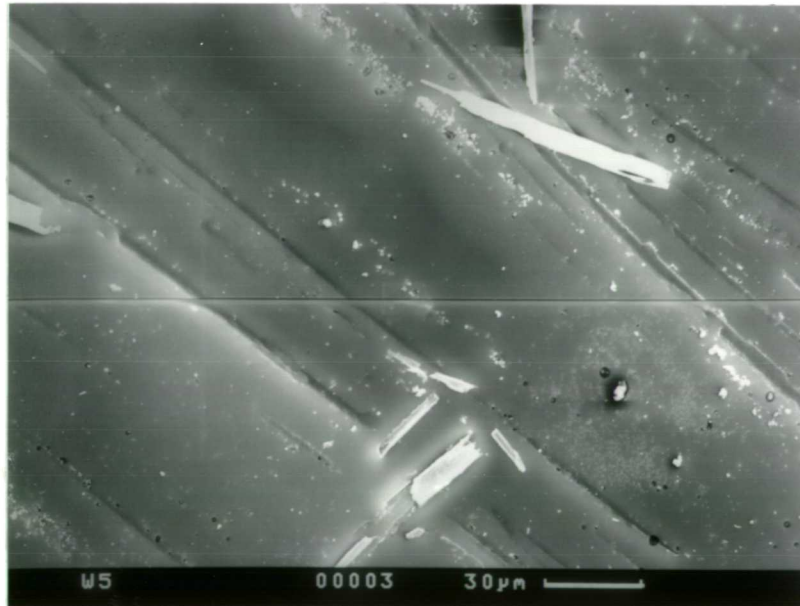


Figure 91: High magnification secondary electron image of the 5<sup>th</sup> pressed glass surface made using the carbon-carbon composite PM-C VCB-20 chopped squares plunger material at an initial plunger temperature of 510°C.

It can be seen from Figure 90 that the surface of the 5$^{th}$ glass sample made using the carbon-carbon composite PM-C VCB-20 chopped squares plunger material at an initial plunger temperature of 510°C appears to be a replica of the plunger material. Figure 91 shows that the grooves seen appear to be fairly deep and were most likely to be caused due to the fibres from the composite. The particles seen on the surface of the pressed glass sample were either metallic, or thought to be carbon. Short carbon fibres can also be seen on the pressed glass surface. This would therefore suggest that the composite material has become unstable possibly due to oxidation of the carbon matrix material during contact with the hot glass.

Figure 92 shows a secondary electron image of the carbon-carbon composite chopped squares plunger material which had been used to make 5 pressed glass samples at an initial plunger temperature of 510°C.



**Figure 92: Secondary electron image of the carbon-carbon composite PM-C VCB-20 chopped squares plunger material used to make 5 pressed glass samples at an initial plunger temperature of 510°C.**

It can be seen from Figure 92 that there does not appear to be a significant amount of the carbon matrix left in the carbon-carbon composite chopped squares plunger material after it had been used to make 5 pressed glass samples at an initial plunger temperature of 510°C. The fibres in this material appear to be loosened and could, therefore, become embedded in the glass surface on contact during pressing.

### 3.1.3.3 Carbon Felt

This type of carbon-carbon composite was made up from randomly oriented carbon fibres in a carbon matrix according to the manufacturer.

Figure 93 and Figure 94 show secondary electron images of the carbon-carbon composite felt material before any contact with hot glass.
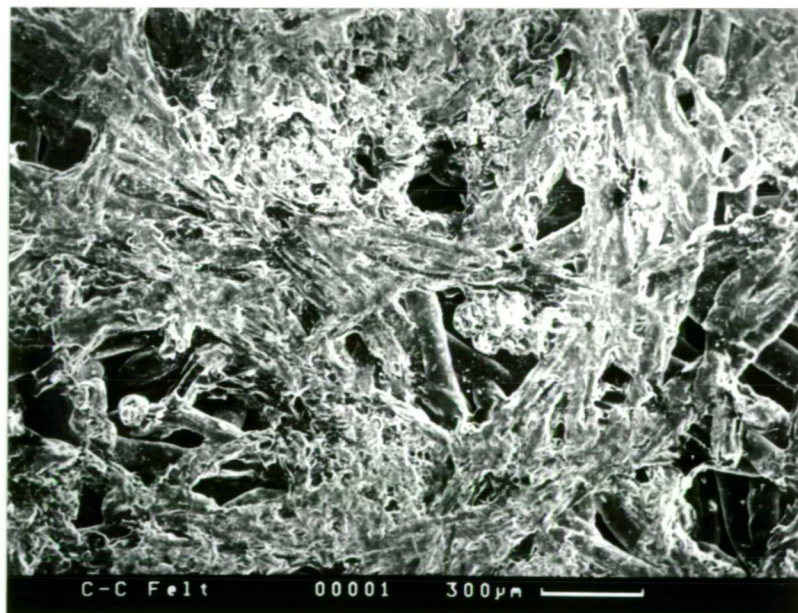


**Figure 93: Secondary electron image of carbon-carbon composite felt material with no previous glass contact.**
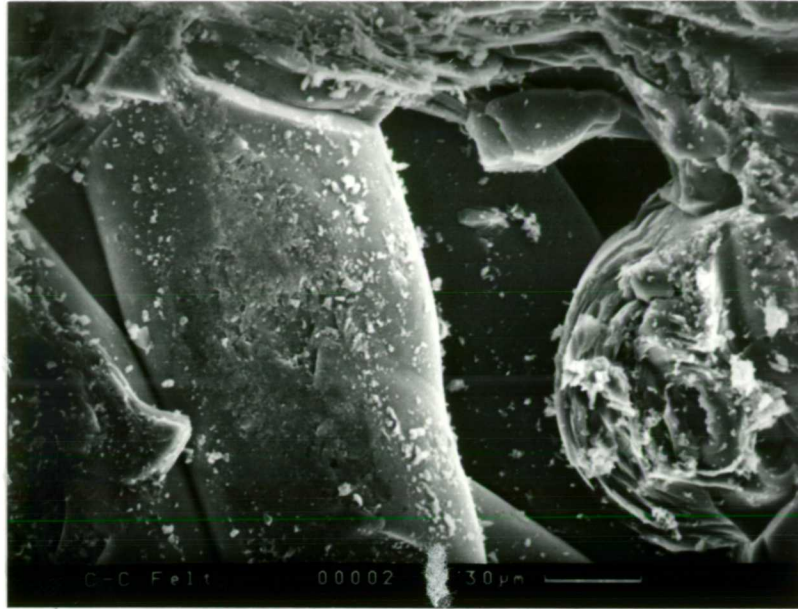
**Figure 94: High magnification secondary electron image of carbon-carbon composite felt material with no previous glass contact.**

It can be seen from Figure 93 and Figure 94 that the fibres in the carbon-carbon composite felt material form a three dimensional material (compared to the laminate (Figure 78 and Figure 79) and chopped squares (Figure 86 and Figure 87) material which were made up from layers). The fibres in the felt material are approximately 80μm in diameter. It is also apparent that the felt material has numerous voids present over the whole surface (and throughout the bulk material) that appear to range in size from about 30μm to 200μm.

Figure 95 shows a secondary electron image of the 5th pressed glass sample made using a carbon-carbon composite felt plunger material at an initial plunger temperature of 300°C.

**Figure 95: Secondary electron image of the 5<sup>th</sup> pressed glass surface made using a carbon-carbon composite felt plunger material at an initial plunger temperature of 300°C.**
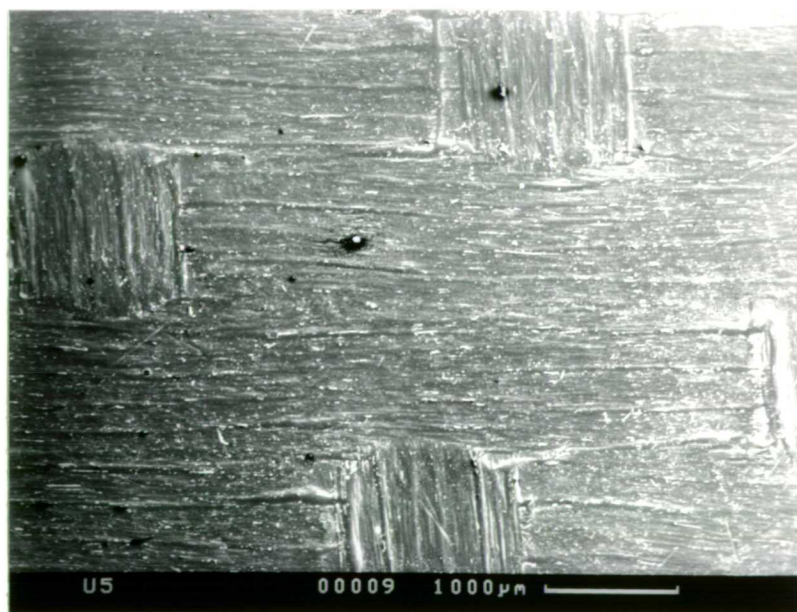
It can be seen from Figure 95 that the surface of the 5<sup>th</sup> glass sample pressed using a carbon-carbon composite felt plunger material at an initial plunger temperature of 300°C appears to be covered in rounded mounds (assuming the image is lit from the top as described in section 2.2.2). These are likely to have formed due to the relatively fluid glass melt entering the voids in the plunger surface a certain distance before becoming too viscous for further flow. The particles seen on the pressed glass surface were found to be metallic or thought to be carbon.

Figure 96 shows a secondary electron image of the carbon-carbon composite felt plunger material that had been used to make 5 pressed glass samples at an initial plunger temperature of 300°C.
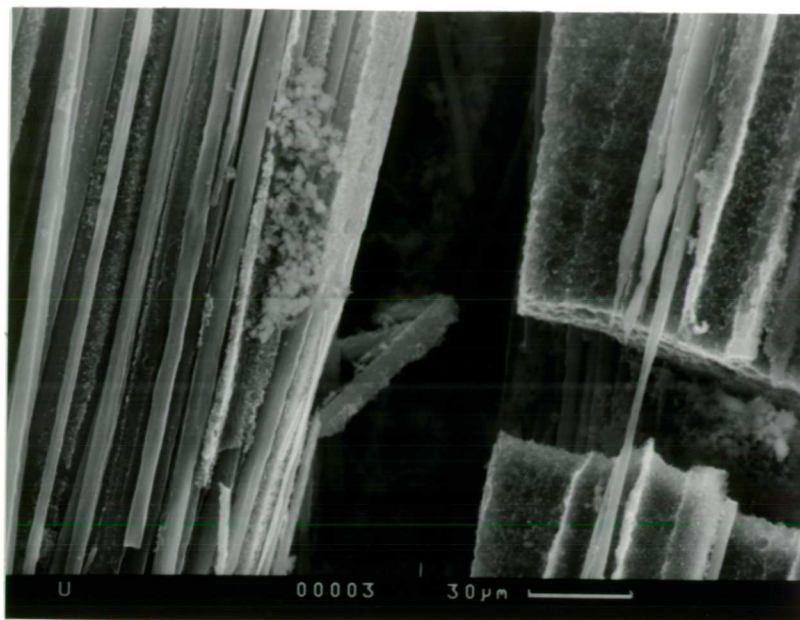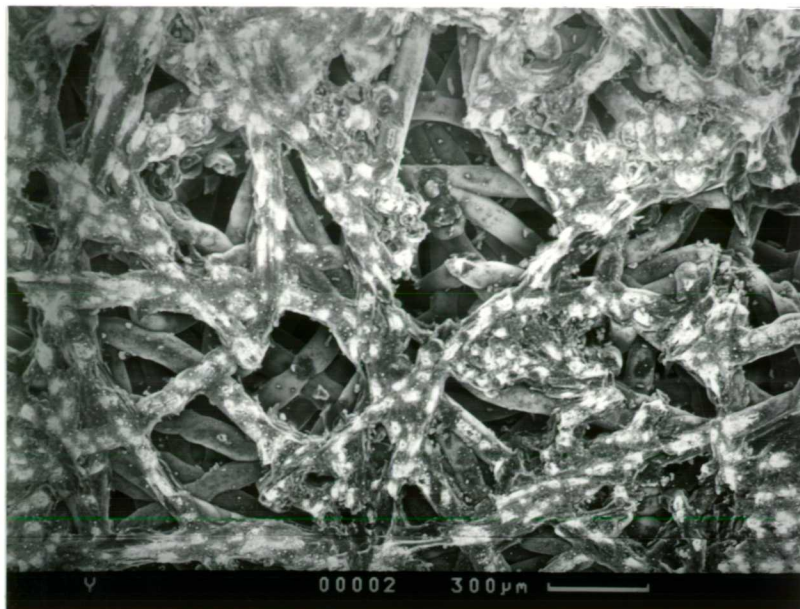
**Figure 96: Secondary electron image of the carbon-carbon composite felt plunger material after making 5 pressed glass samples at an initial plunger temperature of 300°C.**

It can be seen from Figure 96 that there appears to be less of the carbon matrix present on the carbon-carbon composite felt plunger material, and hence larger voids, after making 5 pressed glass samples at an initial plunger temperature of 300°C when compared to the same material with no glass contact (Figure 93). The bright particles seen on the surface of the fibres, which had been in contact with the glass surface, were found to be potassium chloride using EDS (as described in section 3.1.3.1 and section 3.1.3.2).

Figure 97 and Figure 98 show secondary electron images of the 5th glass surface pressed using the carbon-carbon composite felt plunger material at an initial plunger temperature of 510°C.
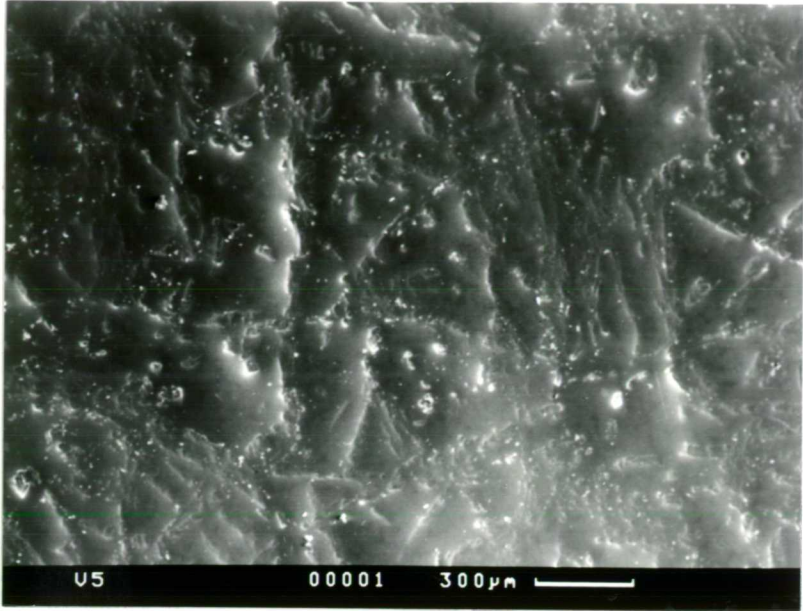
Figure 97: Secondary electron image of the 5th pressed glass surface made using a carbon-carbon composite felt plunger material at an initial plunger temperature of 510°C.



Figure 98: High magnification secondary electron image of the 5th pressed glass surface made using a carbon-carbon composite felt plunger material at an initial plunger temperature of 510°C.

It can be seen from Figure 97 and Figure 98 that rounded mounds the surface of the 5<sup>th</sup> glass sample made using the carbon-carbon composite felt plunger material at an initial plunger temperature of 510°C are now much larger that those seen on the surface of the glass sample made at an initial plunger temperature of 300°C (Figure 95). This may indicate that the amount of carbon matrix present on the surface has decreased a significant amount after contact with the hot glass on pressing.

Figure 99 and Figure 100 show secondary electron images of the carbon-carbon composite felt material after making 5 pressed glass samples at an initial plunger temperature of 510°C.



**Figure 99: Secondary electron image of the carbon-carbon composite felt plunger material after making 5 pressed glass samples at an initial plunger temperature of 510°C.**
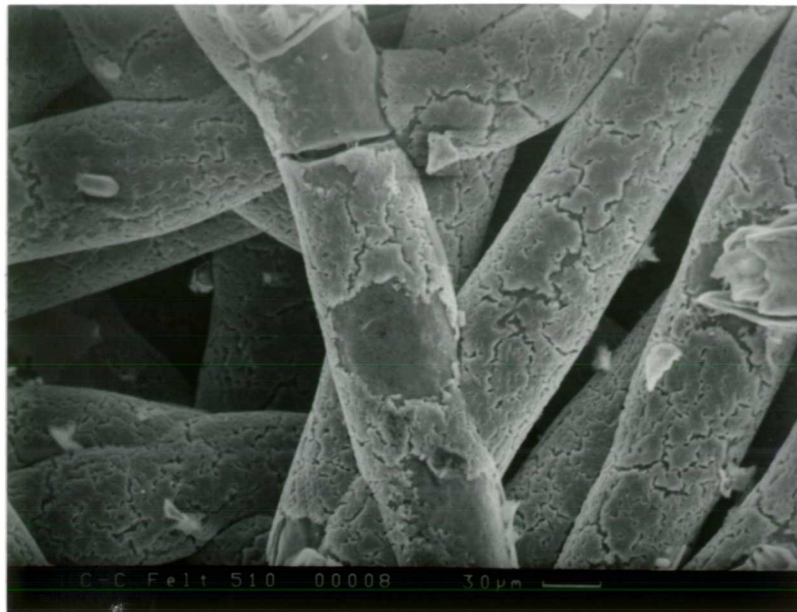
**Figure 100: High magnification secondary electron image of the carbon-carbon composite felt plunger material after making 5 pressed glass samples at an initial plunger temperature of 510°C.**

It can be seen from Figure 99 that there does not appear to be a large amount of the carbon matrix present on the surface of the carbon-carbon composite felt plunger material after making 5 pressed glass samples at an initial plunger temperature of 510°C. Closer examination of the fibres, as seen in Figure 100, shows that they appear to have a flaky coating on the surface. This may therefore indicate that the fibres of the composite, in addition to the matrix, have started to break down due to oxidation and wear.

## 3.2   Present Working Practices

A short survey of local glass container manufacturers was carried out in order to assess the variety of mouldware available for use in container forming and give an

insight into current working practices. Sections 3.2.1 and 3.2.2 summarise some of the findings of the survey.

## 3.2.1 Cast Iron Moulds

As previously described in Chapter 1, moulds used for the formation of glass containers are generally made from a grey cast iron. The molten iron is cast against a cool blank to form an undercooled fine-grained glass contact surface. This fine grained microstructure reduces the possibility of premature oxidation and degradation of the surface which would in turn reduce the quality of the glass containers produced.

The variation in the microstructure across the cast iron mould (i.e. the working surface of the mould compared to the bulk) was examined by taking a section across a used blank mould (*Rockware Glass Ltd., Knottingley, UK*). The mould section was then successively ground and polished as described in section 2.2.1.1 to gain a flat surface that could be examined using optical microscopy. To reveal the grain boundaries and different phases present in the microstructure, the polished section was etched for 5 seconds using 2% Nital (i.e. 2 vol% nitric acid in ethyl alcohol). Figure 101 and Figure 102 show optical micrographs of the blank mould microstructure revealed at the working (i.e. glass contact) surface by polishing and etching, whilst Figure 103 and Figure 104 show the microstructure of the bulk material.
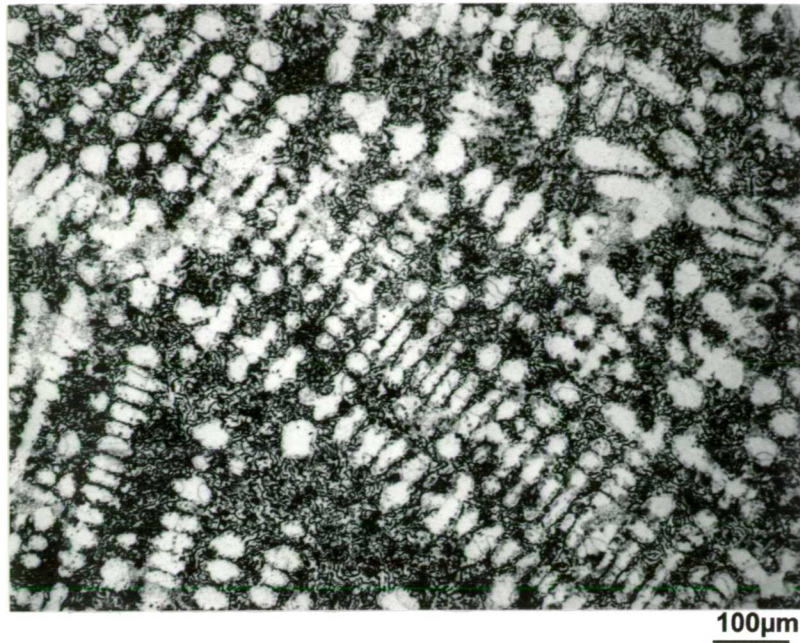
**Figure 101:** Typical optical micrograph of the microstructure found at the working surface of a cast iron blank mould supplied by *Rockware Glass Ltd., Knottingley, UK.*
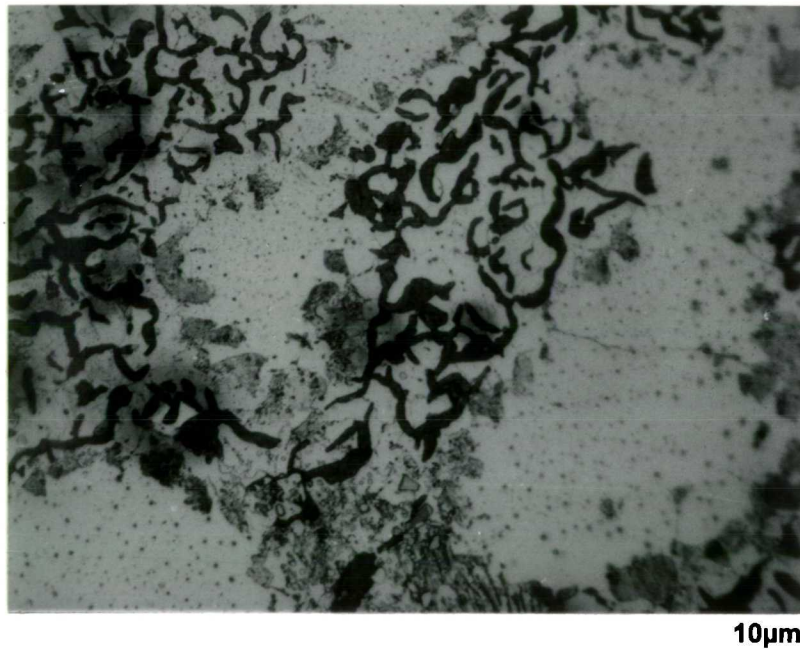


**Figure 102:** Typical optical micrograph of the microstructure found at the working surface of a cast iron blank mould supplied by *Rockware Glass Ltd., Knottingley, UK* taken at a higher magnification to show individual phases present.

British Standard BS EN ISO 945:1994 is internationally recognised as a way of describing the microstructure of graphite in cast irons. The standard describes the form, distribution and size of graphite in cast irons.

Examining the microstructures (Figure 102 and Figure 103) of the working surface of the cast iron blank mould (supplied by *Rockware Glass Ltd., Knottingley, UK*), shows that the graphite flakes in the iron matrix are rounded and clustered together. This form of graphite structure corresponds with the British Standard as being of form III graphite. The flakes are typically 1 - 6μm in length. This size corresponds to a graphite flake size of 7/6 according to the Standard. The distribution of the graphite flakes appears to be that of undercooled graphite (i.e. distribution D). This type of graphite distribution occurs due to the molten iron being cooled quickly (i.e. in this case, being cast against a chill – see section 1.3.1).

The type of iron in the matrix is mainly that of ferrite (that is iron with silicon and manganese in solid solution). The graphite flakes appear to have outlined the primary ferrite dendritic structure. In addition to the graphite flakes in the ferrite matrix, blocky angular crystals approximately 3μm in size can be seen. An examination of the polished surface of the cast iron mould using SEM/EDS, revealed these crystals to be manganese sulphide.

**100µm**

Figure 103: Typical optical micrograph of the bulk microstructure of a cast iron blank mould supplied by *Rockware Glass Ltd., Knottingley, UK.*
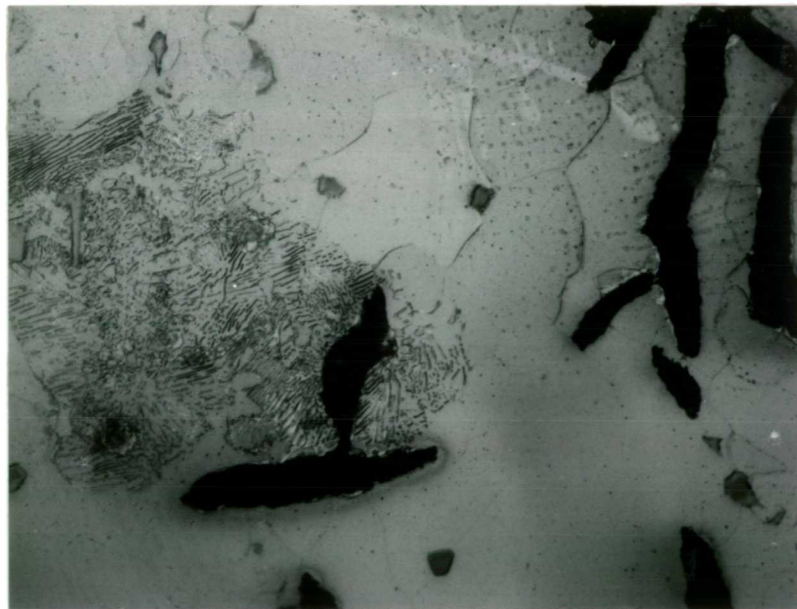


**10µm**

Figure 104: Typical optical micrograph of the bulk microstructure of a cast iron blank mould supplied by *Rockware Glass Ltd., Knottingley, UK* taken at a higher magnification to show individual phases present.

Examining the micrographs of the polished surface of the bulk material of the blank mould (i.e. 30mm from the glass contact surface) found in Figure 103 and Figure 104, it can be seen that the microstructure of the iron is very different to that found at the working surface (Figure 101 and Figure 102). In general, the graphite is coarser and more randomly oriented. A coarser microstructure is needed in the bulk of the mould material as it enables superior heat extraction whereas a fine grained structure is desirable at the working surface as it produces a good surface finish and is more resistant to oxidation and degradation (section 1.3). The length of the graphite flakes appears to range between $80 - 250\mu m$. The graphite structure in the bulk of the cast iron blank mould can therefore be seen to be generally that with distribution type A, form I and size 4/5 according to BS EN ISO 945:1994.

The iron in the matrix appears to be predominantly that of ferrite. However, regions can also be seen which are of pearlite. Pearlite consists of alternate lamellae of iron carbide (cementite) and ferrite; the pearlitic phase occurs due to a phase change where austinite transforms to pearlite at the critical (eutectoid) temperature of 723°C. Angular, blocky crystals can be seen in Figure 104 which have been identified as manganese sulphide using EDS.

Samples of the plungers made from both the virgin cast iron blank mould (supplied by B*irstall Foundary, UK*) and that made from a discarded blank mould (supplied by *Rockware Glass Ltd., Knottingley, UK*) were polished, etched and examined optically. This was carried out to determine whether there was any

substantial change in microstructure of the working surface of the cast iron after it had been used to make glass containers. Optical micrographs of the virgin cast iron plunger and that obtained from a discarded blank mould can be found in Figure 105 and Figure 106 respectively.



**50μm**
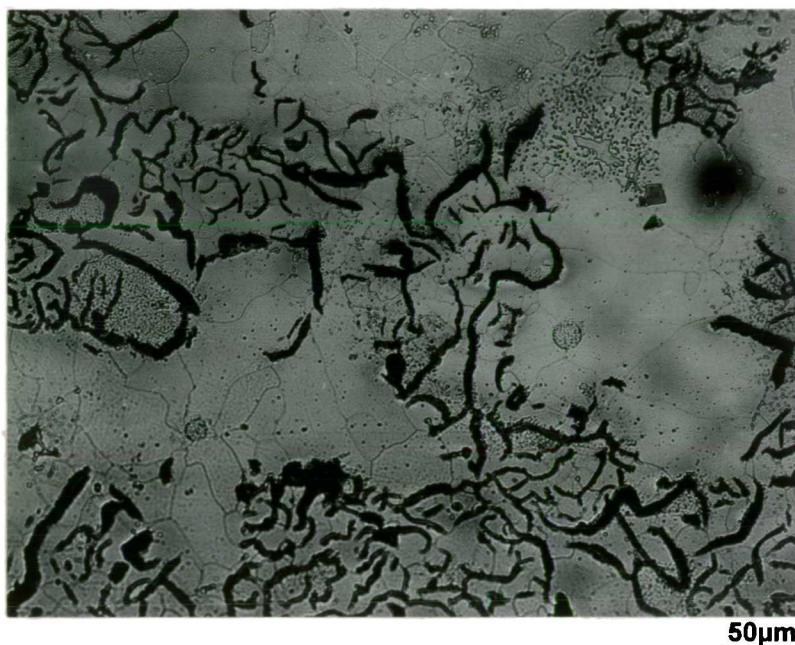
**Figure 105: Typical optical micrograph of the microstructure of the virgin cast iron plunger surface (*Birstall Foundary, UK*).**

It can be seen from Figure 105 that the graphite distribution in the plunger, which had been made from a cast iron blank mould that had had no prior contact with a glass melt, was similar to that found at the working surface of the sectioned mould (Figure 101 and Figure 102). The graphite can therefore be described as having form I, distribution D and size 6/7 according to BS EN ISO 945:1994. Individual ferrite grains can be seen in Figure 105. The size of these ferrite grains appears to be less than 50μm. Blocky manganese sulphide crystals (analysed using EDS) can also be seen in Figure 105.
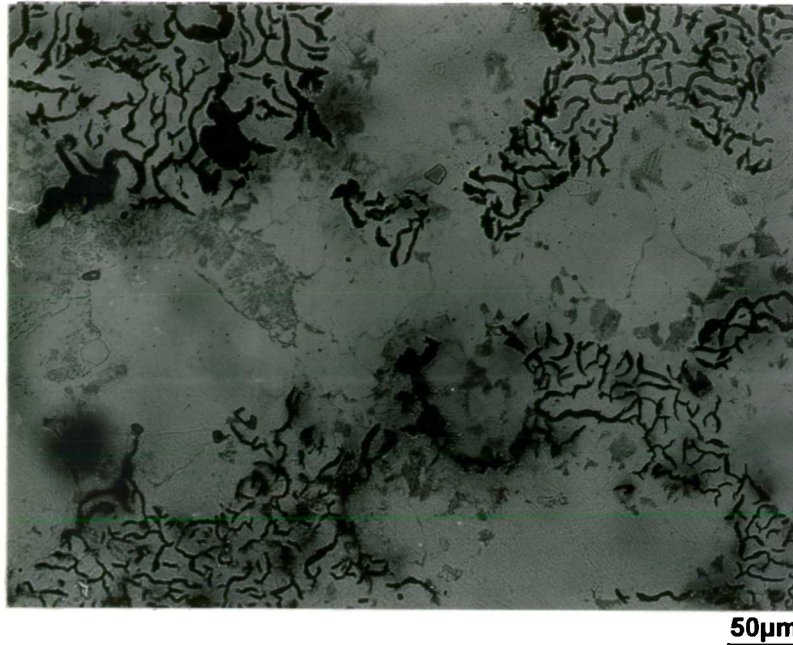
**Figure 106: Typical optical micrograph of the microstructure of the cast iron plunger surface mad from a discarded blank mould (*Rockware Glass Ltd., Knottingley, UK*).**

The microstructure of the plunger made from a discarded blank mould (Figure 105) can be seen to be similar to that of the plunger made from a brand new mould which had had no prior contact with any glass melt (Figure 106).

## 3.2.2 Current Mould Usage

A short survey was carried out which asked UK glass container manufacturers about the grades/compositions of cast irons used for mouldware and the mould suppliers used. Information was also gathered regarding expected service life of mouldware, methods of mould repair and mould cooling methods used.

Cast iron is the most common material in use at the moment for both blank and blow moulds. It appears that a large proportion of the UK glass container industry

currently buys most of its cast iron mouldware from the three main UK glassmaking mould manufacturers: Birstall Foundary, Johnson Radley and Esdale Ltd. Each of these mould manufacturers, however, offers several different grades of cast iron with different compositions that can be used for mouldware. It was suggested that each glass container manufacturer uses at least two of these suppliers depending on current price and availability. This would therefore mean that it is possible that different grades of cast iron are being used which may have different thermal and chemical characteristics that could affect the local chemistry at the glass-to-mould interface.

Blank moulds are typically used for approximately 48 hours before they are removed for cleaning and minor repair. In use they are swabbed, using a mould dope on a cotton mop, approximately every 20 minutes. This mould dope causes a solid build-up on the mould working surface after time. Cleaning is therefore carried out to remove both build-ups of mould dope and heavy oxide coatings by grit blasting the working surface. Chipping (approximately a few millimetres in size) is often found at the edges of the mould due to the brittle nature of the cast iron used to make the moulds. These chips are repaired using a low temperature nickel welding process. The repairing process involves initially heating the affected area. A nickel-based powder is then blown onto the surface that is fired-on using an oxyacetylene flame. The repaired area is then reshaped either by hand or using a lathe if the repaired area is large enough. The working surface of the mould is then refinished before reuse (eg. Blank moulds are finished using a 300 grit emery paper).

The life of a blank mould is approximately 8 to 10 days. This lifetime corresponds with the production of 500,000 to 1,000,000 pieces in a large factory using operating surface temperatures of 450 to 650°C. The lifetime of a blow mould is generally longer with between 750,000 and 1,500,000 pieces being produced. Moulds are taken out of service when the cavity capacity becomes too large (i.e. out of tolerance) due to removal of material during cleaning or when cracking starts to appear.

Additional glass contact materials are used for different forming tools other than blank and blow moulds throughout the industry. At the moment, aluminium bronzes are used for neck rings and bottom plates. Although aluminium bronzes are more efficient at removing heat from the surface of the glass melt during forming, they are approximately 2.5 times the cost of cast iron and as such their use for mouldware is limited to forming parts which are difficult to cool (e.g. neck rings and bottom plates). Plungers are often made from a medium carbon steel (e.g. EN8) which is surface coated with a hard nickel based coating (approximately 650 Vickers hardness). A hard nickel based coating is used as it is a good release agent from glass and is more resistant to wear than the basic plunger material.

A large proportion of glass container manufacturers now use forced air cooling (e.g. vertiflow) to keep the temperature of mouldware stable during production to prevent glass-to-mould sticking due to rising temperatures at the working surface. This is carried out by forcing cool air through holes drilled in the body of the

mould wall (see section 1.3.2). However, for container production using low mould temperatures and slow production speeds, mould cooling is still carried out using cooling fins on the outer mould wall and externally applied cooling air.

## 3.3 Summary

This chapter has summarised the results obtained form experimental pressing using both cast iron and carbon-carbon composite materials as glass melt contact materials. Results from the investigation of several forming parameters were presented to find the effect of the contact material on the glass contact surface and *vice versa*. The forming parameters investigated included heat treatment, plunger surface finish, initial plunger surface temperature and pressing atmosphere. The results presented in this chapter are discussed further in Chapter 4.

# 4. DISCUSSION

In this Chapter the results obtained from this project that were presented in Chapter 3 are discussed. The first part of the discussion will deal with the results acquired from the experimental glass pressing work using both cast iron and carbon-carbon composite plungers. The latter part of this chapter will discuss the current practices used in the glass container industry and attempt to raise some important issues.

## 4.1 Experimental Pressing

Sections 4.1.1 and 4.1.2 discuss the results obtained from experimental pressing using the experimental pressing rig described in section 2.1.1 for cast iron plungers and those made from carbon-carbon composite materials, respectively.

### 4.1.1 Cast Iron Plungers

Presently, grey cast iron is used throughout the glass container industry for hot glass contact materials such as blank and blow moulds, baffles and neck rings as it is inexpensive and easily machinable. However, little is understood about how a container glass melt reacts with the mould materials. It may be possible that there is a chemical reaction of the glass melt with the cast iron that could produce glass with inferior mechanical properties. As the glass container industry is moving towards producing lighter, thinner bottles, it is very important that unfavourable surface reactions that may reduce the strength are avoided.

Two commonly occurring features that have been found, using a scanning electron microscope, which are present on all the pressed glass surfaces produced during this work using the experimental pressing rig are partly embedded, pressed-in particles and pressed-in dimples. The incidence, and size, of pressed-in particles present on the glass surface and appearance of the dimples, however, appears to alter with change in the pressing parameters such as number of glass pressings, plunger surface finish, initial plunger temperature and pressing atmosphere.

### 4.1.1.1 Heat Transfer at the Glass Melt-Mould Interface

During container formation, the heat from the glass melt needs to be extracted by the mould at a high enough rate such that the parison formed holds its shape. However, the amount of heat extracted from the glass melt has been shown to be affected by parameters such as the surface finish of the forming mould and the presence of any mould dope. [McMinn et al., B.T.N. 237_1978 & 262_1979, Fellows et al., B.T.N. 215_1976, Coney et al., B.T.N. 156_1972]. The time of contact between the metal mould and glass melt and the initial temperature of the mould has also been shown to affect the heat flux as shown in Figure 107 [Fellows & Shaw_1978]. However, Fellows and Shaw used a heat resistant AISI 310 steel instead of the more typical mould material of grey cast iron.
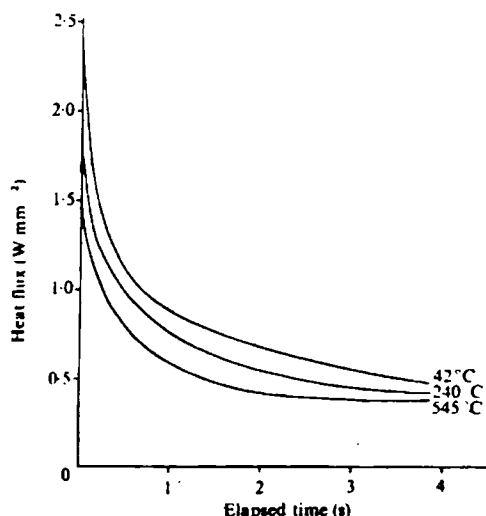
**Figure 107: The effect of the initial mould temperature on the heat flux when pressing a glass sample using an initial glass temperature of 1077±10°C at a constant pressing pressure of 88±8kPa and a mould made from heat resistant AISI 310 steel [Fellows & Shaw_1978].**

It can be seen from Figure 107 that after approximately 4 seconds contact time, the heat fluxes found for all the initial mould temperatures investigated was approximately 0.5 $Wmm^{-2}$. Therefore in the current investigation, where a contact time of 4 seconds has been used throughout the experimentation, the effects of differences in heat flux for each of the different initial plunger temperatures would be minimised. However, at short contact times, the initial temperature of the mould has been shown to affect the heat flux, with greater changes for a lower initial mould temperature. The thermal conductivity of steel, is lower than that of cast iron (i.e. grey ferritic cast iron – 41-49$Wm^{-1}K^{-1}$ whereas steels – 9.9-18.5$Wm^{-1}K^{-1}$)[Kirsch_1993]. As the thermal conductivity of steel is lower than that for cast iron, the heat flux is more likely to become steady at a shorter time than the 4 seconds indicated in Figure 107.

The heat from the glass melt during container production is extracted by the cooler cast iron mould via a mixture of conduction (which is the predominant mode below 200°C) and radiation (which becomes increasingly predominant above 200°C) [Giegerich & Trier_1969]. Heat flow between the glass melt and the metal mould during the formation of containers is therefore complicated, and made more so as the metal surface will not be perfectly smooth and will have layers of oxide and mould dope altering the heat flow characteristics.

The surface texture of the cast iron plunger used in pressing during this project did not have a perfectly smooth texture, but was inevitably made up from a series of ridges and troughs left from the grinding and polishing procedures. This type of uneven surface will also be found on the surface of glass container mouldware which is typically given a 120-300 grit surface finish prior to use. This implies that during the initial stages of pressing, the ridges of the cast iron (i.e. the highest points) would come into more intimate contact with the surface of the glass melt during pressing than the lower points. At the points of intimate contact between the glass melt and the metal mould, one might expect the main form of heat transfer to be that of conduction. Between these points of intimate contact, it is likely that air (if present) would be situated in the voids, which could chemically react with both the plunger and/or glass surface or act as a thermal insulator, as discussed below.

On contact of the plunger with the glass melt during pressing, any air trapped in the voids produced could act as an insulator, therefore restricting the flow of heat

between the glass melt and the relatively cool cast iron plunger. The heat would therefore flow best directly between the points of glass to metal contact during pressing. This would suggest that the surface temperature of the cast iron plunger would not rise as quickly as would be expected from perfect contact. This may help to explain why the surface temperature of the cast iron plunger only appears to rise by approximately 80°C on glass-to-metal contact during pressing (see Section 3.1.2.1). However, it is also well known that container glass has a relatively low effective thermal conductivity (i.e. when compared to a metal such as cast iron) [Jones_1966]. The surface of the glass therefore will be rapidly cooled by the cast iron surface (i.e. faster than heat can be transferred from the bulk of the glass to reheat the surface). This phenomenon will dramatically reduce the effective temperature difference between the glass and moulding surface, which drives heat flow, and will effectively limit the temperature rise on the surface of the mould after the initial contact. The rise in temperature in the current work was measured using fast acting surface thermocouples (made from alumel and chromel foil strips sandwiched between mica strips) and would introduce a possible error of ±5°C.

Previous work has shown that the glass contact surface temperature inside cast iron glassmaking moulds cycles on contact with the glass melt during forming [Trier_1955, Holscher et al._1960]. The temperature fluctuations have been found to be most evident on the contact surface of the mould and decline towards the outer surface. The measurements have shown that the temperature cycles in blank moulds between 50 – 80°C (i.e. between 420°C and 500°C) whilst in blow moulds

it is between 30 – 50°C (i.e. between 450°C and 500°C). Figure 108 shows how the temperature at the glass contact surface of a blank mould varies with time during the manufacture of colourless glass containers.
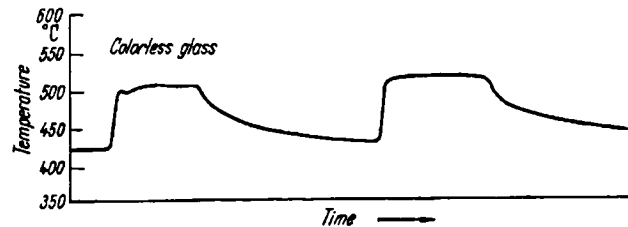


**Figure 108: Temperature of the glass contact surface of a cast iron blank mould at half height during the formation of colourless glass containers [Trier_1955].**

This work confirms that the 80°C temperature rise found in this project on contact of the cast iron plunger with the glass melt during forming is typical of that found in practice during the formation of glass containers.

Corresponding work has also been carried out to investigate how the temperature of the glass melt is affected when brought into contact with a relatively cool blank mould during the formation of glass containers [Trier_1960]. This work involved puncturing the gob and putting a fine line of bubbles in the melt. The subsequent flow of the melt against the mould wall resulted in a distribution of the bubbles in the supercooled glass melt. The position of the bubbles enabled Trier to calculate the temperature distribution curves. However, this method could not be used to determine the actual temperature distribution at the glass-to-mould interface.

Typical temperature distribution curves for a colourless glass melt being formed against a cast iron blank mould held at 470°C can be found in Figure 109.
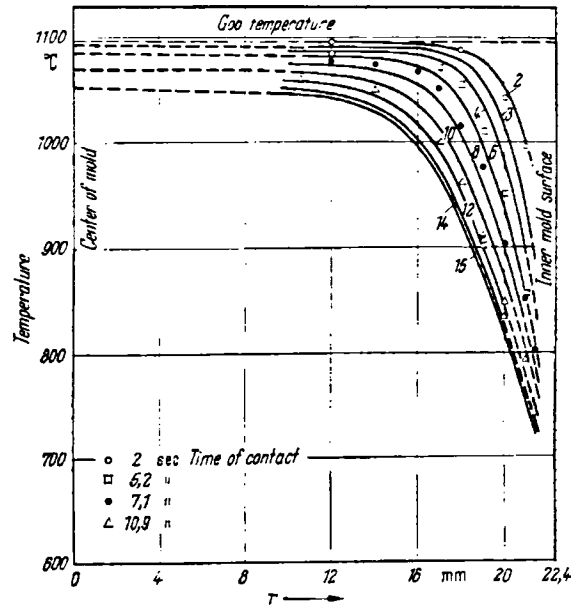


**Figure 109: The temperature distribution in a colourless glass after contact with a cast iron blank mould held at 470°C [Trier_1960].**

It can be seen from this graph that the temperature of the glass melt drops from approximately 1100°C at the centre of the mould to approximately 700°C near to the contact surface of the mould. According to Figure 109, there is a temperature drop of at least 400°C at the very surface of the glass melt (i.e. within 4mm from the glass/mould contact surface). This would have the effect of increasing the viscosity of the glass melt at this location to such an extent that the glass melt should hold its shape for further processing (see section 4.1.1.6 for further discussion of melt viscosity).

On pressing, if air is trapped within the voids formed between the glass melt and the cast iron plunger, it is likely that the air will be compressed tending to increase the potential reactivity, or chemical potential, of species present. Any increase in pressure of the trapped gases would lead to effects such as the increased diffusivity of the gas in the oxide film. The oxygen present in the trapped air under pressure, for example, will have the possibility of directly reacting with any bare iron present on the mould, or diffusing through the oxide layer to react with the underlying metal substrate to increase the thickness of the oxide layer formed. These reactions are discussed in the next section. The oxygen present in the trapped air when under pressure could also react with any species from within the glass melt (e.g. $Na^+$ - see section 4.1.1.7 for a further discussion). Therefore, the partial pressure of the oxygen trapped in the voids would tend to decrease with time if diffusion and reaction processes occur. The nitrogen, from the examination of phase diagrams and free energy information, is fairly unreactive with both the iron and glass melt, and therefore the relative partial pressure of the nitrogen within the voids will increase with time. However, the overall pressure of any trapped air in the voids will decrease (assuming fixed volume).

## 4.1.1.2 Oxidation of Cast Iron

During the parison formation stage of during container formation, the cast iron mould will come into contact with air (containing nitrogen, oxygen, carbon dioxide and water etc.) in addition to the glass melt. Oxygen sources present within the system during the formation of glass containers, other than those available from the air, include the oxide scale itself, the glass melt and possibly oxygen produced from any mould dopes used. An excellent book is available

which is particularly relevant to the investigation of reactions at the glass-to-metal interface during the formation of glass containers and introduces much work from Eastern Europe [Kirsch_1993]. Another relevant general introduction to the high temperature oxidation of metals is also available [Birks and Meier_1983]. This section discusses the possible reactions of the iron in the cast iron with free oxygen from the atmosphere referring to information from these texts.

By examining the micrographs of the oxide scale formed on the surface of the cast iron plungers used to press glass samples, it can be seen that the appearance of the oxide scale changes when the pressing parameters were varied. When pressing a glass sample with an initial plunger temperature of 300°C the oxide scale formed on the cast iron plunger appears to be fairly smooth and relatively thin (e.g. Figure 35). However, after being used to press glass at higher temperatures, the cast iron plunger surface (having the same initial texture and initial heat treatment which has been used to press the same number of glass samples) can be seen to have a relatively thick, fibrous oxide scale present (e.g. Figure 46). As the time of glass melt to metal contact has been the same in all glass pressings, the temperature at which the contact has occurred appears to affect the type of oxide scale formed.

As iron is multivalent, it is possible that a different type of oxide is formed on the surface of the cast iron depending on the glass-to-metal contact temperature. By examining the iron-oxygen phase diagram (see Figure 110), it is possible to determine which oxide phases are likely to form.
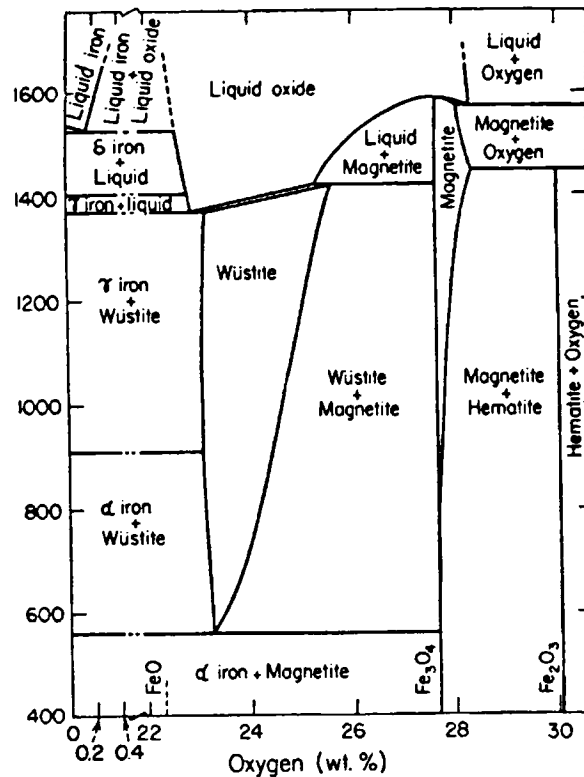
Figure 110: Iron-oxygen phase diagram [Darken & Gurry_1946] at a total pressure of one atmosphere. Oxygen weight% is that in the iron compound itself.

Thus, when held at high temperatures in air, the surface of the cast iron tends to oxidise to form layers of FeO ($FeO_{1.0}$), $Fe_3O_4$ ($FeO_{1.3}$) and/or $Fe_2O_3$ ($FeO_{1.5}$) depending on the successive temperatures at which the iron is held and the chemical availability of the oxygen. Thus, iron could readily form a multilayer system at high temperatures.

At low temperatures (i.e. below 570°C) it can be seen that wustite (i.e. FeO) does not form. This means that if the iron was oxidised below 570°C, only a one or two component oxide system could be formed which contains haematite ($Fe_2O_3$) and/or magnetite ($Fe_3O_4$). This type of oxide layer system is the one that will have formed on the cast iron surface during the initial heat treatment (i.e. holding in air,

with an abundance of oxygen available, for 30 hours at 470°C). It is also most likely that this type of oxide forming system is present on the cast iron plunger surfaces that have been used to press glass samples at low temperatures. The speed at which the oxide scale forms on the surface will be reduced as wustite (which is the phase that has a greater mobility of defects) is not present. This is consistent with the observations made by examining the cast iron plunger surfaces that have been used to press glass samples at low temperatures. Evidence presented in Chapter 3 shows that relatively thin oxide scales appear to have formed on the plunger surface after glass contact (e.g. Figure 25).

At temperatures above 570°C, it can be seen from Figure 110 that it is possible for three iron oxides to form, these being wustite (FeO), haematite ($Fe_2O_3$) and magnetite ($Fe_3O_4$). A mechanism by which iron oxidises to form a three component layer system has been proposed which uses information on the structure of the different oxides formed and their diffusion properties [Birks & Meier_1983]. This mechanism for oxide formation is summarised in Figure 111 and assumes outward cation and electron migration from the cast iron surface through the oxide layers, and backward migration of oxide anions, rather than molecular oxygen.
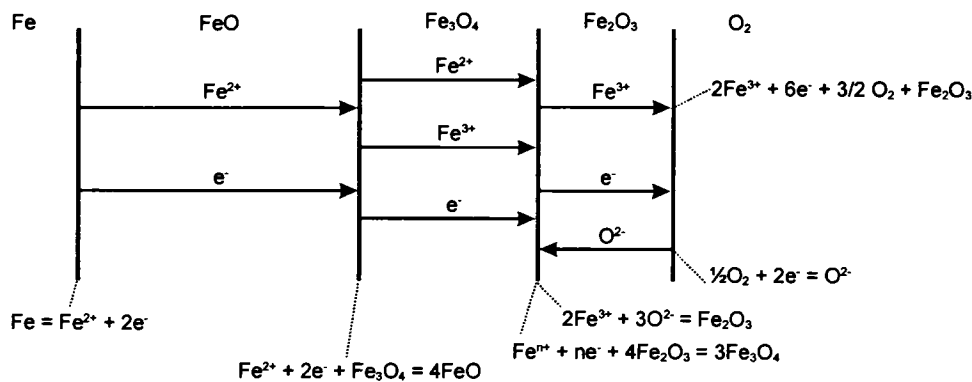
**Figure 111: The oxidation mechanism for iron above 570°C, showing diffusion steps and interfacial reactions [Birks & Meier_1983].**

From Figure 111, it can be seen that at the iron-wustite interface, the iron will ionise to form $Fe^{2+}$ ions (i.e. $Fe = Fe^{2+} + 2e^-$). $Fe^{2+}$ ions, and the corresponding electrons formed, will migrate through the FeO layer over iron vacancies and electron holes respectively. At the wustite-magnetite interface, the magnetite is reduced by the $Fe^{2+}$ ions and electrons to form wustite (i.e. $Fe^{2+} + 2e^- + Fe_3O_4 = 4FeO$) therefore making the oxide layer grow inwards towards the iron surface. The iron ions (both $Fe^{2+}$ and $Fe^{3+}$), and electrons formed, that are surplus to this reaction proceed outward through the magnetite layer. At the magnetite-haemetite interface, magnetite is formed due to the reaction of both types of iron ions formed (i.e. $Fe^{n+} + ne^- + 4Fe_2O_3 = 3Fe_3O_4$, where n = 2 or 3). Evidence of oxide growth in iron by cation diffusion has been found by heat treating iron in different atmospheres (i.e. $CO_2/CO$ and air) and using different temperatures [Bruckman & Simkovich_1972]. The use of platinum markers enabled Bruckman and Simkovich to microscopically determine the extent at which the different oxides had grown and determine which oxides had grown due to the heat treatment applied.

New haematite will form at the $Fe_2O_3$-gas interface if the mobile iron ions, within the haematite already formed, migrate together with electrons over iron ion vacancies. At the haematite-oxygen interface, the oxygen will also ionise (i.e. $\frac{1}{2}O_2$ + $2e^-$ = $O^{2-}$). New $Fe_2O_3$ will then be formed if the oxygen ions diffuse inwards through the $Fe_2O_3$ to react with surplus iron ions and electrons (i.e. $2Fe^{3+}$ + $3O^{2-}$ = $Fe_2O_3$). The corresponding electrons then migrate outwards through the $Fe_2O_3$ to take part in the further ionisation of oxygen.

The wustite layer formed at the metal surface is the fastest growing form of iron oxide in the system and tends to form a thick porous layer that will allow oxygen to pass through to the iron. This therefore means that if iron is held above 570°C, the oxide scale formed is predominantly wustite. The oxide scale which is formed on the glass contact surface of the cast iron plungers, used in the present study, that had been used to press glass samples at high temperatures is therefore most likely to be made up predominantly from wustite (e.g. Figure 28).

During the experiments carried out with vacuum assisted pressing, the amount of air, and hence oxygen, present within the voids, produced due to the contact between the glass melt and metal mould, will be decreased. As the oxygen available for reaction with the two surfaces is minimised, the cast iron is likely to form an oxide layer of $Fe_3O_4$ at temperatures below 570°C or FeO above 570°C, according to Figure 110.

In Chapter 1 (section 1.4.1), previous work describing how a glass melt reacts with a metal substrate during forming was introduced. In particular, the work by Fairbanks *et al.* (1949 – 1964), which examined the temperatures at which a glass melt will adhere to a metal substrate, suggested that the sticking temperature, of a glass melt to a metal substrate on contact, was dependent on the metal investigated. He found that the temperature at which the glass melt stuck to nickel, for example, was higher than that for cast iron. The reason behind this may be due to the type of oxide scale formed on the metal surface (i.e. how stable it is, whether it forms a continuous coating etc.), because it is reasonable to suppose that an oxide melt (containing metal oxides) will have an affinity for adjacent metal oxides. Sticking could therefore be the manifestation of chemical reaction or solubilisation between species present.

It has been suggested that the level of protection that an oxide scale will give to the metal substrate can be defined using a simple ratio (see the Pilling-Bedworth rule in Equation 5) [Kubaschewski & Hopkins._1962].

$$\varphi = \frac{molar.volume.of.oxide}{atomic.volume.of.metal}$$

**Equation 5**

Table 10 shows examples of how the Pilling Bedworth ratio varies with the oxide formed.

| Metal | Oxide | Ratio $\varphi$ |
|-------|-------|-----------------|
| Na | $Na_2O$ | 0.55 |
| Fe | $Fe_2O_3$ | 2.14 |
| Fe | $Fe_3O_4$ | 2.10 |
| Ni | NiO | 1.65 |

Table 10: The Pilling-Bedworth ratio for common glass contact metals [Kubaschewski and Hopkins_1962].

It has been suggested [Kirsch_1993] that if $\varphi < 1$, then the metal surface is not completely covered by a protective oxide layer and therefore oxidation of the metal occurs rapidly (e.g. Na). For oxide films where $\varphi = 1 - 2$, the best protection to the metal surface is provided. However, for oxide scales with values of $\varphi$ greater than 2, the scale is prone to cracking and spalling and oxidation becomes non-uniform. Therefore, nickel surfaces will offer the best protection to further oxidation, whereas iron surfaces will produce an unstable oxide that is prone to spalling. The physical stability of the oxide formed (i.e. resistance to spalling) may explain why some metals have a higher glass-to-metal sticking temperature.

### 4.1.1.3 Reactions at the Interface of the Glass Melt and Cast Iron Mould

The explanations outlined in section 4.1.1.2 above consider the situation if pure metals are held in a gaseous oxygen-containing atmosphere. Container formation has a cycling nature where the mould material is either held in air (i.e. containing nitrogen, oxygen, carbon dioxide, water, hydrogen etc.) at temperature, or is in contact with a highly reactive and corrosive glass melt (possibly with some

additional mould dope or pre-coat present as a barrier). Glass melts are highly reactive at temperature as they have a proportion of non-bridging oxygens available for reaction with the mould material. As we are considering here the reaction of a cast iron mould (i.e. iron alloyed with carbon and silicon etc.) with a glass melt during container formation, the situation may not be the same as that purely for the reaction of iron with pure oxygen.

All possible reactions involved during the contact between the glass melt and plunger in experimental pressing, corresponding to the contact between a gob and blank mould during forming, can be modelled thermodynamically using Ellingham diagrams. Ellingham diagrams allow the immediate visual comparison of the standard free energies of reaction over a wide temperature range without the need for calculation. The greater the free energy of formation, the more stable the reaction product. Therefore, on examining an Ellingham diagram it is possible to determine which reactions are most likely to occur in a given system. The problem is defining the system exactly. The slopes of the plots correspond to the negative entropy change concerned with the formation of the compound.

It is possible that the glass melt/plunger system may come into contact with oxygen from the atmosphere and possibly sulphur and carbon from lubricants. Relevant Ellingham diagrams for the whole temperature range of interest can be found in Figure 112 and Figure 114 which have been constructed for both oxide and sulphide systems using data obtained from Metallurgical Thermochemistry [Kubaschewski & Alcock_1979].
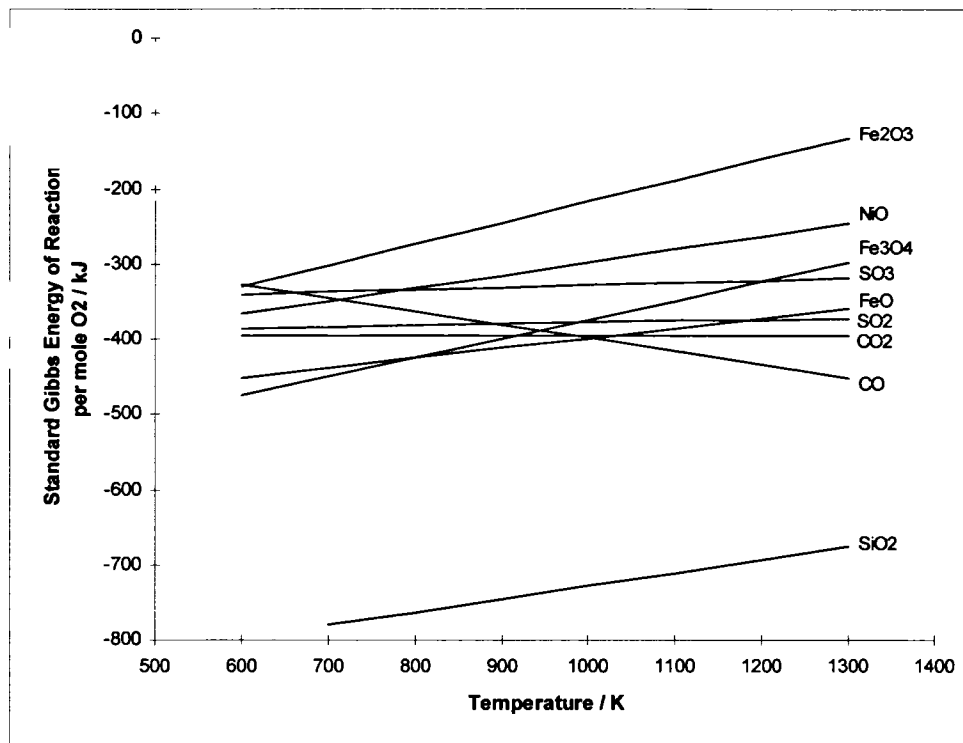
**Figure 112: Ellingham diagram showing how the standard Gibbs' energy of reaction varies when one mole of oxygen combines with possible substances present during container forming.**

Examination of Figure 112 indicates that at temperatures over 1000K, the most stable oxides are CO, $CO_2$, $SiO_2$ and $SO_3$. In the current work, the surface temperature of the glass melt prior to contact with the plunger is 950°C (1223K). This explains why the use of carbon, sulphur and silicon in mould lubricants is beneficial. Elemental sulphur, carbon and silicon produce either gases or silica on reaction with oxygen, which would "mop up" any free oxygen in the system, thus preventing oxygen from reacting with the metal mould surface. The silica produced could be soluble in the glass melt. The diagram seen in Figure 112 is complicated in the temperature range typical of that used in blank moulds,

therefore this portion of interest in the diagram has been expanded and can be found in Figure 113.
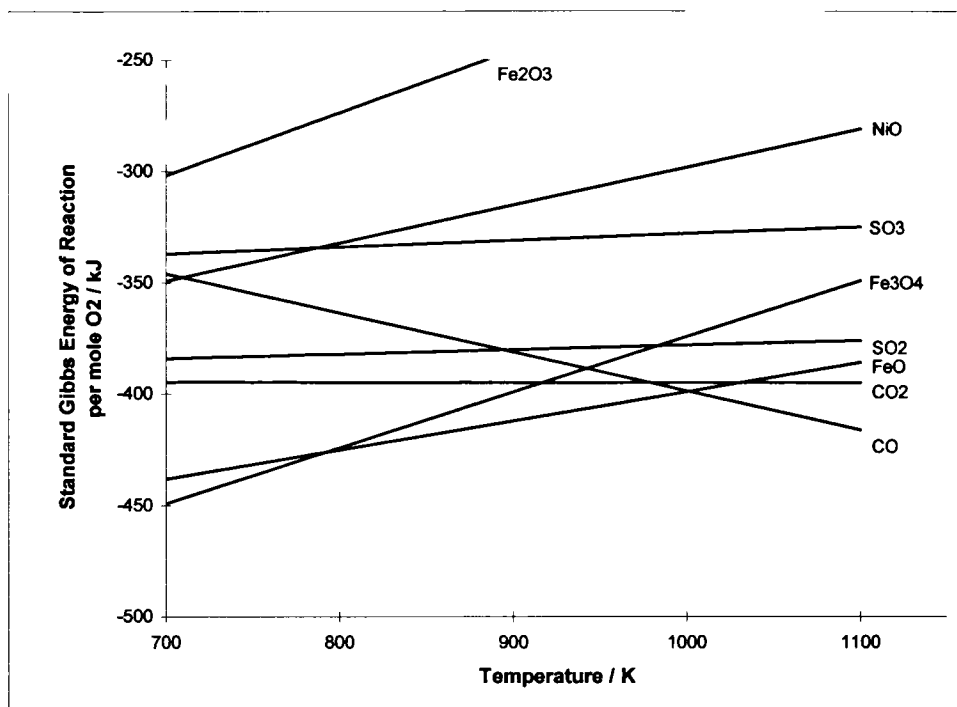


**Figure 113: Ellingham diagram showing how the standard Gibbs' energy of reaction varies when one mole of oxygen combines with possible substances present during container forming at typical plunger temperatures.**

Fairbanks *et al.* (1949 – 1964) have previously reported that glass adheres to nickel surfaces at a higher temperature than that for cast iron. On examination of the Ellingham diagram seen in Figure 112 and Figure 113, it can be seen that at all temperatures, FeO is thermodynamically more stable than any of the other metallic oxides (e.g. NiO, $Fe_2O_3$ etc.). It can also be seen that $SiO_2$ is the most thermodynamically stable oxide within the system. This would mean that free oxygen is most likely to combine with Si to form $SiO_2$ rather than react with iron or carbon at the mould surface. Conversely, it can be seen that the least

thermodynamically stable oxide formed would be $Fe_2O_3$ and as such, this oxide is the least likely to form. At common blank mould temperatures used during the formation of glass containers, it can be seen that the least stable oxides formed are $Fe_2O_3$ and $NiO$. The ability of the metal to form an oxide, which then reacts with the glass surface, is therefore not the only factor involved. Other factors that may be involved include the solubility of the oxide in the glass melt.

By examining Figure 113 in detail over the temperature range which is important for the formation of glass containers, it is possible to determine which oxide is the most likely to form at which temperature:

700K (427°C) – at this temperature, the most stable oxide formed would be $Fe_3O_4$ followed by $FeO$. These iron oxides are more stable than $CO$ or $CO_2$ at this temperature, and hence any oxygen present in the atmosphere is more likely to oxidise the cast iron mould (producing $Fe_3O_4$ then $FeO$) rather than forming a protective layer of gas.

800K (527°C) – at this temperature, the most stable oxides formed are both $FeO$ and $Fe_3O_4$ (having similar thermodynamic stabilities at this temperature). This would mean that, thermodynamically, any oxygen present in the local atmosphere during glass container formation is most likely to oxidise the iron surface (forming $FeO$ and $Fe_3O_4$) rather than producing protective gases.

950K (677°C) – at this temperature, it can be seen that the most stable oxide formed will be FeO, but $CO_2$ is more stable than $Fe_3O_4$. This would mean at this temperature, free oxygen is most likely to form FeO on the mould surface, however the beneficial influences of the formation of protective cushions of gas becomes more likely.

>1025K (>752°C) – above this temperature, it can be seen that CO and $CO_2$ are more stable than the iron oxides. This will mean that any free oxygen in the local atmosphere is more likely to form protective cushions of gas rather than oxidising the cast iron mould surface.
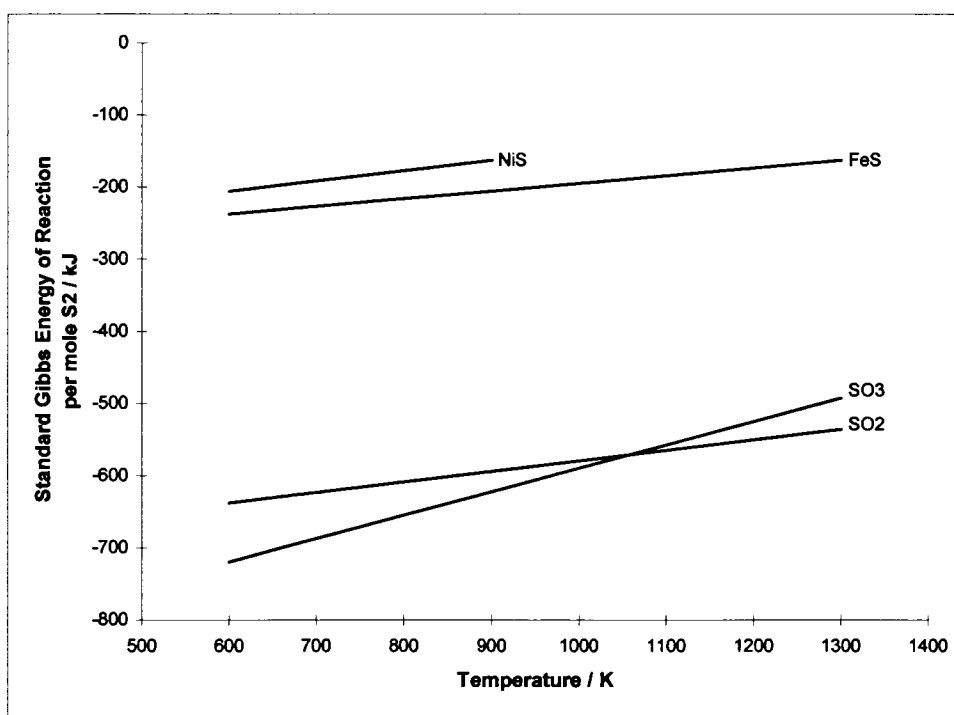


Figure 114: Ellingham diagram showing how the standard Gibbs' energy of reaction varies when one mole of sulphur combines with possible substances present during container forming.

Sulphur is well known to exhibit rather long lasting "non-stick" properties when applied to moulds as a lubricant for container formation. The effect is sustained even after the sulphur has apparently oxidised away from the mould surface. Sulphur has not only been used in the formulation of mould lubricants, but is also known to have been thrown into moulds during container production by the machine operatives as 'flowers of sulphur' [Coney_1995]. This practice was still actually employed surreptitiously after new legislation had banned it according to hearsay. Obviously, sulphur produces noxious gases (e.g. $SO_2$, $SO_3$, $H_2S$, $H_2SO_4$ etc.) in the factory atmosphere, production of which would flout current emission regulations.

Examination of the Ellingham diagram with respect to sulphur (Figure 114) shows that the most stable oxides formed are those of $SO_2$ and $SO_3$. As previously mentioned, formation of these gases would tend to "mop up" free oxygen from the system inhibiting the formation of the metal oxide, which itself may be prone to react with the glass surface. These gases formed may act as a protective cushion to prevent further reaction of the glass melt with the cast iron mould. This alone, however, does not explain why the use of sulphur appears beneficial in the prevention of sticking of the glass melt to the mould during the formation of glass containers. It can be seen from Figure 114 that thermodynamically the compound FeS is less likely than the formation of $SO_2$ and $SO_3$. Examination of the iron – sulphur phase diagram indicates the reaction which is most likely to occur at normal pressing temperatures (Figure 115) once the oxygen has been used up.
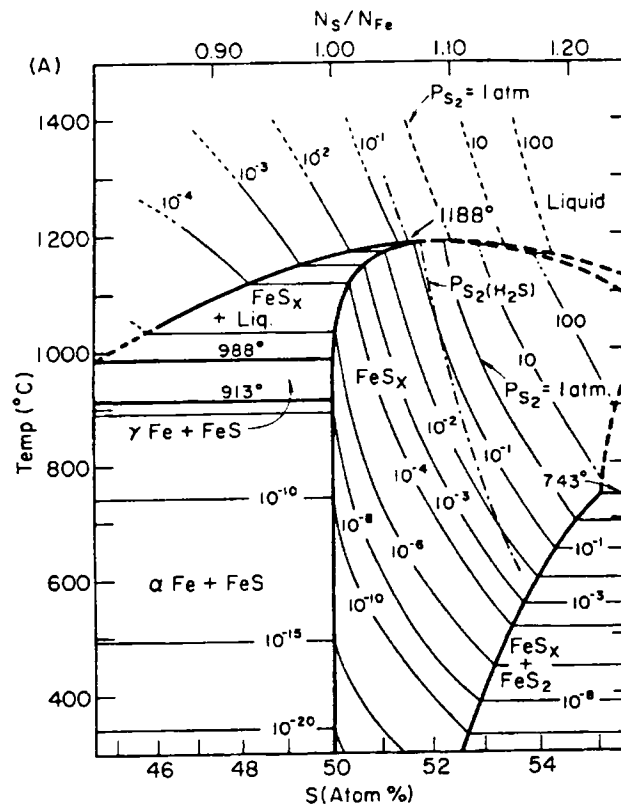
**Figure 115: Iron – sulphur phase diagram [Burgmann et al._1968].**

It can be seen from Figure 115 that, at a pressing temperature of 500°C, at lower concentrations of sulphur (i.e. <50 atomic%), the iron and sulphur will react to form $\alpha$Fe (i.e. ferrite) and FeS. However, as the sulphur concentration increases, iron polysulphides are more likely to form. The formation of iron sulphides, as a reservoir of sulphur, may therefore act as a barrier to the further oxidation of the iron mould by the gradual decomposition of the iron sulphides to form sulphur oxides.

### 4.1.1.4 Possible Corrosion of Cast Iron within Container Formation

In addition to the surface of the cast iron mould reacting with oxygen in the air, it could also react with water vapour in the atmosphere. As previously mentioned in Chapter 1 (section 1.2.4), the trials have been carried out on the use of water based mould lubricants as part of the "Elimination of Manual Lubrication of Forming Moulds" work carried out by British Glass Technology [1994 - 1997] which would also increase the local humidity at the glass-to-mould contact surface. Therefore water in the atmosphere may react with the mould material affecting the oxide/hydrous oxide scale formed, or even the glass melt affecting its temperature-viscosity properties during forming.

Corrosion of iron in an oxygen containing atmosphere is also dependent on parameters such as temperature and local humidity (which is in turn affected by the temperature). If the humidity in an oxygen containing atmosphere is so high that a film of moisture condenses on the surface of the metal, electrochemical corrosion will occur at weak spots in the oxide film [Cottrell_1975]. If the surface of the iron is kept dry (i.e. kept in a less humid atmosphere) aqueous corrosion can still occur, as iron oxides are hygroscopic. In the UK, the relative humidity, at normal temperature and pressure, is usually approximately 60%. The relative humidity in the atmosphere during pressing, at elevated temperatures, will be lower than 60%, but of course the absolute mass of water vapour in the atmosphere will be the same as at normal temperature and pressure. Below this relative humidity, no rusting occurs and only oxidation occurs. However, if the relative humidity in the atmosphere became higher than 60% the likelihood of

rusting will increase [Cottrell_1975]. However, which reaction occurs will also depend upon the temperature and level of oxygen present in the atmosphere.

The corrosion of substances in a water-containing atmosphere can be investigated using a Pourbaix diagram, which indicates which phases are thermodynamically stable as a function of the applied emf and pH, however usually only at ambient temperatures. Figure 116 shows the Pourbaix diagram for the iron – water system at 25°C.
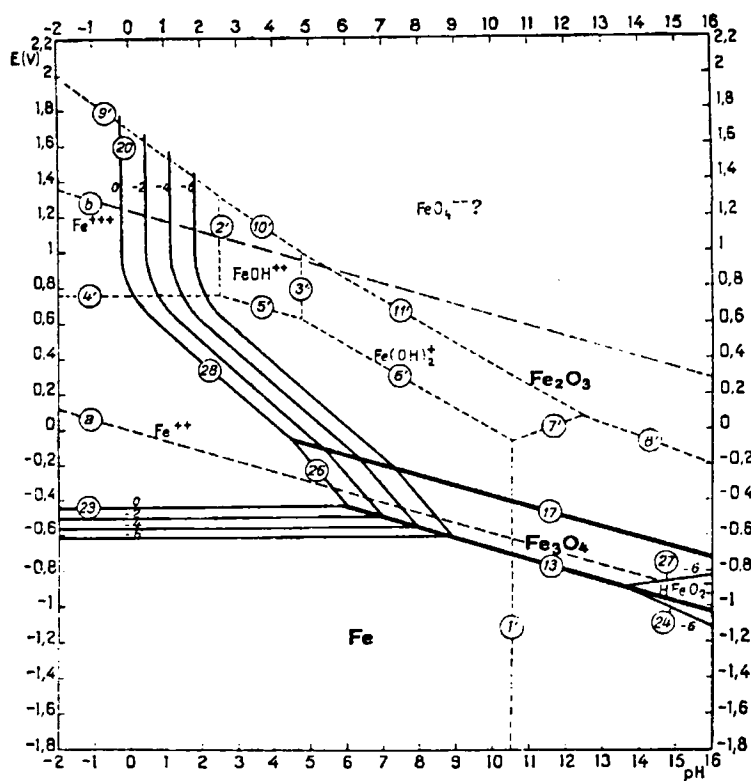


Figure 116: Potential pH diagram for the iron – water system at 25°C [Pourbaix_1963].

The line marked 'a' on Figure 116 shows the hydrogen evolution reaction and 'b' shows the oxygen evolution reaction, which are both pH dependent. Above the oxygen line, oxygen gas is liberated, whilst below the hydrogen line, hydrogen gas is liberated.

It can be seen from Figure 116 that under pH 4 the iron is prone to corrosion, i.e. $Fe^{2+}$ ions form due to dissolution of the iron in water. As the pH increases, less and less $Fe^{2+}$ tends to dissolve in water to form a protective passive film (i.e. $Fe_2O_3$) on the iron. This means that the majority of the corrosion of the cast iron surface will occur if it is in an acidic environment (e.g. if an acidic gas such as $SO_2$ is present in the atmosphere). However, the Poubaix diagram seen in Figure 116 is for the system at 25°C. At elevated temperatures such as those used in the fabrication of glass articles, the situation may be altered due to the change in relative humidity.

It can be seen from Figure 116 that at zero applied emf, there is also the possibility of the formation of hydrous oxides in addition to iron oxides. This would mean that in glass container forming, it is important to consider the formation of insoluble hydrous oxides on the mould surface due to the presence of water in the local atmosphere. Predominance diagrams can be used to determine which hydrous oxides are most likely to be the predominant species at what pH. The predominance diagram for ferrous iron can be found in Figure 117 whilst that for ferric iron can be found in Figure 118.
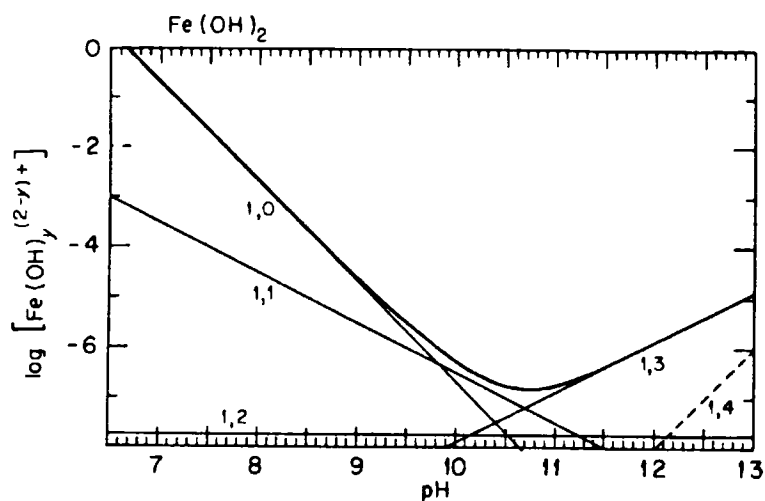
**Figure 117: Predominance diagram for ferrous iron showing the distribution of hydrolysis products in solutions saturated with Fe(OH)₂ at 25°C [Baes &Mesmer_1986].**

It can be seen from Figure 117 that hydrolysis of $Fe^{2+}$ to form a hydroxide does not start until a pH of 7. Between pH 7 and pH 10, it can be seen that the most dominant species are soluble, i.e. $Fe^{2+}$ and $Fe(OH)^+$. Above pH 10 insoluble $Fe(OH)_2$ starts to form and become the most dominant species. Therefore, in this regime, precipitation of insoluble ferrous hydroxide occurs before appreciable hydrolysis products are formed in solution (i.e. $[Fe(H_2O)_2]^{2+} \rightarrow Fe(OH)_2\downarrow + 2H^+$). This insoluble ferrous hydroxide is likely to be present in the layers of corrosion product on the surface of the cast iron mould if the pH was allowed to rise above 10, however, is unlikely to be crystalline.
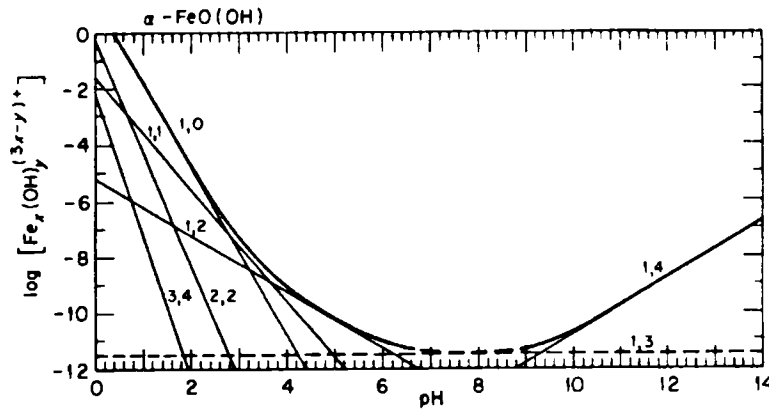
Figure 118: Predominance diagram for ferric iron showing the distribution of hydrolysis products in solutions saturated with α-FeO(OH) at 25°C [Baes &Mesmer_1986].

It can be seen from Figure 118 that hydrolysis of $Fe^{3+}$ starts at pH1 and hence occurs across the whole pH scale, generally forming soluble products such as $Fe(OH)^{2+}$ in acidic solutions. Here, the most insoluble ferric hydroxide is α-Fe(O)(OH)↓ which is likely to be a crystalline phase [Baes &Mesmer_1986]. Thus, Fe(O)(OH) could be present in the corrosion layers of a cast iron glass container mould that had been used in a humid atmosphere.

### 4.1.1.5 Material Transfer During the Pressing of Glass Samples

Iron rich particles, which have become detached from the cast iron plunger surface during the production of the pressed glass samples, have been seen to become embedded in the surface of the pressed glass sample (e.g. Figure 62). These particles are most likely to have occurred due to oxidation of the cast iron surface (as discussed above). Oxide layers do not adhere well to the parent metal and can detach from the surface of the cast iron plunger.

Industrially, such embedded particles may have detrimental effects upon the strength of the finished glass article. Previous work by Puyane [1976] has shown that materials that are purposely dropped onto the surface of a glass melt decrease strength of the glass sample by differing amounts depending on the temperature of the glass and the type of damaging material used. For example, when iron oxide particles were dropped onto the surface of a glass at 600°C, the mean fracture stress of the resulting glass sample was found to be $249.8\pm44.6$MNm$^{-2}$ whereas if they were dropped on a glass melt at 1000°C the mean fracture stress decreases to $83.1\pm8.8$MNm$^{-2}$, compared to a mean fracture stress of $264.8\pm42.7$MNm$^{-2}$ for glass discs with no deliberate damage [Puyane & Rawson_1979].

These decreases in strength seen could be attributed to differences in thermal expansion coefficient between the embedded material and glass. The thermal expansion coefficient of a typical soda-lime-silica glass is approximately $8 - 9 \times 10^{-6}$K$^{-1}$, whereas the approximate thermal expansion coefficient of a cast iron is $12.5 - 14\times10^{-6}$K$^{-1}$ [Kirsch_1993]. This differential thermal expansion coefficient between the cast iron and glass may cause circumferential cracking. Previously, circumferential cracking has been observed around embedded particles [Puyane_1976] and has also been seen around large embedded particles in the current work.

The halo effect seen on scanning elecron micrographs of the pressed glass surface in the current study (e.g. Figure 57) may suggest that there has been some dissolution of the iron rich particles embedded in the melt during pressing

[Lee_1997]. Any dissolution of the iron in the glass melt around the particle may give an iron rich glass with different physicochemical properties from the surrounding glass. Similar halo effects around embedded particles have not been observed using back-scattered electron imaging (which should show changes in composition). This may suggest that the halos seen with secondary electron imaging could be due to a shadowing effect. The resolution of back-scattered electron detectors, however, is lower than that found for secondary electron detectors and therefore, if small (dimensionally) compositional changes are found, it may not be possible to resolve them using back-scattered electron imaging.

Experimentation at the beginning of the work reported in this thesis was carried out to examine the effect of increasing the iron content of a soda-lime-silica glass on the glass properties (see Appendix B for further details). It was found that as the iron content of the soda-lime-silica glass was increased, the glass transition temperature ($T_g$) decreased. For example, a drop of approximately 30°C in $T_g$ occurred for a 12 wt% addition of $Fe_2O_3$ to a $SiO_2$-$Na_2O$-$CaO$-$Al_2O_3$ melt [Hollands_1995]. It should be noted, however, that the melt used in the current work was not the same as that used when $Fe_2O_3$ was added deliberately; the composition of the base glass used in the current work was approximately 73wt.% $SiO_2$, 2wt.% $Al_2O_3$, 11.5w.t% $CaO$ and 13wt.% $Na_2O$ whereas the composition of the base glass used in the iron doping work was 72wt.% $SiO_2$, 2wt.% $Al_2O_3$, 12wt.% $CaO$ and 14wt.% $Na_2O$ to which the iron oxide was added. Thus, for instance, a glass with a 12wt.% $Fe_2O_3$ addition was produced by adding 12g of $Fe_2O_3$ to 100g of the base glass ($72SiO_2$-$2Al_2O_3$-$12CaO$-$14Na_2O$). A graph of the

effect of iron content on the glass transition temperature of the glass melt can be

seen in Figure 119.
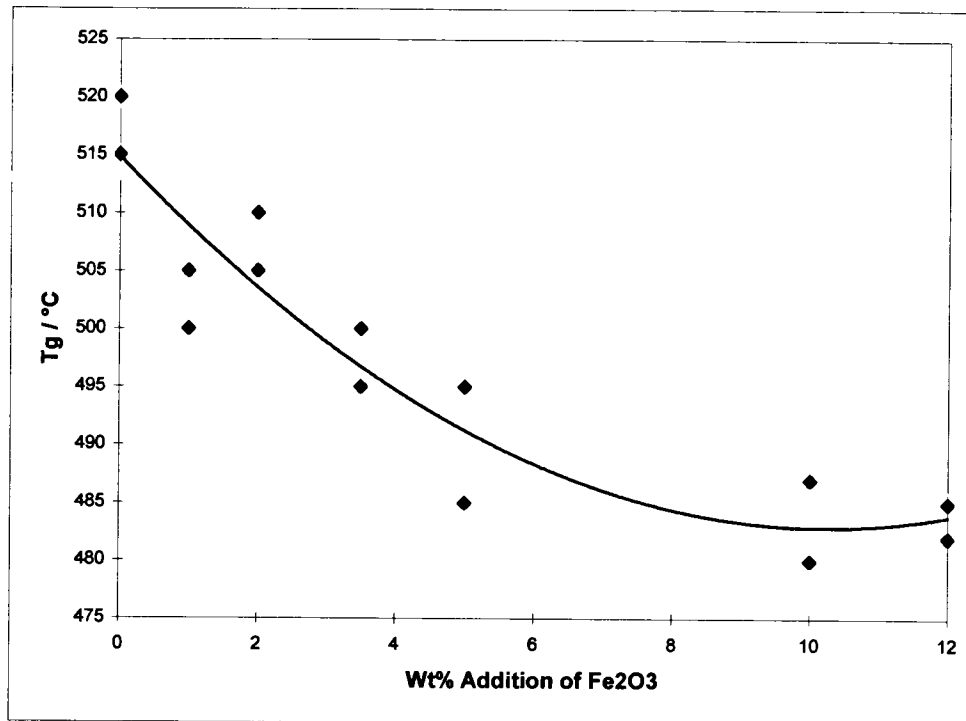


Figure 119: The effect of iron content on the glass transition temperature (T$_g$) of a SiO$_2$-Na$_2$O-CaO-Al$_2$O$_3$ glass [Hollands_1995].

A decrease in T$_g$ would suggest that in areas where the concentration of iron was

high, the glass melt would have a different viscosity to the rest of the melt that

would affect the surface of the glass article during forming. Any local changes in

the viscosity at the surface of the glass melt could mean that higher than normal

stresses could occur in localised points on the surface of the article due to areas

solidifying faster than others.

The thermal expansion coefficient of an iron enriched soda-lime-silica glass has been seen to increase with increasing $Fe_2O_3$ content to a maximum of to a 5% wt% addition of $Fe_2O_3$ and then decreases as the iron content increases further [Hollands_1995]. A graph showing the effect of iron content on the thermal expansion coefficient of the glass can be found in Figure 120.
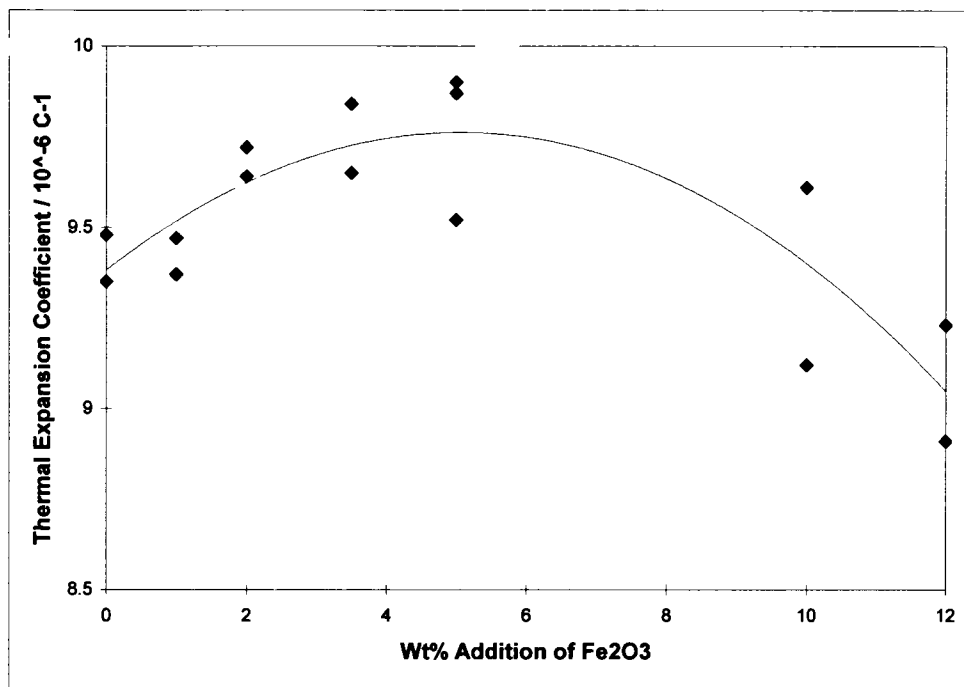


Figure 120: The effect of iron content on the thermal expansion coefficient of a $SiO_2$-$Na_2O$-$CaO$-$Al_2O_3$ glass [Hollands_1995].

The thermal expansion of glass depends on the strength of the bonds within the glass with weak, floppy bonds giving more expansion. The production of $Fe^{2+}$ ions within the glass would produce weaker bonds than those for $Fe^{3+}$ ions, as the charge is lower. It may therefore be possible from the influence of the increase in iron content in the glass on the thermal expansion coefficient to infer that the

number of $Fe^{3+}$ ions in the melt increases until a 5 wt% concentration is achieved, and then the number of $Fe^{2+}$ ions present increases.

UV-visible spectroscopy of these glasses was carried out to try and establish whether the hypothesis discussed above was the case.
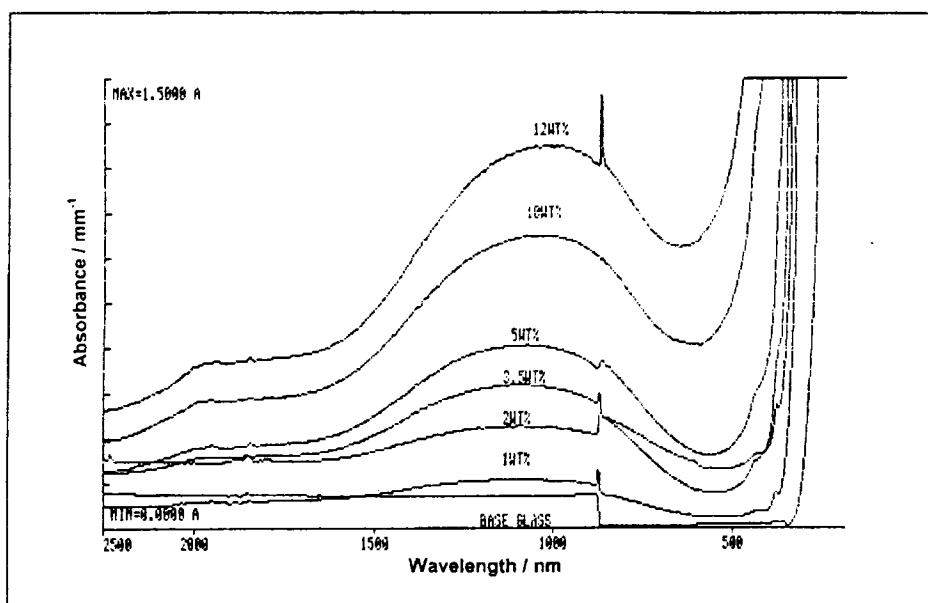


Figure 121: The effect of iron content on the UV-visible spectra of a $SiO_2$-$Na_2O$- $CaO$-$Al_2O_3$ glass showing iron present as $Fe^{2+}$ (in both octahedral and tetrahedral sites) and $Fe^{3+}$ [Hollands_1995].

It can be seen from Figure 121 that $Fe^{2+}$ is present in both octahedral sites (2000nm) and tetrahedral sites (1100nm). However, the peak for $Fe^{3+}$ (400nm) coincided with the UV cut off edge of the glasses containing greater concentrations of iron and hence the theory could not be tested. An XPS examination of the iron rich glasses was therefore carried out to establish the

ferrous to ferric ratio in the iron rich glasses. However, the peak observed for iron was too small to determine the $Fe^{2+}$ to $Fe^{3+}$ ratio even for glasses containing large amounts of iron.

### 4.1.1.6 Viscosity Characteristics of the Glass Melt

It has been found by examining scanning electron micrographs and comparing these to three dimensional atomic force microscope (AFM) images, that the size and depth of the pressed-in dimples seen on the pressed glass surface alter with changes in the plunger properties. From the experimental work, it can be seen that narrower, deeper dimples are produced in the pressed glass surface as the plunger temperature is increased. AFM evidence in Figure 42 shows the texture of a glass sample pressed using a low plunger temperature of 300°C (cast iron finish of 1200 grit). The dimples formed have been found to be approximately 150-200nm deep and are approximately 15μm across with fairly shallow sides. This can be compared to the AFM evidence shown in Figure 48 which shows a glass surface which had been pressed using a similar cast iron plunger using a higher plunger temperature of 510°C. At this higher initial plunger temperature, the dimples have been found to be 400nm deep and approximately 8μm across. This evidence would indicate that the glass melt has flowed further into the imperfections in the cast iron surface at higher initial plunger temperatures. The changes in viscosity of the surface of the glass melt on contact with the relatively cool plunger may explain the observed changes in surface texture found on the pressed glass surface.

The viscosity-temperature characteristics of the glass melt used in this project can be modelled using the Vogel-Tamman-Fulcher equation [Rawson_1980] (equation 1-1) which was described in section 1.1.1. The three constants from the Vogel-Tamman-Fulcher equation (i.e. B, A and $T_0$) can be calculated from the known composition of the glass melt using the Lakatos equations [Lakatos_1972] (found in equations 1-2, 1-3 and 1-4 respectively). Figure 122 shows the calculated viscosity-temperature characteristics of the glass melt used in this project.
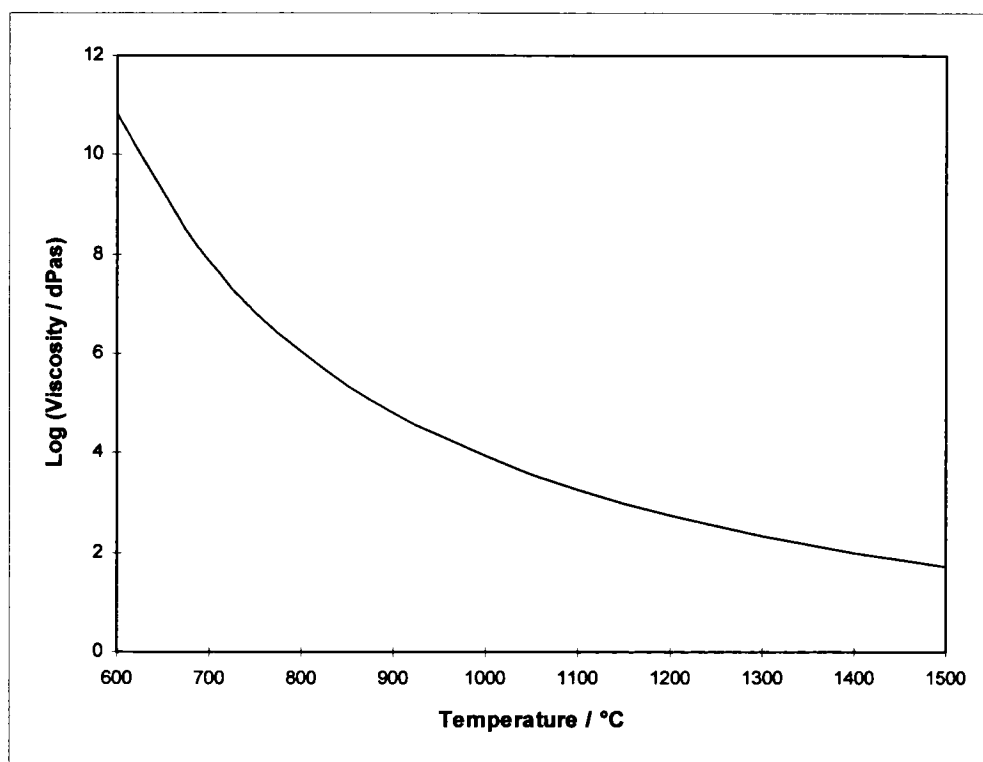


Figure 122: The viscosity-temperature characteristics of the glass melt (72.64wt% $SiO_2$ - 11.43wt% CaO - 13.00wt% $Na_2O$ - 1.68wt% $Al_2O_3$ - 0.56wt% $K_2O$ - 0.19wt% $SO_3$ - 0.14wt% MgO - 0.046wt% $Fe_2O_3$) calculated using the Vogel-Tamman-Fulcher and Lakatos equations (where B=3848, A=1.47 and $T_0$=287°C).

During the formation of glass containers, heat needs to be withdrawn from the surface of the glass melt to form a rigid glass skin. Examining the viscosity-

temperature characteristics shown in Figure 122, it can be seen that the surface temperature must fall from the initial glass melt surface temperature of 950°C (approximate viscosity $10^4$ dPas) to at least 700°C (corresponding to an approximate viscosity of $10^8$ dPas) which are the values for appropriate viscosities outlined in Table 1 [ed. Zarzycki_1991].

During the pressing operation, the glass melt will tend to be forced into any imperfections in the surface of the plunger. The glass melt will therefore flow to try and follow the texture of the plunger until the surface of the glass melt becomes so viscous that the pressing pressure used cannot force the glass melt to flow any further.

The surface finish of the plunger has been shown to affect the resulting texture found on the pressed glass sample (c.f. Figure 45 with Figure 48). A coarser finish to the cast iron plunger has been shown to give a coarser texture to the resulting pressed glass surface.

Pressing glass samples at low plunger temperatures will mean that initially the heat will be withdrawn faster from the surface of the glass melt than glass samples pressed using a higher initial plunger temperature. This may explain why the dimples found on the surface of glass samples which were pressed using a lower initial plunger temperature were shallower than those seen on pressed glass samples which were pressed using higher initial plunger temperatures.

When pressing glass samples using vacuum assisted pressing, the glass melt is pulled into the surface of the cast iron plunger. This means that the glass melt will tend to flow deeper into crevices and imperfections in the cast iron plunger during pressing. The use of a vacuum to aid pressing produces a glass surface that has deeper pressed-in dimples (Figure 77) than that found on glass samples where vacuum assistance was not used (Figure 45). Alternatively, the vacuum used may evacuate any trapped air within the press head which would have acted as a cushion to the flow of the glass melt around the imperfections in the cast iron plunger surface. The latter of the two explanations for the difference in resulting surface finish of the glass sample when vacuum assistance is used in pressing is less likely as the fit between the plunger sample and the plunger housing in the press head was not tight (see Figure 6). This would therefore mean that any air within the press head would be forced out through the small gap between the plunger sample and its housing during pressing. However, if the air had been trapped in between the cast iron plunger and glass melt during pressing, the gas contained would have become compressed, which would affect the reactivity of the species present (see section 4.1.1.1).

Unfortunately, glass-to-plunger sticking could not be observed using the experimental pressing temperatures achievable, as described in Chapter 2, due to heat losses to the surrounding atmosphere. It is worth noting that it has been suggested previously [Manns *et al.*_1995] that sticking occurs if the contact temperature becomes high enough to reduce the viscosity of the glass melt at the glass-to-mould interface enough to overcome the surface tension of the glass melt.

*4.1.1.7 Sodium Transfer Between the Glass Melt and Cast Iron Mould*

During pressing of the glass samples using a cast iron plunger, it was observed (using x-ray photoelectron spectroscopy (XPS)) that in addition to bulk iron oxide material transfer from the plunger to pressed glass surface (seen by the inclusion of embedded iron rich particles in the glass surface using scanning electron microscopy (SEM)), there also appears to be sodium ion migration. XPS, however, has not shown any evidence of iron transfer from the plunger to the pressed glass surface despite the overwhelming scanning electron microscope evidence. This lack of XPS evidence for iron on the pressed glass surface may be due to the low detection limit (approximately 1 at%) of the XPS equipment used.

XPS results have indicated that the surface of cast glass is depleted in sodium. It can be seen in Table 2 that the atomic ratio of sodium (i.e. $100 \times$ at% Na/$\Sigma$(at% Si, Na, Ca)) for the bulk composition found using XRF (x-ray fluorescence spectroscopy) is 18 when compared to 2 for the surface composition using XPS. Previous work has also shown that surfaces of glass bottles have a layer depleted in sodium and calcium [Anderson *et al._*1975, Fox_1981]. Other published work, however, suggests that both calcium and sodium will migrate from the glass surface when irradiated during an XPS examination due to a positive charge building up on the glass surface [Binkowski *et al._*1976]. This latter explanation may explain why, even with the crude depth profiling carried out, the calcium and sodium levels in the glass apparently remained static (see Figure 41).

XPS examination of the surface of a cast iron plunger that had been used to press 30 glass samples has shown it to have evidence of sodium at the surface (see Figure 68, Figure 69 and Figure 70). The sodium present appears to be that pertaining to $Na_2O$, as the binding energy of the sodium peak was found to lie at 1072.4eV which compares well with the published value of 1072.5eV [Briggs & Seah_1990]. Migration of the sodium ion should be easy due to its size and charge. The large temperature gradient found in the very surface of the glass melt during forming (see Figure 109) would tend to increase, at the higher temperature, the mobility of sodium ions. It is concluded that it is entirely feasible that $Na_2O$ has been transferred from the glass to the cast iron plunger on contact with the glass melt on pressing. The surface of the glass will then have a depleted sodium layer. Another possible explanation for the presence of sodium on the cast iron surface could be due to local sticking of the glass melt to the cast iron plunger during pressing. However, examining the expected silicon:sodium atomic ratio for bulk glass transfer (i.e. 100:36±2) when compared to the results found using XPS (i.e. 100:48±5) suggests that bulk glass transfer is less likely as there appears to be an excess of sodium present.

This phenomenon of sodium transfer from the glass to plunger materials has been reported by others very recently [Falipou et al._1997]. It has been suggested that sodium oxide within the glass surface is reduced to sodium at the expense of oxidation of the metallic elements in the plunger, which is acceptable thermodynamically. The metallic sodium on the plunger surface is then re-oxidised using oxygen in the ambient atmosphere. Thus for the glass samples

which were pressed using vacuum assistance (i.e. with an oxygen depleted atmosphere), the migration of sodium in the glass melt to the cast iron mould during the formation of glass containers may be restricted. However, this point was not followed up in this study due to lack of time.

## 4.1.2  Carbon-Carbon Composite Plungers

The use of an alternative material to that of cast iron should be investigated due to the instability of the oxide surface produced on cast iron and subsequent problems for glass articles. Recently, several alternative possible contact materials and protective coatings have been investigated [e.g. Falipou *et al._*1997, Manns *et al._*1995]. As carbon is used in glass-to-metal lubricants, the use of carbon as a glass contact material is a possible candidate. The work carried out by Fairbanks *et al.* [1949 – 1964] suggested that graphitic carbon had a high sticking temperature. However, graphitic carbon itself does not have the mechanical durability necessary for glass container manufacture. Carbon is already extensively used for hot end handling in the glass container industry, although it does not have the mechanical strength and oxidation resistance required [Williams_1989]. For these reasons, it was decided that the feasibility of carbon-carbon composite materials as possible hot glass contact materials should be investigated here.

Examination of the pressed glass surfaces made using carbon-carbon composite plungers with the scanning electron microscope (SEM) has revealed dimples and pressed–in particles present which were similar in appearance to those found when the glass was pressed using cast iron (e.g. Figure 80, Figure 83 and Figure 84

etc.). The appearance of the pressed-in dimples appeared to alter with the type of composite investigated (i.e. the surface finish due to fibre orientation) and the initial plunger temperature. The presence of pressed-in particles present on the glass surface, however did not appear to alter when the pressing parameters were altered. In all cases, the glass surfaces pressed using carbon-carbon composite materials appeared to have evidence of both metallic (i.e. containing iron, chromium and nickel) and carbonaceous particles. The most likely source of the metallic particles is from the tools used to prepare the plunger samples.

In general, the dimples/grooves produced in the glass surfaces that were pressed using carbon-carbon composites were better defined and closer replicas of the material surface even when pressed at lower temperatures than the glass samples pressed using cast iron. In the case of the carbon-carbon composite laminate material, the pressed glass surface appeared as a replica of the laminate material itself (e.g. compare the laminate material shown in Figure 78 with the pressed glass surface in Figure 80). This amount of replication of the original plunger texture appeared to be more evident when pressing at higher initial plunger temperatures. The better definition, compared to those features found using cast iron plungers, may be due to the size and geometry of the features present on the carbon-carbon composite surface (i.e. rounded fibres between 10-80$\mu$m in diameter) which allowed the glass melt to flow around easier. From the suppliers information, the thermal conductivity of the carbon-carbon composite material is 28Wm$^{-1}$K$^{-1}$ in plane and 8Wm$^{-1}$K$^{-1}$ crossply. Therefore, as the thermal conductivity is lower than that for cast iron (i.e. 41-49Wm$^{-1}$K$^{-1}$), the surface

temperature of the carbon-carbon composite remains higher for a longer period of time (i.e. not drawing the heat from the glass melt) thus making the glass melt fluid enough to flow for a longer period of time than when cast iron was used. In addition to the larger features present on the surface, there is also evidence of porosity on the plunger surface (e.g. Figure 79). This porosity may suggest that any air present between the glass melt and plunger sample would permeate the composite, therefore eliminating the possibility of a protective cushion of air which could prevent damage to the surface of the glass melt. The porosity of the surface of carbon-carbon laminates has been reported to give variable surface characteristics to the hot glass contacted when used industrially for hot end handling equipment such as takeout tongs [Budd & Vickers_1990].

The use of the carbon-carbon composites supplied as high temperature glass contact materials for use as moulds and baffles etc., however, may not be possible due to oxidation which forms gases such as CO, $CO_2$ etc. (see Figure 112). SEM examination of the surface of the composites which had been used to press glass samples has shown there to be degradation in both the matrix and fibres (e.g. Figure 99 and Figure 100). This would therefore indicate that the graphite oxidises at pressing temperatures and therefore would also oxidise if it were used in mouldware for the formation of glass containers. This means that during pressing, the carbon in the fibres and matrix is likely to react with oxygen in the atmosphere and within the glass melt itself to produce gaseous $CO_2$. It can be seen from the Ellingham diagram (in Figure 112) that at all temperatures of interest, the formation of $CO_2$ is likely. Thus, it is probable that the integrity of the composite

will not be maintained during use, meaning a short lifetime. Oxidation resistant graphitic materials are available that are produced by undergoing a complex heat treatment process which alters the crystalline structure and by the introduction of oxidation inhibitors. These oxidation resistant graphite carbon materials may be more suitable for the production of glass containers as they will be less prone to degradation at the working temperatures used [Gerber_1994]. If carbon-carbon composites such as the ones investigated here were to be used in the glass container industry for items such as moulds, a method for maintaining stability of the material at the temperatures required needs to be determined (e.g. a TiC coating [Rossing_1995]). The use of a coating or other method to stabilise possible oxidation of the carbon surface, however, could mean that the attractive properties of using this type of material would be lost.

In addition to the carbon materials investigated here, there is scope for examining the effect of glass melts on other carbonaceous materials such as vitreous carbon. Vitreous carbon, however, may be oxidised too quickly in the normal atmosphere at the temperatures required. Evacuation or the use of an inert atmosphere could theoretically be used to reduce oxidation, however this would slow down the processing and is unlikely to be easily implemented in practice.

The use of coatings on the surface of mouldware could increase longevity and decrease the need for using mould dope. Synthetic diamond-like coatings could produce a surface on a mould which is likely to increase the resistance to surface

damage. This type of coating should be investigated further to establish how it would react at the elevated temperatures used in the formation of glass containers.

## 4.2   Current Practice

The work carried out in this project has concentrated on the examination of the reaction between cast iron and a soda-lime-silica container glass in a static press (i.e. with little glass movement). However, in practice, it is likely that the use of a mould lubricant or mould pre-coat will be utilised to prevent the glass melt from sticking to the mould due to the high temperatures and speeds normally encountered. These mould lubricants may provide protection to the glass melt from the unstable iron oxide surface by the formation of a protective gas layer. The formation of a container is a two stage process where initially the glass melt is either stretched over a plunger to fill a blank mould (in the press and blow process), or blown into a blank mould, to form a parison. The parison is then allowed to reheat to form a more fluid surface and blown further into the final blow mould. Thus the glass melt will flow and "slide" over the surface of the mouldware. The practice used in the formation of glass containers would be different to the situation used here in the experimental pressing work, where the glass melt is statically held with no protective barrier between the glass melt and plunger. However, the work carried out in this investigation has given some important clues about what happens at the glass-to-metal interface during the formation of glass samples.

In a meeting with one of the UKs major cast iron mould manufacturers (*Birstall Foundry*, 1997), many issues were raised about the limitations of cast iron as a mould material to be used in the glass industry. At today's high production speeds and temperatures, cast iron is considered to be near to the limits of its usable range. Therefore, alternative manufacturing techniques and/or materials need to be explored in order to progress.

The lifetime of cast iron mouldware is limited by two major factors: material and misuse. Cast iron as a material is limited in that softer areas such as graphite and ferrite are removed from the surface at a faster rate to the rest of the iron resulting in features such as surface pitting. Another contributory factor to premature failures of mouldware can be attributed to misuse. Misuse can arise from:

1) storage problems such as storing mouldware in humid areas or stacked up against walls resulting in corrosion and

2) thermal shock due to rapid cooling (e.g. operatives dropping hot moulds into a bucket of cold water to cool them).

One of the main problems highlighted is with the use of forced mould cooling. The temperature gradient across the surface of the mouldware would be increased with the use of vertical mould cooling$^2$. The more traditional types of mould consist of a solid piece of cast iron. This type of mould gave slow production speeds, but the mould was structurally sound with no stress raisers (Figure 123).
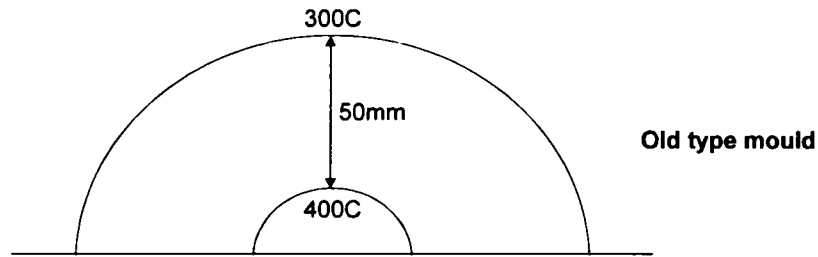
**Figure 123: Schematic diagram of the heat transfer involved within a mould using no mould cooling.**

New type moulds consist of a solid piece of cast iron which have a number of holes drilled through the length of the wall. These holes are used to pipe cooling air through the mould, facilitating cooling and consequently allowing production speeds to be increased. The drilled holes however act as stress raisers, and also the temperature gradient near the mould surface is much higher than in undrilled moulds.
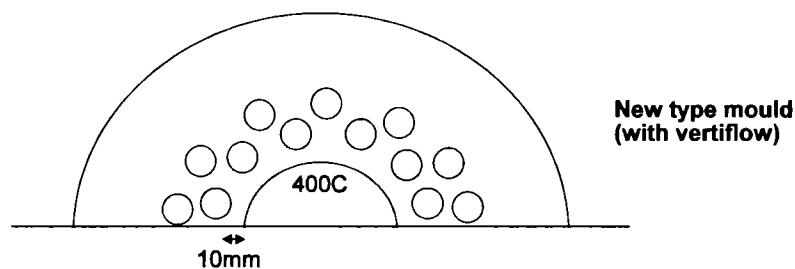


**Figure 124: Schematic diagram of the heat transfer involved within a mould using vertical mould cooling.**

---

[2] Such as Vertiflow

It can be seen from Figure 123 that in traditional moulds a temperature drop of about 100°C can be observed through about 50mm of material (i.e. the whole thickness of the mould) whereas new type moulds with vertical cooling have a potential temperature drop of 300°C through 10mm at the working surface (Figure 124).

If a mould has failed prematurely due to cracking, it is often thought that this is due to the material from which the mould has been made. If one of these moulds is sectioned it is more usually found that the crack has initiated from one of the cooling holes and not from the surface of the material (see Figure 125).
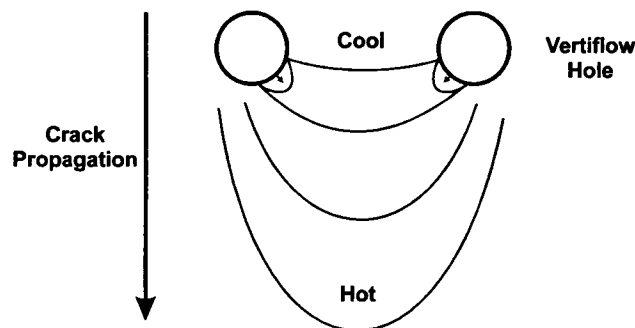


**Figure 125: Schematic diagram showing how cracks in cast iron mouldware form and propagate**

In Figure 125, the crack can be seen to grow from the relatively cool vertical cooling hole to the working surface of the mould resulting in the crack seen on the surface. Evidence of this behaviour can apparently often be found if a failed mould is sectioned.

On initial use of mouldware, the moulds are worked up to the desired working temperature from a lower preheated temperature. The mould cooling is then switched on to maintain this temperature. This increased amount of mould cooling could give rise to thermal shock leading to the increased likelihood of premature failure.

Mould cooling at present is generally carried out by forcing relatively cool air through a series of vertical holes close to the working surface of the mould. It has been shown that this type of mould cooling has its own associated problems with limiting the life of the mould. An alternative technique by which moulds are cooled between the glass contact cycle to ensure that production speeds are maintained needs to be investigated. One possible idea is using a cooling jacket with temperature feedback that is placed around the mould.

The work that has been presented in this thesis has shown that the use of cast iron as a mould material for use in the formation of glass containers has its drawbacks. The instability of the iron surface when exposed to an oxygen-containing atmosphere is one of the major problems. Therefore, work needs to be carried out to find a new material or coating which is stable in oxidising atmospheres at high temperatures but does not detrimentally react with the glass surface, or to exclude oxygen, but this would be difficult to achieve without jeopardising production rates.

## 4.3 Summary

This chapter has discussed the results obtained from the experimental pressing investigation for both cast iron and carbon-carbon composite plunger materials. In addition, a number of concerns raised by one of the UKs leading cast iron mould manufacturers has been addressed. Chapter 5 will outline the conclusions that have been reached from this project and attempt to suggest areas of specific interest where future work should be carried out.

# 5. CONCLUSIONS AND FUTURE WORK

## 5.1   Conclusions

Previous work carried out within this field has not really explained exactly what happens when a hot mould material contacts a glass melt during the formation of glass articles such as containers. However, much of this previous work had been carried out before modern instruments such as x-ray photoelectron spectroscopy were commonplace. The current work has attempted to increase the general understanding for both the moulding material used and the resulting pressed glass surface made using a semi-automated experimental pressing rig.

In general for all the mould materials investigated in the current work, the pressed glass surface could be seen to contain defects such as embedded pressed-in particles and pressed-in dimples. These defects are likely to have an effect of the mechanical strength of the final article formed. It could be seen that the appearance of the pressed glass surface was affected by process parameters such as the initial temperature of the plunger used, the surface finish of the plunger material and whether or not vacuum assisted pressing had been used.

As might be expected, the surface finish of the cast iron plunger material used had a direct effect on the texture of the pressed glass surface. It could be seen that for finer plunger finishes the resulting texture of the pressed glass surface was improved. However, the surface of the pressed glass sample was not an exact

replica of the tool used to make it. The most likely reason for this is due to the viscosity of the surface of the glass melt becoming too great for it to fully flow into the defects in the plunger surface.

In addition, the initial plunger temperature used during pressing appeared to affect the surface finish of the pressed glass surface. It was largely found that using an initial pressing temperature of below 450°C resulted in a randomly rippled 'chilled' glass surface. The reason for this behaviour is likely to be that the temperature of the surface of the glass melt was reduced at such a rate on contact with the plunger that it resulted in the surface of the melt rapidly gaining a high viscosity. As the viscosity of the melt became too high for flow into the defects found on the plunger surface, it in effect, 'sets' resulting in the ripples seen. As the initial temperature of the plunger was increased, the surface texture of the pressed glass sample became a closer replica to that of the plunger.

The thermal conductivity of the plunger material used also appears to affect the extent to which the surface finish was replicated on the pressed glass surface. It was found that the glass surfaces pressed using plungers made from carbon-carbon composites had a much closer finish to that of the plunger material used than when compared to a glass surface which had been pressed using a cast iron plunger at the same pressing temperature. This would indicate that using a material with a lower thermal conductivity (such as this type of carbon-carbon composite when compared to cast iron) would keep the viscosity of the glass melt higher for longer, thus resulting in the melt flowing deeper into any surface

defects (when using a contact time of 4 seconds). However, in practice, using a material with a lower thermal conductivity would imply that longer processing times would be required than are presently used.

The surfaces of the cast iron and carbon-carbon composite plungers appear to have been affected by the initial plunger temperature used. As the initial pressing temperature was increased, the amount of oxidation seen also appeared to increase.

Examination, using x-ray photoelectron spectroscopy, of both the pressed glass surfaces and the plunger material used to make them indicates that migration of sodium ions from the glass melt to the plunger has occurred during forming. The migration of sodium ions from the glass has resulted in the surface of the supercooled glass melt sample being depleted in sodium and a layer of sodium oxide being present on the cast iron plunger surface.

## 5.2 Future Work

Much of the work carried out in the present investigation adds to the current understanding of the interaction between the glass melt and mould material during the formation of glass containers. However, it can be seen that there is still a substantial amount of work that needs to be carried out in order to follow up some of the important threads.

The experimental work carried out in the current study indicates that the initial temperature at which a cast iron plunger contacts a soda-lime-silica glass melt appears (visually) to affect the type of scale formed on a cast iron plunger surface. In addition, it has been discussed within section 4.1.1 that the cast iron plunger could react with all components in the surrounding atmosphere (i.e. oxygen, water, the glass melt itself etc.). It is therefore important to establish what reactions have actually taken place at the glass melt to plunger interface. This could be carried out using x-ray diffraction on the cast iron plunger surfaces immediately after the formation of glass samples, which would establish which crystalline phases are present on the surface of the cast iron plunger. Once it has been established which crystalline phases are present on the cast iron surface after being in contact with a glass melt, it might be possible to suggest a method for increasing the resistance of the iron surface to oxidation/corrosion such as the use of a coating or the use of an alternative atmosphere. If the resistance to oxidation/corrosion on the surface of a cast iron mould were increased, the possibility of iron rich particles from the scale becoming embedded within the surface of the glass article is likely to decrease. It might also be interesting to establish whether the surface of the cast iron is affected by pressing glass samples in an inert atmosphere (such as nitrogen) or where the relative humidity had been increased.

It has been seen in the current work that migration of sodium ions from the surface of the glass melt to the surface of the cast iron mould has occurred. The action of the sodium ions migrating from the immediate surface of the glass melt may assist

in producing a layer on the surface of the final glass article with a different stress pattern to that of the bulk. Further work needs therefore to be carried out to determine whether forming parameters such as the temperature, time of contact, pressing pressure required etc. affect the amount of sodium migration from the glass melt to the forming tool. The depth of the sodium depleted layer in the surface of the glass article will affect any stress pattern at the immediate surface of the final article. Therefore a study is required which could determine the depth and extent of any sodium migration during the pressing of glass samples. A study of this type would require the forming parameters used during the pressing of glass samples to be systematically altered such as temperature, time of contact and sodium content of the glass melt to determine their effect on the amount of sodium migration. The pressed glass surfaces could then be investigated using a combination of argon ion beam milling (to remove atomic layers from the surface of the glass article) and x-ray photoelectron spectroscopy to allow a detailed depth profile to be carried out.

The temperature at which the glass melt adhered to the plunger during forming was not achievable using the present design of pressing rig. Previous work has indicated that elevated forming temperatures produce stronger glass articles. Therefore, the design of the current pressing rig needs to be rethought to allow the investigation of the glass melt to plunger material immediately prior to sticking to be investigated. Alternatively, hot stage microscopy could be used to determine how a glass melt reacts with a metal substrate at elevated temperatures up to the point at which sticking occurs.

The results from the use of carbon-carbon composites in this project did not appear to suggest that these materials, in their current form, would be useful as potential mould materials for the manufacture of glass containers. However, if a method for stabilising the material at the elevated temperatures required for the formation of glass containers could be found, carbon-carbon composite materials could still be possible candidates for the mould material of the future. In addition, the use of alternative materials and coatings as possible glassmaking mould materials needs to be investigated.

It was suggested by one of the UKs leading mould manufacturers that there is a problem with the use of forced air mould cooling. It may therefore be useful to model the stresses set up in the surface of the cast iron mould using a technique such as finite element analysis. This type of modelling would allow the user to visualise where the stresses are too high, therefore allowing modifications to the design of the cooling to be carried out which may in turn increase the lifetime of the current moulds. Alternatively, a new method for the cooling of cast iron glassmaking mouldware needs to be sought in order to maintain the current production levels.

# REFERENCES

Abramovich B. G., Kalashnikov G. E., GLASS AND CERAMICS, 1981, 38, pp349 - 350

Anderson P. R., Bacon F. R., Byrum B. W., J. NON-CRYST. SOLIDS, 1975, 19, pp251 – 262

Baes C. F., Mesmer R. E., "THE HYDROLYSIS OF CATIONS", Reprint Edition, Robert E. Krieger Publishing Co., 1986

Baiocchi E., Bettinelli M., Montenero A., J. AM. CERAM. SOC. (COMMUNICATIONS), 1982, March, ppC-39 - C-40

Binkowski N. J., Heitzenrater R. F., Stephenson D. A., J.. AM. CERAM. SOC., 1976, 59 (3-4), pp153-157

Birks N., Meier G. H., "INTRODUCTION TO HIGH TEMPERATURE OXIDATION OF METALS", 1$^{st}$ Edition, Edward Arnold, 1983

Boow J., Turner W. E. S., J. SOC. GLASS TECHNOL., 1942, 26, pp215-237

Bourne R., Cowen N. D., Budd S. M., GLASS TECH., 1984, 25 (3), pp145 - 147

Brearley W., Holloway D. G., PHYS. CHEM. GLASSES, 1963, 4 (3), pp69 – 75

Briggs D., Seah M. P., "PRACTICAL SURFACE ANALYSIS – VOLUME 1 AUGER AND X-RAY PHOTOELECTRON SPECTROSCOPY", 2$^{nd}$ Edition, John Wiley and Sons, 1995

Bruckman A., Simkovich G., CORROSION SCI., 1972, 12, pp595-601

BSI Standards BS EN ISO 945:1994, "CAST IRON – DESIGNATION OF MICROSTRUCTURE OF GRAPHITE"

Budd S. M., Vickers T. A. Y., GLASS, 1990, 67, pp365 – 366

Burgmann W., Urbain G., Frohberg M., MEM. SCI. REV. MET., 1968, 65(78), pp572

Clark-Monks C., GLASS TECH., 1974, 15 (2), pp31 - 34

Coney S. S., Kent R., BGIRA TECHNICAL NOTE NO. 140, 1971

Coney S. S., Kent R., BGIRA TECHNICAL NOTE NO. 151, 1971

Coney S. S., Shaw. F., Kent R., BGIRA TECHNICAL NOTE NO. 156, 1972

Coney S. S., Sherborne D. J., Kent R., BGIRA TECHNICAL NOTE NO. 176, 1973

Coney S. S., Sherborne D. J., Shaw F., BGIRA TECHNICAL NOTE NO. 179, 1973

Coney S. S., PRIVATE COMMUNICATION, 1995

Copley G. J., Rivers A. D., Smith R., J. MAT. SCI., 1973, 8, pp1049 - 1051

Copley G. J., Rivers A. D., Smith P., J. MAT. SCI, 1975, 10, pp1285-1290

Copley G. J., Rivers A. D., J MAT. SCI., 1975, 10, pp1291-1299

Cottrell A., "AN INTRODUCTION TO METALLURGY", 2nd Edition, Edward Arnold, 1975

Darken L. S., Gurry R. W., J. AM. CERAM. SOC., 1946, 68(5), pp799

Dartnall R. C., Fairbanks H. V., Koehler W. A., J. AM. CERAM. SOC., 1951, 34 (11), pp357 - 360

Dengel A., Roeder E., GLASTECH. BER., 1991, 64 (10), pp268 – 271

Dietzel A., Brückner R., GLASTECH. BER., 1955, 28, pp455-467

Donet J. B., Bansal R. C., "CARBON FIBRES", 2nd Edition, Marcel Dekker Inc., 1990

Dowling W. C., Fairbanks H. V., Koehler W. A, J. AM. CERAM. SOC., 1950, 33 (9), pp269 - 273

Edgington J. H., GLASS, 1995, February, pp68, 70

Ensor T. F., GLASS TECH., 1970, 11 (2), pp42 - 47

Ensor T. F., GLASS TECH., 1978, 19 (5), pp113 - 119

Ensor T. F., GLASS TECH., 1990, 31 (3), pp85 – 88

Ernsberger F. M., "RESEARCH INTO GLASS", Volume I, pp19-31

Ernsberger F. M., RESEARCH INTO GLASS, 1970, Volume II, pp21 - 37

Evans A. G., Davidge R. W., GLASS TECH., 1971, 12 (6), pp148 - 154

Fairbanks H. V., SYMPOSIUM SUR LE CONTACT DU VERRE CHAUD AVEC LE METAL, 1964, pp575 – 595

Falipou M., Donnet C., Maréchal F., Charenton J.C., GLASTECH. BER. GLASS SCI. TECH., 1997, 70(5), pp137-145

Fellows C. J., McKerrow A. S., Shaw F., BGIRA TECHNICAL NOTE NO. 215, 1976

Fellows C. J., McKerrow A. S., Shaw F., BGIRA TECHNICAL NOTE NO. 222, 1976

Fellows C. J., Shaw F., GLASS TECH., 1978, 19 (1), pp4 - 9

Foster S., McKerrow A. S., Shaw F., BGIRA TECHNICAL NOTE NO. 276, 1980

Foster T. V., GLASS IND., 1984, September, pp27 - 28

Fox K. E., Furukawa T., White W. B., PHYS. CHEM. GLASSES, 1982, 23 (5), pp169-178

Fox P. G., GLASS TECH., 1981, 22 (2), pp67 – 78

Gerber D., GLASS PROD. TECH. INT., 1994, pp153-156

Giegerich W., GLASTECH. BER., 1953, 26, pp333

Giegerich W., Trier W., "GLASS MACHINES – CONSTRUCTION AND OPERATION OF MACHINES FOR THE FORMING OF HOT GLASS", Chapter 1, Springer Verlag, 1969

Glass Manufacture – An Open Learning Course, Section V – Glass Forming Processes, Module 19: Blowing, Glass Training Ltd.

Golden J. T., GLASS INT., 1983, (60), pp50, 52

Griffel H., GLASS TECH., 1987, 28 (3), pp121 – 123

Hand R., Seddon A. B., PHYS. CHEM. GLASSES, 1997, 38(1), pp11-14

Hannoyer B., Lenglet M., Dürr J., Cortes R., J. NON-CRYST. SOLIDS, 1992, 151, pp209-216

Hollands L. J., FIRST YEAR RESEARCH REPORT, University of Sheffield, 1995

Holloway D. G., PHIL. MAG., 1959, Series 8 (4), pp1101 – 1106

Holscher H. H., Coleman J. G., Cooke C. C., GLASS IND., 1960, 41, (2) pp74-81, 113-114, (3) pp 142-147, 181-182

Howse T. K. G., Kent R., Rawson H., GLASS TECH., 1971, 12 (4), pp84 – 93

Jones S. P., BGIRA Information Circular No. 60, 1966

Kapnicky J. A., Fairbanks H. V., Koehler W. A., J. AM. CERAM. SOC., 1949, 32 (10), pp305 – 308

Kent R., Rawson H., GLASS TECH., 1971, 12 (5), pp117 – 127

Kirsch R., "METALS IN GLASSMAKING", Elsevier, 1993

Kolotilkin O. B., Volchok I. P., GLASS AND CERAMICS, 1983, 40, pp355 - 357

Kropotov D. P., GLASS AND CERAMICS, 1975, (6), pp383 - 384

Kubaschewski and Alcock, "METALLURGICAL THERMOCHEMISTRY", 5th Edition, Pergamon Press, 1979

Kubaschewski O., Hopkins B. E., "OXIDATION OF METALS AND ALLOYS", Butterworths, 1962

Lacourse W. C, GLASS IND., 1987, June, pp14 - 18, 23

Lakatos T., Johansson L.-G., Simmingsköld B., GLASS TECH., 1972, 13 (3), pp88-95

Lee W., PRIVATE COMMUNICATION, 1997

Lynch E. D., Tooley F. V., J. AM.CERAM. SOC., 1957, 40 (4), pp107 - 112

Müller-Simon H, Wagner J, Lenhart A, GLASTECH BER, 1994, 67 (5), pp134 - 142

Müller-Simon H, Wagner J, Lenhart A, GLASTECH BER, 1994, 67 (7), pp196 - 201

Manns P., Döll W., Kleer G., GLASTECH. BER. GLASS SCI. TECH., 1995, 68(12), pp389-399

Mcgraw D. A., GLASTECH. BER., 1973, 46 (5), pp89 - 91

McMinn J. J., Shaw F., McKerrow A. S., BGIRA TECHNICAL NOTE NO. 236, 1977

McMinn J. J., McKerrow A. S., Shaw F., BGIRA TECHNICAL NOTE NO. 237, 1978

McMinn J. J., McKerrow A. S., Shaw F., BGIRA TECHNICAL NOTE NO. 262, 1979

Meichel E., GLASS, 1990, 67 (November), pp455

Merchant, Harish D., BULL. AM. CERAM. SOC., 1963, 42 (2), pp57 - 64

Mishchenko N. A., GLASS AND CERAMICS, 1977, 34 (10), pp627 - 630

Moder H. J., Wasylyk J. S., GLASS UDYOG, 1985, 14 (1), pp39 - 46

Oel H. J., Gottschalk A., GLASS, 1967, 44 (7), pp398 - 401

Orlov A. N. et al, GLASS AND CERAMICS, 1977, 34 (4), pp231 - 233

Pantano C. G., RIV. STN. SPER. VETRO, 1990, 6, pp123-135

Pask J. A, Fulrath R. M., J. AM. CERAM. SOC., 1962, 45 (12), pp592 – 596

Penlington R., Sarwar M., Lewis D. B., Marshall G. W., Cockerham G., PROC. EAST CONF., Germany, Nov. 1993a, pp86-90

Penlington R., Sarwar M., Lewis D. B., Marshall G. W., Cockerham G., PROC. EUROPEAN SOC. OF GLASS SCI. AND TECH., 2nd INT. CONF. ON FUNDAMENTALS OF GLASS SCIENCE AND TECHNOLOGY, Venice, Italy, Jun. 1993b, pp279-284

Penlington R., Sarwar M., GLASTECH. BER. GLASS SCI. TECH., 1995, 68(C2), pp164-171

Penlington R., Sarwar M., Lewis D. B., SURFACE COATINGS TECHNOLOGY 1995, 76-77, pp81-85

Pourbaix M., "ATLAS D' EQUILIBRES ELECTROCHEMIQUES À 25°C", Gauthiers- Villars, Paris, 1963

Proctor B. A., Whitney I., Johnson J. W., PROC. ROY. SOC., 1966, 297, pp534 - 557

Puglisi O., Torrisi A., Marletta G., J. NON-CRYST. SOLIDS, 1984, 68, pp219-230

Puyane R., PHD THESIS UNIVERSITY OF SHEFFIELD, 1976

Puyane R., Rawson H., GLASS TECH., 1979, 20 (5), pp186 - 193

Rawson H., Wlosinski W. K., GLASS TECH., 1968, 9 (2), pp45 - 51

Rawson H., GLASTECH. BER., 1988, 61 (9), pp231 - 246

Rawson H., "PROPERTIES AND APPLICATIONS OF GLASS", 1st Edition, Elsevier, 1980

Ritter J. E., Cooper A. R., PHYS. CHEM. GLASSES, 1963, 4 (3), pp76 – 78

Rossing B. R., GLASS, 1995, 72(9), pp363

Ryabov V. A., Fedoseyev D. V, GLASS TECH., 1968, 9 (2), pp32 - 35

Shaw F., Coney S. S., Sherborne D. J., BGIRA TECHNICAL NOTE NO. 202

Sil'vestrovich S. I., Pavlushkin N. M., Koshel'kova V. S., Mikhailenko N. Yu., GLASS AND CERAMICS, 1970, 27 (12), pp719 - 722

Simpson W, GLASS PROD. TECH. INT., 1990, pp137 - 138

Smrcek A., SILIKATY, 1967a, 11 (3), pp267 - 277

Smrcek A., SILIKATY, 1967c, 11 (4), pp339 - 344

Smrcek A., SILIKATY, 1967b, 11 (4), pp345 – 351

Trier W., J. AM. CERAM. SOC., 1961, 44, pp339-345

Trier, W, GLASTECH. BER., 1994, 67(10), pp280 - 291

Vickers T., GLASS IND., 1988, November, pp15 - 19

Warren G., MSc(TECH) THESIS UNIVERSITY OF SHEFFIELD, 1973

Wasylyk J. S., GLASS MACH. PLANTS AND ACCESS., 1991, 4 (6), pp37 - 43

Williams H. P., GLASS TECH., 1985, 26 (6), pp248 - 251

Williams H. P., GLASS TECH., 1989, 30 (3), pp99 - 101

Winther S., Schaeffer H. A., GLASTECH. BER., 1988, 61 (7), pp184 - 190

Zarzycki J., "MATERIALS SCIENCE AND TECHNOLOGY: A COMPREHENSIVE TREATMENT. VOLUME 9 – GLASSES AND AMORPHOUS MATERIALS, Chapter 1 (M. Cable) 1991

# APPENDIX A – XPS

## A.1 Experimental Parameters Used

The following experimental parameters were typically used for glass and cast iron samples measured using XPS:

**Instrument** – VG Clam 2

**X-ray source** - MgKα (1253.6eV)

**Slit width** – 4mm

**Analyser type** –hemispherical electrostatic electron energy analyser

**Vacuum quality** – minimum of $10^{-6}$Pa

**Take off angle** – the take off angle on the instrument used is variable, however, a typical experiment used a take off angle of 30°

**Step size** – 0.6eV for widescans (survey scan), 0.1eV for narrow scans

**Dwell time** – 0.1s for widescans, 0.5s for narrow scans

**Number of scans** – 2

## A.2 Peak Characterisation

Using X-ray photoelectron spectroscopy, in addition to the characteristic peaks used to identify elements, additional peaks can be observed which occur due to photoelectrons being ejected from different shells within the atom. The following information shows the line positions (in binding energy) for all the elements of interest in the current work using a MgKα source [Briggs & Seah_1990]:

C – Photoelectron lines **1s 287eV**, Auger lines **993eV**

O – Photoelectron lines **1s 531eV**, 2s 23eV, Auger lines 779eV, 764eV, **743eV**

Na – Photoelectron lines **1s 1072eV**, 2s 64eV, 2p 31eV, Auger lines 332eV, 303eV, **264eV**

Si – Photoelectron lines 2s 153eV, 2p$_{1/2}$ 103eV, **2p$_{3/2}$ 102eV**

Cl – Photoelectron lines 2s 270eV, 2p$_{1/2}$ 201eV, **2p$_{3/2}$ 199eV**, 3s 17eV, Auger lines **1071eV**

Ca – Photoelectron lines 2s 439eV, 2p$_{1/2}$ 350eV, **2p$_{3/2}$ 347eV**, 3s 44eV, 3p 25eV, Auger lines 964eV, **961eV**

Fe – Photoelectron lines 2s 847eV, 2p$_{1/2}$ 723eV, **2p$_{3/2}$ 710eV**, 3s 93eV, 3p$_{1/2}$ 56eV, 3p$_{3/2}$ 55eV, Auger lines 659eV, 608eV, **553eV**


It should be noted that the line positions in bold type are the strongest characteristic peaks which are used for element identification and quantification.


Once charge referencing has been carried out (i.e. referencing to the C1s peak at 285eV) to account for charging in non-conducting samples, small shifts in the peak position may be observed which may be used to determine the local chemistry of each element detected.

## A.3   Quantification

Quantification of the surface composition of the samples was carried out by data processing the characteristic peaks on widescan traces using *Spectra 6* (the software used to operate the spectrometer).

In order to quantify the species on the surface of a sample, a number of steps were carried out. Initially, the normalised intensity of each of the characteristic peaks was determined by subtracting the background (linear for the glass samples and Shirley for the cast iron samples). A Shirley background subtraction is used where the background is curved; the background intensity at a point is determined using an iterative process, as being proportional to the intensity of the total peak area above the background and to higher energy [Briggs & Seah_1990]. The analyser used has a varying sensitivity over the whole compositional range, and as such the normalised intensity alone cannot be used for quantification. A number of sensitivity factors (relative to C 1s = 1.00) have been determined for the *VG Clam 2* for each of the elements which takes this variation into account. The sensitivity factors (expressed as ratios against the C1s peak) used in this work are as follows:

C – 1.00

O – 2.46

Na – 22.00

Si – 0.89

Cl – 2.89

Ca – 6.30

Fe – 15.70

Using the normalised intensity ($N$) in addition to the sensitivity factor ($S$) and number of scans ($m$), quantification of the surface was carried out using the following equations:

e.g. for a glass sample, the amount of silicon present on the surface ($n_{Si}$) can be approximated to:

$$n_{Si} \propto \frac{N}{mS}$$

This process was repeated for the other elements of interest, and quantification was carried out using the following:

$$\%Si = \frac{n_{Si}}{(n_{Si} + n_C + n_O + n_{Ca} + n_{Na})}$$

It should be noted that the spectrometer used is generally applied to the examination of polymeric samples. As such, the sensitivity factors used may not be appropriate for the quantification of glass samples (due to different absorption and enhancement effects in the sample matrix).

# APPENDIX B – IRON CONTAINING GLASS

At the beginning of the project, several soda-lime-silica based glasses were melted with an iron content that was higher than typical for soda-lime-silica glasses to determine what effect an elevated iron content had on glass properties. This was carried out in order to determine the effect of any material transfer between the mould material and glass on the resultant glass.

## B.1 Glass Composition

The base glass used was a basic four component system (i.e. 72wt.% $SiO_2$, 14wt.% $Na_2O$, 12wt.% CaO and 2wt.%$Al_2O_3$) with 1-12wt.% additions of $Fe_2O_3$ (i.e. 1, 2, 3.5, 5, 10 and 12 wt.%). The varying iron additions were made to constant wt.% proportions of the base glass components (eg for a nominal 1wt.% addition, 1g of $Fe_2O_3$ was added to 100g of the base glass).

The batch materials used (i.e. L.A. sand, soda ash, limestone and aluminium hydroxide and iron (III) oxide $Fe_2O_3$ ) were weighed out to two decimal places to make 100g batches and mixed thoroughly. All the glasses were melted in an electric furnace at 1450°C in a platinum crucible for 1 hour (in order to reach the batch free time) then stirred using a platinum stirrer for a further 5 hours in order to ensure a homogeneous melt. The glass melt was then cast into slabs and annealed by holding at 560°C for 1 hour and then slowly cooled at 1°C per minute.

# B.2  Characterisation

The doped 1-12wt.% iron enriched glasses were characterised using the following techniques:

### B.2.1  DTA to determine the glass transformation temperature

The glass samples were ground to a fine powder using an agate pestle and mortar. 150mg samples of glass were heated in a platinum crucible in static air at 10°C/minute to a maximum temperature of 750°C and compared against 150mg of a standard fused alumina sample using a *Stanton Redcroft 374* DTA.

### B.2.2  Thermal Expansion Coefficient

Rods of the glass samples were machined to have a diameter of between 2 - 5mm and to be 25 - 70mm in length with ground parallel ends from a cast glass slab. The thermal expansion of the samples was measured using a silica dilatometer by heating from room temperature to a maximum of 700°C at 5°C per minute. The sample was located between two silica rods, and placed under a small compressive load in the furnace of the dilatometer. The change in length was constantly monitored throughout heating. In order to take account of the expansion due to the silica rods, a comparative silica rod was measured in parallel. The thermal expansion coefficient of the samples was determined between 200 – 400°C.

### B.2.3 UV-Visible Spectroscopy

This technique was used to try and determine the ferric and ferrous iron contents present in the high iron glass samples. The specimens produced for analysis were ground and polished in order to give samples of approximately 10mm by 10mm and less than 1mm optical pathlength in order for light to pass through. The UV-Visible spectra were measured over a wavelength range of 200 – 2500nm using a *Perkin-Elmer 330* spectrophotometer. The absorbance traces obtained were all normalised to a 1mm pathlength in order to compare the traces from the different experiments.